Extension of the effectiveness-NTU Model to Liquid-to-Air Membrane Energy Exchangers (LAMEEs)

A Thesis Submitted to the College of

Graduate Studies and Research

In Partial Fulfillment of the Requirements

For the Degree of Master of Science

In the Department of Mechanical Engineering

University of Saskatchewan

Saskatoon

By

Houman Kamali

Permission to Use

In presenting this thesis in partial fulfilment of the requirements for a Postgraduate degree from the University of Saskatchewan, I agree that the Libraries of this University may make it freely available for inspection. I further agree that permission for copying of this thesis in any manner, in whole or in part, for scholarly purposes may be granted by the professor or professors who supervised my thesis work or, in their absence, by the Head of the Department or the Dean of the College in which my thesis work was done. It is understood that any copying or publication or use of this thesis or parts thereof for financial gain shall not be allowed without my written permission. It is also understood that due recognition shall be given to me and to the University of Saskatchewan in any scholarly use which may be made of any material in my thesis.

Requests for permission to copy or to make other use of material in this thesis in whole or part should be addressed to:

Head of the Department of Mechanical Engineering

3B48 Engineering Building, University of Saskatchewan

57 Campus Drive, Saskatoon, SK (S7N 5A9)

Abstract

Liquid-to-air membrane energy exchangers (LAMEEs) enable simultaneous heat and moisture exchange, with a minimal cross-contamination, between air and liquid desiccant solution by separating the streams with porous membranes that are permeable to water vapor. This thesis has two main objectives. The first objective is to identify and introduce a new set of dimensionless parameters to which the effectiveness of LAMEEs for heat and moisture exchange can be correlated. The second objective is to develop methods to predict the effectiveness of LAMEEs based on these new dimensionless parameters.

The standard effectiveness-NTU model correlates the effectiveness of heat exchangers to the dimensionless parameters: number of transfer units (NTU) and heat capacity rate ratio (Cr). The standard effectiveness-NTU models is widely used in the industry as a simple method for initial design and sizing of heat exchangers, however, as a result of the coupling between heat and moisture exchange in LAMEEs, this model is not directly applicable to LAMEEs. To extend this model to LAMEEs, two new dimensionless parameters that are analogous to Cr are introduced and defined: effective heat capacity rate ratio (effective Cr) and effective mass flow rate ratio (effective m*). Furthermore, two models (termed the simplified-extended effectiveness models) are introduced as analogs of the standard effectiveness-NTU model. These models correlate the effectiveness of LAMEEs for heat exchange to the dimensionless parameters: number of transfer units (NTU) and effective Cr, and correlate the effectiveness of LAMEEs for moisture exchange to the dimensionless parameters: number of moisture transfer units (NTUm) and effective m*. To verify these models, a number of experimental data previously published for a small-scale LAMEE and also a hollow fiber membrane contactor were used. The discrepancies between the estimations of the simplified-extended effectiveness models and the experimental measurements for heat and

moisture effectiveness do not exceed 16%. However, a major drawback of this method is that to calculate the new dimensionless parameters (effective Cr and effective m*), in addition to the inlet operating conditions of both the air and solution streams, the outlet operating conditions of the air stream are also required, which results in an iterative design procedure.

To achieve the second objective of this thesis, a set of methods are proposed for estimating effective Cr and effective m* as a function of the inlet operating conditions of the air and solution streams and the LAMEEs' design parameters. To verify that these proposed methods result in accurate estimations, a number of previously published experimental data points and 10,000 numerical data points for different designs of LAMEEs were used. The methods developed in this thesis were used to estimate effective Cr and effective m* for these data points. Then, these estimations for effective Cr and effective m*, along with NTU and NTUm corresponding to each data point, were substituted into the simplified-extended effectiveness models to predict the changes in the temperature and moisture content of the air stream for each of the data points. The estimated changes in the temperature and moisture content of the air stream differed from the experimental measurements and numerical calculations by less than 2.1 °C and 2.8 g/kg. For comparison, the estimations provided by the standard effectiveness-NTU model for the outlet air temperature differed from the numerical calculations by up to 7.2 °C and from the experimental measurements by up to 5.1 °C.

Acknowledgements

I would like to express my appreciation for the guidance, support and encouragement that my supervisors, and friends, Professor C. J. Simonson and Professor Emeritus R.W. Besant provided as I worked to develop and finish this thesis.

I would also like to acknowledge financial assistance from the Department of Mechanical Engineering at the University of Saskatchewan.

Table of Contents

List of Tables

List of Figures

Nomenclature

Acronyms

C&D	Cooling and dehumidification
C&H	Cooling and humidification
ERV	Energy recovery ventilator
H&D	Heating and dehumidification
H&H	Heating and humidification
HFMC	hollow fiber membrane contactor
HVAC	Heating, ventilation and air conditioning
LAMEE	Liquid-to-air membrane energy exchangers
LDAC	Liquid-desiccant air conditioning
RAMEE	Round-around membrane energy exchanger
SHR	Sensible heat ratio

English Symbols

A	Total area of the membranes (m^2)
c_p	Specific heat capacity $(J/kg \cdot K)$
C_{air}	Heat capacity rate of air (W/K)
C_{sol}	Heat capacity rate of solution (W/K)
Cr	Heat capacity rate ratio
Cr_e	Effective heat capacity rate ratio
d_{air}	Width of the air channel (m)
dCr_e	Differential effective heat capacity rate ratio
$\overline{dCr_e}$	Average differential effective heat capacity rate ratio
dm_{e}^*	Differential effective mass flow rate ratio
$\overline{dm_{\mathrm{e}}^*}$	Average differential effective mass flow rate ratio
d_m	Membrane thickness (mm)
d_{sol}	Width of the solution channel (m)
D_h	Hydraulic diameter of air channel (m)
D_{va}	Diffusivity coefficient of vapor in air (s/m)
h	Convective heat transfer coefficient $(W/K \cdot m^2)$
h_{fg}	Specific heat of evaporation of water (J/kg)
h_m	Convective mass transfer coefficient (m/s)
H	Height of the exchanger (m)
HCR	Heat conduction resistance of membrane $(K \cdot m^2/W)$
k	Thermal conductivity of membrane $(W/K \cdot m)$
k_{air}	Thermal conductivity of air $(W/K \cdot m)$
k_m	Vapor permeability of membrane $(kg/s \cdot m)$
l	Dimensionless position along the length of the exchanger

L	Length of the exchanger (m)
$\dot{m}$	Mass flow rate (kg/s)
$\dot{m}_W$	Moisture transfer rate (kg/s)
m^*	Mass flow rate ratio
m_e^*	Effective mass flow rate ratio
$m_{e,in}^*$	Inlet effective mass flow rate ratio
$m_{e,IWD}^*$	Inlet humidity ratio difference effective mass flow rate ratio
n	Total number of membrane sheets
NTU	Number of transfer units
NTU_m	Number of moisture transfer units
Nu	Nusselt number for air
P	Total pressure (Pa)
Pr	Prandtl number
P_v	Partial water vapor pressure (Pa)
q_L	latent heat transfer rate (W)
q_s	Sensible energy exchange rate (W)
$q_{s,air}$	Rate of sensible energy transfer to air (W)
$q_{s,sol}$	Rate of sensible energy transfer to solution (W)
Re	Reynolds number
R^2	Coefficient of determination
Sh	Sherwood number for air
Sc	Schmidt number
T	Temperature (K)
U	Overall heat transfer coefficient $(W/K \cdot m^2)$
U_m	Overall mass transfer coefficient $(kg/s \cdot m^2)$
VDR	Vapor diffusion resistance of membrane $(s \cdot m^2/kg)$
W_{air}	Humidity ratio of air (kg/kg)
W_{sol}	Equilibrium humidity ratio of solution (kg/kg)
x	Position along the length of the exchanger (m)
X_{sol}	Concentration of salt solution

Greek Symbols

α_1	Coefficient (g/kg)
α_2	Coefficient (g/kg)
β	Coefficient $(1/K)$
δ	thickness of the membrane (m)
Δ	Difference operator
ϵ	Effectiveness of heat exchangers for sensible energy exchange
ϵ_m	Effectiveness of energy exchangers for moisture exchange
ϵ_s	Effectiveness of energy exchangers for sensible energy exchange

ρ_{air}	Density of dry air (kg/m^3)

Subscripts

air	Air
B	Component B
HX	Heat exchanger
in	Inlet
IWD	Inlet humidity ratio difference
max	Maximum
min	Minimum
MX	Moisture exchanger
out	outlet
sol	Solution

Chapter 1

Introduction

1.1. Liquid-to-Air Membrane Energy Exchangers (LAMEEs)

Liquid-to-air membrane energy exchangers (LAMEEs) are equipment that separate air and liquid desiccant solution streams using semi-permeable porous membranes that are pervious to water vapor but impervious to liquid water (under normal operating pressures of LAMEEs, which are $\sim 1\ atm$). These porous membranes enable LAMEEs to simultaneously exchange sensible energy and moisture between the air and solution streams. In contrast, heat exchangers use solid materials to separate the streams and thus enable only sensible energy exchange between the streams. The two main perceived applications for LAMEEs are (a) energy recovery ventilation and (b) air dehumidification and humidification. Photograph of two LAMEE prototypes is presented in Figure 1.1 [1].

Figure 1.1 Photograph of the two fully assembled LAMEEs [1]

Energy recovery ventilation refers to the use of energy recovery ventilators (ERVs) in the heating, ventilation and air conditioning (HVAC) systems. ERVs reduce the energy consumed for conditioning the outdoor ventilation air by recovering some of the energy from the exhaust air of buildings. For example in summer, the hot and humid supply air that is used to ventilate the building should first be cooled and dried, thus the intended purpose of ERVs in the summer is to use the cool and dry exhaust air of buildings to partially cool and dry the supply air. Noting that the energy that is used to change the temperature of the air is termed sensible energy and the energy that is used to change the moisture content (humidity) of the air is termed latent energy, the advantage of LAMEEs over heat exchangers for the purpose of energy recovery ventilation becomes clear: LAMEEs enable the recovery of latent energy in addition to sensible energy. That is, if only heat exchangers are used in an ERV, that ERV cannot exchange moisture between the supply and the exhaust air streams, and thus cannot be used to recover the latent energy. Round-around membrane energy exchangers (RAMEEs) are ERVs that consist of two LAMEEs which couple the supply and the exhaust air streams using a liquid desiccant solution and enable simultaneous sensible and latent energy recovery [2]. Rasouli et al. demonstrated that RAMEEs can reduce the annual heating and cooling energy consumption of hospitals in North American climates by up to nearly 70% and 20%, respectively [3]. The importance of reducing heating and cooling energy demand becomes clear under the light that in Canada alone in 2009, "commercial business owners and institutions spent $24 billion on energy", and that 53% of that energy was consumed for space heating and cooling [4]. Furthermore, Rasouli et al. concluded that RAMEEs can be used to reduce the capacity of the heating and cooling equipment by nearly 50% and 25%, respectively, which directly affects the capital cost of the HVAC equipment.

Liquid desiccant solutions in LAMEEs are aqueous solutions of salts such as $MgCl_2$ and $LiCl$. By controlling the concentration of the salt and the temperature of the desiccant solutions, it becomes possible to either humidify or dehumidify the air that exchanges moisture with the desiccant solutions inside LAMEEs. For the applications in which the temperature and concentration of the desiccant solution in a LAMEE are controlled, the LAMEE are said to operate as either active dehumidifiers or active regenerators, depending on whether the air is dehumidified or humidified, respectively [2]. The advantage of using liquid desiccant air conditioning equipment, e.g. LAMEEs, for air dehumidification is that, compared to the conventional method of condensing the vapor in the air in order to reduce the moisture content of the air, the cycle of cooling the air to a lower than required dew point temperature and then heating it back to the desired temperature is eliminated [5] [1]. This is because similar to solid desiccants (e.g. silica gel beads), liquid desiccant solutions at appropriate concentrations (e.g. an aqueous solution of $LiCl$ salt with the ratio of mass of the salt to mass of the water equal to 0.3), can absorb humidity from air at room temperature and maintain relative dryness in the air adjacent to the desiccant.

To facilitate the design of better performing liquid desiccant air conditioning (LDAC) systems that incorporate LAMEEs, it can be helpful if the designers have access to simple models that can be used to evaluate the performance of LAMEEs. These should also provide an insight into how the design parameters and the operating conditions affect the performance of LAMEEs. The objective of this thesis is to provide simple to understand models for LAMEEs, so that understanding the models does not become a challenge itself and so that the models can be used to quickly make decisions at the initial stages of design.

[1] In conventional dehumidifiers, the humid air stream is first cooled to a temperature below its dew point, after which the water vapor in the air condenses into liquid and the moisture content of the air decreases. However, the cooled air typically needs to be heated back to a higher temperature appropriate for supply to an occupied space.

1.2. Effectiveness of Heat Exchangers

In air conditioning systems, power plants, refineries, and several other applications, heat exchangers are used to transfer sensible energy from one medium to another, typically from a fluid stream to another fluid stream. There are different basic designs of heat exchangers, among which, plate heat exchangers and shell and tube heat exchangers are two of the more common designs [6]. The main purpose of heat exchangers is to separate two fluid streams at different temperatures from each other, e.g. by solid plates in plate heat exchangers, and enable heat exchange between the two streams as the streams flow past each other inside the heat exchanger. In this thesis, it is assumed that heat exchangers are isolated from the environment, and thus heat exchange occurs only between the two streams flowing inside the heat exchanger, and not between the streams and the environment. Figure 1.2 presents a schematic of two adjacent channels of a counter-flow flat-plate heat exchanger, where counter-flow refers to the situation where the streams are flowing parallel to each other but in the opposite directions. The hot stream enters the exchanger at the temperature $T_{h,in}$ $(°C)$ and the cold stream enters the exchanger at the temperature $T_{c,in}$ $(°C)$. As heat transfers from the hot stream to the cold stream, the temperature of the hot stream decreases and it leaves the exchanger at a temperature $T_{h,out}$ that is lower than the temperature at which the hot air stream entered the exchanger. Similarly, the temperature of the cold stream increases and leaves the exchanger at a higher temperature of $T_{c,out}$ at the outlet.

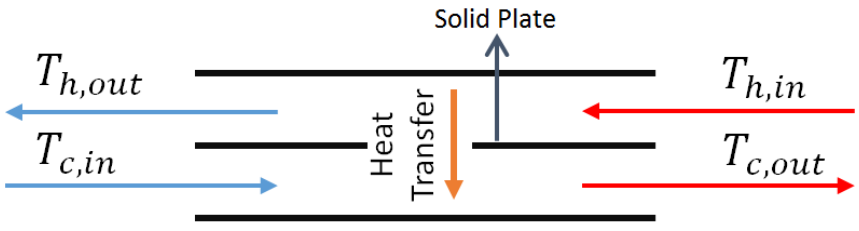

Figure 1.2 Schematics of heat exchange between two adjacent channels of a flat heat exchanger

The deriving potential for heat exchange between the streams is the difference between the temperatures of the streams. Heat transfer through the solid plate is governed by Fourier's law of heat conduction, which, in its one-dimensional form is stated as [7]

$$q''_x = -k\frac{dT}{dx} \tag{1.1}$$

where q''_x (W/m^2) is the local heat flux density in the x direction (e.g. normal to the solid plate in Figure 1.1), k $(W/K \cdot m)$ is the local thermal conductivity of the material through which heat transfer is occurring (e.g. the thermal conductivity of the solid plate in Figure 1.1), and T (K) is the local temperature.

In addition to the inlet temperatures of the cold and hot streams, i.e. $T_{h,in}$ and $T_{c,in}$, the heat capacity rates of the streams is another important property of the streams. The heat capacity rates of the cold and hot streams are, respectively, denoted C_c and C_h, which are defined as

$$C_c = \left(c_p \dot{m}\right)_c \tag{1.2}$$

$$C_h = \left(c_p \dot{m}\right)_h \tag{1.3}$$

where $\dot{m}$ (kg/s) is the mass flow rate of a stream and c_p $(J/kg \cdot K)$ is the specific heat capacity of a fluid, and subscripts c and h refer to the cold and hot fluid. Denoting the total rate of heat transfer from the hot stream to the cold stream by q_s (W), and assuming steady-state conditions, the principle of conservation of energy can be used to calculate the changes in the temperatures of the streams as follows

$$T_{h,out} - T_{h,in} = \Delta T_h = -\frac{q_s}{C_h} \tag{1.4}$$

$$T_{c,out} - T_{c,in} = \Delta T_c = \frac{q_s}{C_c} \tag{1.5}$$

where $\Delta T_h(°C)$ and $\Delta T_c\ (°C)$ are the changes in the temperatures of the hot and cold streams. Equating Eq. (1.4) and Eq. (1.5), one can conclude that

$$-\Delta T_h C_h = \Delta T_c C_c = q_s \tag{1.6}$$

Furthermore, denoting the change in the temperature of the stream with the maximum heat capacity with ΔT_{min} and the change in the temperature of the stream with the minimum heat capacity with ΔT_{max} (i.e. if $C_c \leq C_h$ then $\Delta T_{min} = \Delta T_h$ and if $C_h \leq C_c$ then $\Delta T_{min} = \Delta T_c$), from Eq. (1.6) it can be concluded that

$$|\Delta T_{min} C_{max}| = |\Delta T_{max} C_{min}| = q_s \tag{1.7}$$

Thus the stream with the minimum heat capacity rate will undergo the maximum change in the temperature inside the heat exchanger. However, the maximum possible value for $|\Delta T_{max}|$ is equal to the difference between the inlet temperatures of the streams [7] in heat exchanger, while the actual value of $|\Delta T_{max}|$ depends on the effectiveness of the heat exchanger:

$$|\Delta T_{max}| = \epsilon \left(T_{h,in} - T_{c,in}\right) \tag{1.8}$$

where ϵ is the effectiveness of a heat exchanger and for heat exchangers it assumes a value between 0 and 1

$$0 \leq \epsilon \leq 1 \tag{1.9}$$

Substituting Eq. (1.8) into Eq. (1.7), it can be concluded that

$$\frac{|\Delta T_{max} C_{min}|}{\left(T_{h,in} - T_{c,in}\right) C_{min}} = \frac{q_s}{q_{s,max}} = \epsilon \tag{1.10}$$

Thus, the effectiveness of a heat exchanger quantifies the ability of the heat exchanger to achieve $q_{s,max}\ (W)$, the maximum possible heat exchange between the streams. Since in heat exchangers there is no conversion of energy from one form to another, the concept of efficiency is

not applicable to the process of heat exchange that occurs in heat exchangers. The concept of effectiveness of heat exchangers is introduced here because this concept will be used as the basis for defining effectiveness of LAMEEs for heat and moisture exchange in the subsequent sections of this thesis.

1.3. Simultaneous Heat and Moisture Exchange in LAMEEs

In this thesis, it is assumed LAMEEs are isolated from the environment, and thus heat and moisture exchange occurs only between the two streams flowing inside the LAMEEs, and not between the streams and the environment. Figure 1.3 presents a schematic showing simultaneous heat and moisture exchange between two adjacent channels of a LAMEE. The air stream enters the exchanger at temperature $T_{air,in}$ $(°C)$ and humidity ratio $W_{air,in}$ (kg/kg) , and solution stream enters the exchanger at the temperature $T_{sol,in}$ $(°C)$ and salt concentration $X_{sol,in}$ $(\%)$. As a result of heat and moisture exchange between the streams inside the LAMEE, the temperature and humidity ratio of the air stream change to $T_{air,out}$ and $W_{air,out}$ at the outlet, and temperature and humidity ratio of the solution stream change to $T_{sol,out}$ and $X_{sol,out}$ at the outlet.

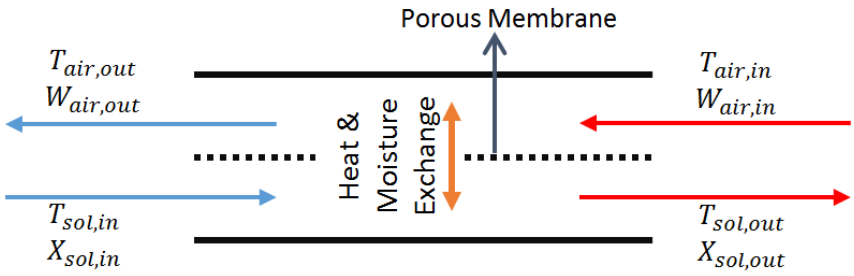

Figure 1.3 Schematics of simultaneous heat and moisture exchange between two adjacent channels of a LAMEE

The difference between the concentrations (densities) of water vapor on each side of the membrane is the driving potential for the moisture exchange between the streams in LAMEEs.

Mass exchange through the porous membrane (water vapor exchange in LAMEEs, since the porous membranes of LAMEEs are impervious to liquid water under normal operating pressures) is governed by Fick's law of diffusion. Fick's law, in its one-dimensional form, is stated as [8]

$$\dot{m}_B{''}_x = -\rho D \frac{d(\frac{\rho_B}{\rho})}{dx} \tag{1.11}$$

where $\dot{m}_B{''}_x$ $(kg/s \cdot m^2)$ is the local mass flux density of component B in the x direction (e.g. normal to the porous membrane in Figure 1.2), D (m^2/s) is the local diffusivity of the material through which mass transfer is occurring (e.g. the water vapor diffusivity of the porous membrane in Figure 1.2), the ratio ρ_B/ρ is the local concentration of the component B (e.g. humidity ratio on each side of the porous membrane in Figure 1.2), and ρ (kg/m^3) is the local density of the matter. Comparing Eq. (1.11) with Eq. (1.1), it becomes clear that Fick's law of diffusion is analogous to the Fourier's law of heat conduction, and thus there is an analogy between heat transfer and mass transfer. This analogy is encountered several times in this thesis and thus it is important to note it.

Researches have used experimental studies ([9], [10], [11] and [12]), numerical models ([13], [14] and [15]), neural network models ([16] and [17]), or simplified iterative-analytical models ([11]) were developed to determine the performance of LAMEEs. In particular, Vali [13] and Seyed-Ahmadi [14], respectively developed numerical models for steady-state and transient performance of LAMEEs. Zhang developed an iterative-analytical solution for a simplified steady-state model of the coupled heat and moisture exchange in hollow fiber membrane contactors (HFMCs) [18]. Zhang's solution was later extended to LAMEEs by Ge et al [11]. It should be noted that in some cases, the effectiveness of LAMEEs may exceed 100%, because the maximum

possible heat or moisture exchanger rates are not fully defined. However, calculating the maximum possible values for heat and moisture exchange in LAMEEs is out of the scope of this thesis.

1.4. Thesis Objectives and Overview

Although Ge's extension of the simplified analytical model of Zhang to LAMEEs and the numerical models of Vali and Seyed-Ahmadi provide accurate predictions for the performance of LAMEEs for summer air-conditioning applications, neither of the models directly provide an insight into how the performance of LAMEEs is affected by different design parameters and operating conditions. Furthermore, using these models for the initial stages of design and sizing of LAMEEs requires substantial programming to implement the models in the form of executable applications/modules that can be used by designers.

In contrast to LAMEEs, the initial design and sizing of heat exchangers, is quite straightforward. A method that is widely used for analysis of heat exchangers is the standard $\epsilon - NTU$ (effectiveness-NTU) model. This model expresses the performance of heat exchangers in terms of the two dimensionless parameters heat capacity rate ratio Cr and number of transfer units NTU [7]. Design of heat exchangers using this model is very simple and the relationship between the performance of heat exchangers and the dimensionless parameters NTU and Cr is quite straight forward: effectiveness increases with NTU and decreases with Cr. It would not be far from truth to state that if the standard $\epsilon - NTU$ model was directly applicable to LAMEEs, it would become the sole model that would be used in the initial stages of design and sizing of LAMEEs. However, as a result of the coupling between heat and moisture exchange, the standard $\epsilon - NTU$ model is not directly applicable to LAMEEs. The purpose of thesis, in short, is to extend the application of standard $\epsilon - NTU$ model to LAMEEs. To achieve this purpose, the two major objectives of this MSc. thesis are as follows:

1. To correlate the heat and moisture effectiveness of isolated counter-flow LAMEEs, i.e. LAMEEs isolated such that heat and moisture exchange with the environment is prevented, to a set of new dimensionless parameters using models that are analogous to the standard $\epsilon - NTU$ model.

2. To use models analogous to the standard $\epsilon - NTU$ model to predict the change in the temperature and moisture content of the air stream inside isolated counter-flow LAMEEs as a function of the inlet operating conditions of the air and solution streams and the LAMEEs' design parameters (i.e. geometric ratios and material properties).

The listed objective are achieved, respectively, in the following research manuscripts

1. H. Kamali, G. Ge, R. W. Besant, C. J. Simonson, "Extension of the Concepts of Heat Capacity Rate Ratio and Effectiveness-NTU Model to the Coupled Heat and Moisture Exchange in Liquid-to-Air Membrane Energy Exchangers," to be submitted to *ASME Journal of Heat Transfer*

2. H. Kamali, R. W. Besant, C. J. Simonson, "Estimating Changes in the Temperature and Humidity Ratio of the Air Stream inside Liquid-to-Air Membrane Energy Exchangers using Analogs of the Effectiveness-NTU Model," to be submitted to *ASME Journal of Heat Transfer*

The 1st manuscript composes Chapter 2 and is concerned with achieving the 1st objective, i.e. development of the relevant dimensionless parameters and the models analogous to the standard $\epsilon - NTU$ model for counter-flow LAMEEs. The 2nd manuscript composes Chapter 3 and is concerned with achieving the 2nd objective, i.e. using the models developed in Chapter 2 to predict the change in the temperature and moisture content of the air stream inside isolated counter-flow

LAMEEs. Finally, a summary of the conclusions of this thesis and possibilities for future research compose Chapter 4.

Chapter 2

Extension of the Concepts of Heat Capacity Rate Ratio and $\epsilon - NTU$ Model to LAMEEs

2.1. Overview of Chapter 2

In this chapter, two new dimensionless parameters (effective heat capacity rate ratio, Cr_e, and effective mass flow rate ratio, m_e^*) are developed and introduced as the extensions of the concept of the dimensionless parameter heat capacity rate ratio Cr for the coupled heat and moisture exchange in LAMEEs. Furthermore, analytical derivations of some extended versions of the standard $\epsilon - NTU$ model are presented in this chapter. These derivations are concluded by proposing simplified-extended $\epsilon - NTU$ and $\epsilon_m - NTU_m$ models as the analogs to the standard $\epsilon - NTU$ model which are applicable to the coupled heat and moisture exchange in LAMEEs under certain conditions. Finally, the applicability of the simplified-extended $\epsilon - NTU$ and $\epsilon_m - NTU_m$ models is verified using previously published experimental data for a small-scale LAMEE and a hollow fiber membrane contactor. It is demonstrated that for these experimental data points, the simplified-extended $\epsilon - NTU$ and $\epsilon_m - NTU_m$ models can be used to correlate the effectiveness of LAMEEs for heat exchange ϵ_s to the dimensionless parameters number of transfer units NTU and Cr_e and correlate the effectiveness of LAMEEs for moisture exchange ϵ_m to the dimensionless parameters number of moisture transfer units NTU_m and m_e^*, respectively. That is, for LAMEEs, $\epsilon_s = f(NTU, Cr)$ and $\epsilon_m = f(NTU_m, m_e^*)$. Thus, the 2nd chapter is dedicated to achieving the 1st objective of this thesis, which was to correlate the heat and moisture effectiveness of isolated counter-flow LAMEEs to a set of dimensionless parameters using models that are analogous to the standard $\epsilon - NTU$ model. The theories were developed and the manuscript #1

was written by the author of this thesis (Houman Kamali), and the co-authors (Gaoming Ge, Robert W. Besant and Carey J. Simonson) provided feedback on the research and on the manuscript #1.

Manuscript #1: H. Kamali, G. Ge, R. W. Besant, C. J. Simonson, "Extension of the Concepts of Heat Capacity Rate Ratio and Effectiveness-NTU Model to the Coupled Heat and Moisture Exchange in Liquid-to-Air Membrane Energy Exchangers," to be submitted to *ASME Journal of Heat Transfer*

2.2. Summary

Background: The heat and moisture exchange between the air and liquid desiccants inside liquid-to-air membrane energy exchangers (LAMEEs) are coupled. As a result, the effectiveness of LAMEEs, for sensible energy and moisture exchange, is strongly dependent on the inlet operating conditions, i.e. temperatures and humidity ratios, of the air and solution streams. The main objective of this paper is to provide a simple-to-understand explanation for this dependency.

Method of approach: First, extended versions of the effectiveness-NTU model are analytically derived. Then, these extended versions are simplified and are proposed as analogs to the effectiveness-NTU model that can be used for analysis of LAMEEs. These analogs are denoted simplified-extended effectiveness models and correlate the effectiveness of LAMEEs for sensible energy exchange to dimensionless parameters number of transfer units and effective heat capacity rate ratio, and correlate the effectiveness of LAMEEs for moisture exchange to dimensionless parameters number of moisture transfer units and effective mass flow rate ratio. The inlet and outlet operating conditions of the streams are needed to calculate the effective heat capacity rate ratio and effective mass flow rate ratio.

Results: The simplified-extended effectiveness models are used to estimate the effectiveness of LAMEEs for some previously published experimental data on LAMEEs. The results show that the maximum discrepancy between the estimated effectiveness values and the measured effectiveness values does not exceed 16%. For comparison, the estimations provided by the standard effectiveness-NTU model can differ from the measured effectiveness values by more than 45%.

Conclusions: The number of heat transfer units and number of moisture transfer units for LAMEEs, as defined in this paper, are independent of the operating conditions and the simplified-extended effectiveness models are identical in form to the standard effectiveness-NTU model. Thus, for the experimental data considered in this paper, the dependency of the effectiveness of LAMEEs on the inlet operating conditions can be correlated to the dependency of the effective heat capacity rate ratio and effective mass flow rate ratio on the inlet operating conditions. Equivalently, it can be stated that the considered LAMEEs operate analogously to a heat exchanger for which the heat capacity rate ratio is dependent on the inlet operating conditions.

Keywords: coupled heat and moisture exchange, effectiveness-NTU, heat capacity rate ratio, mass flow rate ratio, LAMEE

2.3. Abstract

In this paper, as a first step toward extending the application of the standard effectiveness-NTU model to the coupled heat and moisture exchange in liquid-to-air membrane energy exchangers (LAMEEs), two new dimensionless parameters are introduced as analogs of heat capacity rate ratio Cr: effective heat capacity rate ratio (effective Cr) and effective mass flow rate ratio (effective m*). It is demonstrated that models analogous to the standard effectiveness-NTU

model can be used to correlate the dependency of the effectiveness of LAMEEs on the inlet operating conditions of the air and solution streams to effective Cr and effective m*.

2.4. Introduction

A recent assessment by Intergovernmental Panel on Climate Change expects that the energy demand for residential air conditioning in summer will increase more than 30 times in this century, "from nearly 300 TWh in 2000, to about 4,000 TWh in 2050 and more than 10,000 TWh in 2100", while, comparatively, energy demand for heating in winter is expected to increase only slightly [19]. To sustain this increase in air conditioning energy demand, more efficient HVAC equipment should be developed. Desiccant air conditioning systems have the potential to significantly reduce energy demand for air conditioning in summer for most non-desert climate zones, where sensible heat ratio (SHR), the ratio of sensible to total cooling demand, is between 0.4 to 0.7 [20]. This is because for small SHRs, these desiccant air conditioning systems can meet the latent cooling load and achieve the desired dehumidification without overcooling and reheating the air [5]. In particular, liquid-to-air membrane energy exchangers (LAMEEs) can be used to design liquid desiccant air conditioning (LDAC) systems, that, with a proper control strategy, can operate with SHRs are as low as 0.3 to 0.5 under different operating conditions [21].

LAMEEs are composed of adjacent rectangular air and solution channels, and have a geometric design similar to counter-flow flat plate heat exchangers. LAMEEs enable simultaneous heat and moisture exchange between air and liquid desiccant streams through porous membranes that are permeable to vapor, but are impermeable to liquids under normal operating pressures of LAMEEs (~1 atm). Figure 2.1 presents a simplified schematic of a single-panel counter-flow LAMEE [22], where L and H are the length and height of the channels, respectively, and d_{sol} and d_{air} are the widths of the solution and air channels, respectively. In Figure 2.1, one air channel is

between two solution channels and hence the LAMEE shown is a single-panel LAMEE [22], however, depending on the design, many adjacent pairs of air and solutions channels might exist in a larger-scale LAMEE [10]. Solutions used in LAMEEs are liquid desiccants that are able to store and transfer heat and water. Two common types of liquid desiccants are aqueous solutions of Lithium Chloride ($LiCl$) and Magnesium Chloride ($MgCl_2$).

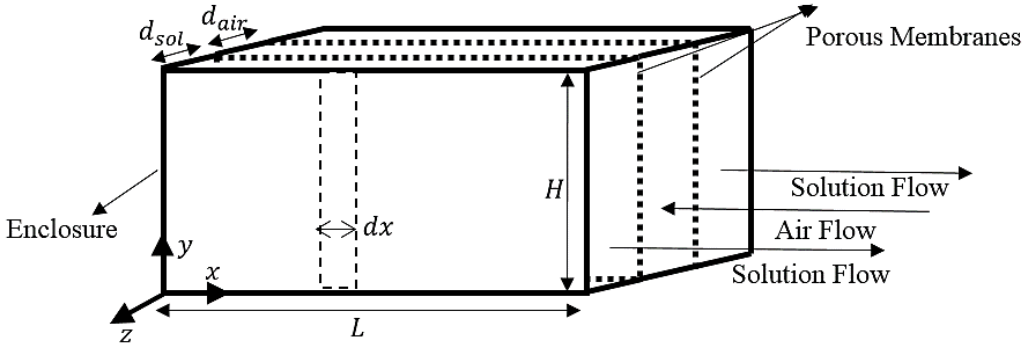

Figure 2.1 Schematics of a counter-flow single-panel LAMEE with an air channel and two adjacent solution channels. Hdx represents a differential area of a membrane, through which heat and moisture are exchanged between two adjacent air and solution streams.

Since LAMEEs enable simultaneous heat and moisture exchange between the air and solution streams, two different effectiveness concepts can be defined to quantify their performance: sensible heat exchange effectiveness ϵ_S and moisture exchange effectiveness ϵ_m, which quantify the effectiveness of LAMEEs for changing temperature and humidity ratio of the air stream. In this paper, it is assumed that heat capacity rate of the solution stream is higher than that of the air stream ($C_{air} = C_{min}$), and following the conventions of ASHRAE standard 84-2013 [8], the effectiveness equations are defined as follows

$$\epsilon_s = \frac{actual\ sensible\ energy\ transfer}{inlet\ potential\ for\ heat\ transfer} = \frac{T_{air,out} - T_{air,in}}{T_{sol,in} - T_{air,in}} \tag{2.1}$$

$$\epsilon_m = \frac{actual\ moisture\ transfer}{inlet\ potential\ for\ moisture\ transfer} = \frac{W_{air,out} - W_{air,in}}{W_{sol,in} - W_{air,in}} \quad (2.2)$$

Subscripts air and sol refer to the air and solution streams, respectively. Subscripts in and out refer to the respective inlets and outlets of each stream. T $(°C)$ refers to the bulk temperature of a either the air or solution stream. W_{air} (g_{water}/kg_{air}) refers to the bulk humidity ratio of the air stream and W_{sol} (g_{water}/kg_{air}) refers to the equilibrium humidity ratio of the solution stream, which indicates the equilibrium humidity ratio of the air at the solution-air interface.

Several prototypes of LAMEEs, with different configurations and dimensions, have been developed and tested experimentally to investigate the performance of LAMEEs under various operating conditions [11], [23], [22] and [10]. To theoretically evaluate the performance of LAMEEs, a numerical model for transient heat and moisture transfer in LAMEEs was developed by Seyed-Ahmadi [14]; however this numerical model was too slow to be used for hourly energy analysis [17]. Later, Zhang developed an iterative analytical solution for heat and moisture transfer in hollow fiber membrane contactors [18], which was extended to LAMEEs by Ge [11]. Compared to the numerical model, this analytical model was fast enough to be used in hourly energy analysis [21]. Akbari et al. also developed a fast Neural Network model to replicate the numerical model developed by Ahmadi et al. for LAMEEs [17]. These models are suitable for academic research, but they do not directly provide an intuitive understanding into why ϵ_s and ϵ_m of LAMEEs are dependent on inlet operating temperatures and humidity ratios of the streams.

A widely used model for analysis and calculating effectiveness of heat exchangers that can be used to intuitively evaluate their performance, is the standard $\epsilon - NTU$ model, which expresses ϵ_s of heat exchangers in terms of the dimensionless parameters: number of transfer units NTU and

heat capacity rate ratio Cr. For example, for heat exchangers with counter-flow arrangements, which is the flow arrangement exclusively considered in this paper, one can obtain [24]

$$\epsilon_s = \frac{1 - \exp[-NTU\ (1 - Cr)]}{1 -\ Cr\ \exp[-NTU\ (1 - Cr)]} \tag{2.3}$$

Models for simultaneous heat and moisture exchangers have depended on whether the heat and moisture exchange are coupled or uncoupled. For the case of coupled heat and moisture exchange in rotating energy wheels, Simonson and Besant [25] and [26] correlated ϵ_s and ϵ_m to the pairs of governing dimensionless parameters NTU and Cr and NTU_m and m^*. Number of moisture transfer units NTU_m and mass flow rate ratio m^* are dimensionless parameters analogous to NTU and Cr, but for mass exchange. However, as result of the coupling between heat and moisture exchange in the energy wheels, the correlations of Simonson and Besant were functions of the operating conditions. In contrast, for the case uncoupled heat and moisture exchange in air-to-air energy exchangers, Zhang and Niu later demonstrated [27] that ϵ_s and ϵ_m can be estimated as a function of the pairs of dimensionless parameters NTU and Cr and NTU_m and m^*, using correlations that are not dependent on the operating conditions. For LAMEEs, as is the case for energy wheels, heat and moisture exchange are coupled and thus it is not possible to use correlations that are independent of the operating conditions to estimate ϵ_s and ϵ_m of LAMEEs as a function of the pairs of dimensionless parameters NTU and Cr and NTU_m and m^*.

An approach that has been adapted for evaluating performance of equipment with coupled heat and moisture exchanger, is to use the enthalpy difference between the air stream and the solution stream as the driving potential for energy exchange between the streams [28] and [29, pp. 6.9-6.13]. However, the shortcomings and the complexities associated with this approach [30] do

not align with the main motivation behind this study, namely, providing simple-to-understand methods for evaluating performance, i.e. for calculating ϵ_s and ϵ_m, of LAMEEs in terms of a number of dimensionless parameters.

In this paper, the already established concepts of Cr and m^* are used to define two dimensionless parameters: effective heat capacity rate ratio Cr_e and effective mass flow rate ratio m_e^*, per Eq. (2.5) and Eq. (2.9). Then, it will demonstrated that if Cr_e is used instead of Cr, it can be possible to correlate ϵ_s to NTU and Cr_e using a correlation identical in form to the standard $\epsilon - NTU$ model, with the difference between the temperatures of the streams acting as the driving potential for sensible energy exchange. This correlation is denoted the simplified-extended $\epsilon - NTU$ model, presented by Eq. (2.37). The dimensionless parameter Cr_e quantifies the ratio between the total changes in the temperatures of the solution streams across the exchanger and represents the same ratio for LAMEEs that Cr represents for heat exchangers

$$Cr = \frac{C_{air}}{C_{sol}} \tag{2.4}$$

$$Cr_e = -\frac{T_{sol,out} - T_{sol,in}}{T_{air,out} - T_{air,in}} \tag{2.5}$$

where C_{air} (W/K) and C_{sol} (W/K) are the heat capacity rates of the air and solution streams, defined as

$$C_{air} = \left(c_p \dot{m}\right)_{air} \tag{2.6}$$

$$C_{sol} = \left(c_p \dot{m}\right)_{sol} \tag{2.7}$$

where c_p $(J/kg \cdot K)$ and $\dot{m}$ (kg/s) are specific heat capacity rate and the mass flow rate of either of the streams. Similarly, it will demonstrated that if m_e^* is used instead of m^*, it can be possible to correlate ϵ_m to NTU_m and m_e^* using a correlation identical in form to the standard $\epsilon -$

NTU model, with the difference between the humidity ratio of the streams acting as the driving potential for moisture exchange (and the associated latent energy exchange). This correlation is denoted the simplified-extended $\epsilon_m - NTU_m$ model, presented by Eq. (2.42). m_e^* quantifies the ratio between the total changes in the humidity ratios of the streams across the exchanger and represents the same ratio for LAMEEs that m^* represents for air-to-air energy exchangers

$$m^* = \frac{\dot{m}_{air}}{\dot{m}_{sol}} \tag{2.8}$$

$$m_e^* = -\frac{W_{sol,out} - W_{sol,in}}{W_{air,out} - W_{air,in}} \tag{2.9}$$

To validate the simplified-extended models for LAMEEs, previously published experimental studies on a small-scale LAMEE [23] and [22] and also a hollow fiber membrane contactor [18] are used. Cr_e and m_e^* are calculated for each experimental data point based on the measured inlet and outlet operating conditions, and then the simplified-extended models are used to estimate ϵ_s and ϵ_m for each corresponding experiment. The results show that for some typical summer operating conditions, for which experimental data were available, the discrepancy between the estimated and the experimentally measured values of ϵ_s and ϵ_m is less than 10% on average and the ϵ_s and ϵ_m can be correlated to the dimensionless parameters NTU, Cr_e, NTU_m and m_e^*.

As a final note, it should be emphasized that, in this paper, both the inlet and outlet operating conditions were used to calculate Cr_e and m_e^* for each experiment. Furthermore, because of the coupling between heat and moisture exchange, ϵ_s and ϵ_m of LAMEEs are not bounded between 0 and 1 for all the operating conditions, and the simplified-extended models are not directly applicable to such operating conditions. The objective of this paper, hence, is limited to demonstrating that if, at all, it is possible to use the simplified-extended models to estimate ϵ_s and

ϵ_m of LAMEEs for some typical operating conditions for which ϵ_s and ϵ_m are bounded between 0 and 1. The validation of this possibility is imperative to further investigations which can e.g. lead to methods for estimating Cr_e and m_e^* from the inlet operating conditions and the design parameters.

2.5. The Governing Equations of LAMEEs

A thorough discussion on the governing equations of LAMEEs can be found in either [31] or [14]. Here, a short summary of the most important equations is provided, which can be derived following a number of simplifying assumptions, including those presented in Table 2.1 [31], [14] and [32].

Table 2.1 Major assumptions used to simplify the governing equations of LAMEEs

1) Exchangers are operating in steady-state conditions.
2) Fluid properties are uniform along the height of the exchanger.
3) Heat and mass exchange occurs only between the two streams through the membranes.
4) Heat and moisture transfer occur only in the direction normal to the membranes.
5) Deflection of the porous membranes and flow mal-distributions are negligible.
6) Overall heat and mass transfer coefficients are constant inside LAMEEs.
7) Mass flow rates and heat capacity rates of the flows are constant inside LAMEEs.

Neglecting edge effects (assumption 2 in Table 2.1), the differential sensible energy transfer rate $dq_S\ (W)$ and the differential moisture transfer rate $d\dot{m}_W\ (kg/s)$ can be expressed as

$$dq_S = L\ H\ U\ (T_{sol} - T_{air})_l\ dl \tag{2.10}$$

$$d\dot{m}_W = L\ H\ U_m\ (W_{sol} - W_{air})_l\ dl \tag{2.11}$$

where $H\ (m)$ and $L\ (m)$ are height and length of a channel, l is the dimensionless position along the length of the exchanger

$$l = \frac{x}{L} \tag{2.12}$$

and U $(W/K \cdot m^2)$ and $U_m(kg/s \cdot m^2)$ are the overall heat and moisture transfer coefficients, respectively.

Defining the heat conduction resistance HCR $(K \cdot m^2/W)$ and the vapor diffusion resistance VDR (s/m) of the membrane as follows

$$VDR = \frac{\delta}{D_{vm}} \tag{2.13}$$

$$HCR = \frac{\delta}{k} \tag{2.14}$$

then, U and U_m can be calculated as [14]

$$U = \left(HCR + \frac{1}{h_{air}}\right)^{-1} \tag{2.15}$$

$$U_m = \rho_{air}\left(VDR + \frac{1}{h_{m,air}}\right)^{-1} \tag{2.16}$$

where h $(W/K \cdot m^2)$ is the convective heat transfer coefficient, δ (m) is the thickness of the membrane, k $(W/K \cdot m)$ is the thermal conductivity of the membrane, D_{vm} (m^2/s) is the diffusivity coefficient of vapor through the membrane, ρ_{air} (kg/m^3) is the density of dry air, and h_m (m/s) is the convective mass transfer coefficient for air. Since the diffusivity coefficient of vapor in water and the thermal conductivity of the desiccant solutions are an order of magnitude larger than those of the air [33] and [34], it is assumed that the solution side contributes little to the overall resistance to heat and mass transfer. Convective heat and mass transfer coefficients can be calculated from the following definitions for Nusselt number Nu and Sherwood number Sh,

and their correlations are a function of the dimensionless parameters Reynolds number Re, Prandtl number Pr, Schmidt number Sc, and the flow channel geometry ratios

$$Nu = \frac{hD_h}{k_{air}} \tag{2.17}$$

$$Sh = \frac{h_m D_h}{D_{va}} \tag{2.18}$$

where D_h (m) is the hydraulic diameter of the air channel, k_{air} is the thermal conductivity of the air, and D_{va} is the diffusivity coefficient of air. In this study, to calculate the Sherwood number, it is assumed that the analogy between heat and mass transfer is applicable and the Lewis relationship can be used as follows [35]:

$$h_m \cong \frac{h}{\rho_{air}\, c_{p,air}} \tag{2.19}$$

Zhang et al. [36] and Haung et al. [37] have investigated values of Nu and Sh numbers for coupled heat and moisture transfer in, respectively, hollow fiber membrane modules and membrane parallel-plate channels for laminar flows. For the cases they studied, the Lewis relationship was not exactly applicable, but it was approximately valid. This is because, for laminar flows, the Nusselt number and analogously the Sherwood number, are strongly dependent on heat and mass transfer boundary conditions. However, for turbulent flow, this dependency is weak [32, p. 446] and the Lewis relationship is applicable [35]. Assuming that the overall heat and mass transfer coefficients are constant (assumption 6 in Table 2.1), the total sensible energy exchange rate and moisture exchange rate can be calculated as

$$q_S = n\, L\, H\, U \int_0^1 (T_{sol} - T_{air})_1\, dl = A\, U \int_0^1 (T_{sol} - T_{air})_1\, dl \tag{2.20}$$

$$\dot{m}_W = n\,L\,H\,U_m \int_0^1 (W_{sol} - W_{air})_l\, dl = A\,U_m \int_0^1 (W_{sol} - W_{air})_1\, dl \tag{2.21}$$

where n is total number of membrane sheets and A (m^2) is total area of the membranes.

2.5.1. Mass balance in LAMEEs

Assuming no mass exchange with the environment (assumption 3 in Table 2.1), the principle of conservation of mass can be used to express the ideal mass balance equation for LAMEEs as

$$\frac{d\dot{m}_{air}}{dl} = \frac{d\dot{m}_{sol}}{dl} = \frac{d\dot{m}_W}{dl} \tag{2.22}$$

where $\dot{m}_{air}$ (kg/s) and $\dot{m}_{sol}$ (kg/s) are mass flow rates of the moist air and solution streams, respectively. In terms of the change in the humidity ratio of the air stream, mass balance results in

$$\frac{dW_{air}}{dl} = \frac{1}{\dot{m}_{air}} \frac{d\dot{m}_W}{dl} \tag{2.23}$$

where it has been assumed that the mass flow rate of the dry air is nearly equal to that of the moist air, because, for air conditioning applications, W_{air} is typically less than $0.04\ kg/kg$ and the percentage changes in $\dot{m}_{air}$ are nearly two orders of magnitude smaller than the percentage changes in W_{air}.

2.5.2. Energy Balance in LAMEEs

Assuming that the air stream inside a LAMEE is heated or cooled only as result of sensible heat exchange with the solution stream (assumption 3 in Table 2.1), and neglecting the moisture content of the air (since $W_{air} \leq 0.04\ kg/kg$ for most air-conditioning applications), the energy balance for the air stream can be stated as

$$\frac{dq_{s,air}}{dl} = C_{air}\frac{dT_{air}}{dl} = \frac{dq_S}{dl} \tag{2.24}$$

However, the temperature of the solution stream not only changes as a result of heat exchange with the air stream, but also as a result of release/absorption of the phase change energy associated with the moisture exchange between the streams. This is because the membranes in LAMEEs, under normal operating pressures ($\sim 1\ atm$), are permeable only to vapor. Therefore, for air dehumidification, first vapor transfers to the solution stream and then condenses there. Similarly, for air humidification, water evaporates from the solution stream and then transfers as vapor to the air stream. The released/absorbed phase change energy is nearly equal to the latent heat transfer rate to the air stream $q_L\ (W)$. Thus, the energy balance for the solution stream can be stated as

$$\frac{dq_{s,sol}}{dl} = C_{sol}\frac{dT_{sol}}{dl} = \left(\frac{dq_s}{dl} + \frac{dq_L}{dl}\right) \tag{2.25}$$

where

$$\frac{dq_L}{dl} = \mathrm{h_{fg}}\frac{d\dot{m}_W}{dl} \tag{2.26}$$

and $h_{fg}\ (J/kg)$ is the specific heat of evaporation of water. Thus, the ideal energy balance equation in LAMEEs can be expressed as

$$C_{air}\frac{dT_{air}}{dl} + C_{air}\frac{h_{fg}}{c_{p,air}}\frac{dW_{air}}{dl} = C_{sol}\frac{dT_{sol}}{dl} = \frac{dq_s}{dl} + \frac{dq_L}{dl} \tag{2.27}$$

2.5.3. Properties of Salt Solutions

Given the total pressure $P\ (Pa)$ and partial water vapor pressure $P_v\ (Pa)$ at an air-solution interface, the equilibrium humidity ratio of the solution W_{sol}, which in fact indicates the equilibrium humidity ratio of the air adjacent to the solution, can be calculated as [35]

$$W_{sol} = \frac{0.622 P_v}{P - P_v} \tag{2.28}$$

In this paper, correlations for P_v and other properties of ordinary water were obtained from ASHRAE Fundamentals [35]. P_v of a salt solution is a function of the salt type, and also concentration X_{sol} and temperature of the salt solution T_{sol}, as follows

$$P_v(\text{salt solution}) = f(salt, T_{sol}, X_{sol}) \tag{2.29}$$

where the concentration of the salt solution is defined as the ratio between the mass (flow rate) of the dry salt $\dot{m}_{salt}$ (kg/s) and mass (flow rate) of the solution $\dot{m}_{sol}$ (kg/s)

$$X_{sol} = \frac{\dot{m}_{salt}}{\dot{m}_{sol}} \tag{2.30}$$

To obtain P_v and other properties of $LiCl$ and $MgCl_2$ salt solutions, the correlations developed by Conde [33], Cisternas and Lam [38], and Zaytsev and Aseyev [34] have been used in this paper. In this paper, it has been assumed that the air adjacent to the solution stream is at standard atmospheric pressure (at zero altitude) in addition to the partial vapor pressure, i.e. it has been assumed that $P - P_v = 101.325\, kPa$. The contribution of pumping pressure to the total pressure is not insignificant in the typical applications of LAMEEs, or otherwise it should have been considered as well. Equilibrium humidity ratio curves for $LiCl$ and $MgCl_2$ desiccant solutions at typical concentrations encountered in LAMEEs are shown in Figure 2.22.

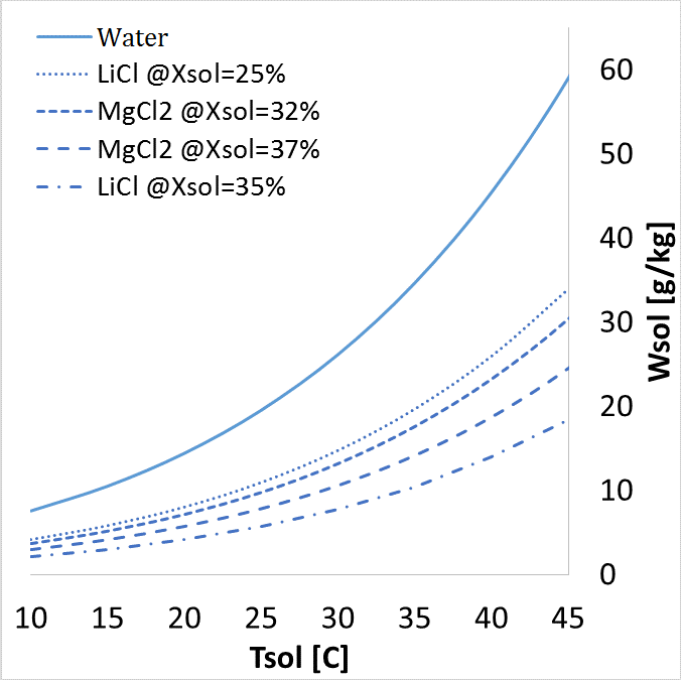

Figure 2.2 Equilibrium Humidity ratio curves of $MgCl_2$ and $LiCl$ desiccant solutions at select concentrations

2.6. Development of the Extended $\epsilon - NTU$ and $\epsilon_m - NTU_m$ Models

In this section, an extended $\epsilon - NTU$ model is presented that expresses ϵ_s as a function of three dimensionless parameters: average differential effective heat capacity rate ratio $\overline{dCr_e}$, effective heat capacity rate ratio Cr_e, and number of transfer units NTU. This extended $\epsilon - NTU$ model can be simplified to the standard $\epsilon - NTU$ model if $\overline{dCr_e}$ and Cr_e are both equal to the heat capacity rate ratio Cr, as is the case for heat exchangers. An extended $\epsilon_m - NTU_m$ model is also presented, which expresses ϵ_m as a function of three dimensionless parameters: average differential effective mass flow rate ratio $\overline{dm_e^*}$, effective mass flow rate ratio m_e^*, and number of moisture transfer units NTU_m. Then, simplified-extended $\epsilon - NTU$ and $\epsilon_m - NTU_m$ models are developed, which express heat transfer effectiveness as a function of NTU and Cr_e and moisture transfer effectiveness as function of NTU_m and m_e^*. The constraints that limit validity of these models are also discussed. The process of obtaining the simplified-extended effectiveness models

is a methodical procedure that follows from the extended effectiveness models and avoids potential errors that could occur if the simplifications were to be applied arbitrarily.

2.6.1. Extended $\epsilon - NTU$ model

An extended *ϵ-NTU* model can be developed, as presented in the appendix, which expresses sensible heat transfer effectiveness equation for a counter-flow exchanger as

$$\epsilon_s = \frac{T_{air,out} - T_{air,in}}{T_{sol,in} - T_{air,in}} = \frac{1 - \exp\left[-NTU\left(1 - \overline{dCr_e}\right)\right]}{1 - Cr_e \exp\left[-NTU\left(1 - \overline{dCr_e}\right)\right]} \tag{2.31}$$

where dCr_e is the differential effective heat capacity rate ratio and is calculated as

$$dCr_e = \left(\frac{dT_{sol}}{dT_{air}}\right)_l \tag{2.32}$$

and $\overline{dCr_e}$ is the average differential effective heat capacity rate ratio and is calculated as

$$\overline{dCr_e} = \int_0^1 dCr_e \tag{2.33}$$

and NTU is the number of heat transfer units for the air stream, defined as

$$NTU = \frac{UA}{C_{air}} \tag{2.34}$$

Eq. (2.31) is valid as long as long as $T_{sol,in} \neq T_{air,in}$, dCr_e is continuous and bounded, and NTU is constant along the exchanger. Since U is assumed to be constant and the variations in C_{air} are negligible, NTU can be assumed to be constant for LAMEEs. However, depending on the operating conditions, it is possible that T_{air} becomes equal to T_{sol} at some point along a LAMEE, in which case dCr_e will be discontinuous, since from Eq. (2.24) it can be observed that at such a point $dq_s/dl = 0$ and thus $dT_{air}/dl = 0$.

2.6.1.1.Simplified Extended $\epsilon - NTU$ Model

It is easy to verify that for heat exchangers $dCr_e = Cr_e = Cr$, and therefore Eq. (2.31) can be simplified to the standard $\epsilon - NTU$, that is a function of NTU and Cr, as expressed in Eq. (2.3). In contrast, for LAMEEs, using Eq. (2.27) one can verify that

$$dCr_e = Cr\left(1 + \frac{h_{fg}}{c_{p,air}}\frac{dW_{air}}{dl}\Big/\frac{dT_{air}}{dl}\right) = Cr\left[1 + \frac{h_{fg}}{c_{p,air}}\frac{NTU_m}{NTU}\left(\frac{W_{sol} - W_{air}}{T_{sol} - T_{air}}\right)_l\right] \tag{2.35}$$

Therefore, due to the coupling between heat and moisture transfer, it is difficult to make any assumptions with regard to the profile or value of dCr_e along a LAMEE. However, T_{air} is bounded between $T_{air,in}$ and $T_{air,out}$ as long as dCr_e is continuous along the exchanger (i.e. as along as $T_{sol} - T_{air} \neq 0$). As such, it is reasonable to assume that if the extended $\epsilon - NTU$ model is valid, T_{air} can be approximated as a linear function along the exchanger, and then

$$\overline{dCr_e} = \frac{1}{T_{air,in} - T_{air,out}}\int_0^1 \frac{dT_{sol}}{dl}dl = -\frac{T_{sol,out} - T_{sol,in}}{T_{air,out} - T_{air,in}} = Cr_e \tag{2.36}$$

$$\epsilon_s = \frac{1 - \exp[-NTU\,(1 - Cr_e)]}{1 - Cr_e\,\exp[-NTU\,(1 - Cr_e)]} \tag{2.37}$$

Comparing Eq. (2.37) with the standard $\epsilon - NTU$ model in Eq. (2.3), it is clear that the simplified-extended model has a form identical to that of the standard model and the only difference between the two is that the simplified-extended model is in terms of Cr_e and NTU instead of Cr and NTU.

2.6.2. Extended $\epsilon_m - NTU_m$ Model

The extended $\epsilon_m - NTU_m$ model, which is developed in the appendix, can be used to express the moisture transfer effectiveness for a counter-flow exchanger as

$$\epsilon_m = \frac{1 - \exp\left[-NTU_m \left(1 - \overline{dm_e^*}\right)\right]}{1 - m_e^* \exp\left[-NTU_m \left(1 - \overline{dm_e^*}\right)\right]} \tag{2.38}$$

where dm_e^* is the differential effective mass flow rate ratio, defined as

$$dm_e^* = \left(\frac{dW_{sol}}{dW_{air}}\right)_l \tag{2.39}$$

and $\overline{dm_e^*}$ is the average differential effective mass flow rate ratio, which is calculates as

$$\overline{dm_e^*} = \int_0^1 dm_e^* \, dl \tag{2.40}$$

and NTU_m is the number of moisture transfer units for the air side, defined as

$$NTU_m = \frac{U_m A}{\dot{m}_{air}} \tag{2.41}$$

Eq. (2.38) is valid as long as long as $W_{sol,in} \neq W_{air,in}$, dm_e^* is continuous and bounded, and NTU_m is constant along the exchanger. Since U_m is assumed to be constant and the variation in $\dot{m}_{air}$ along the exchanger is negligible, NTU_m can be assumed to be constant for LAMEEs. However, depending on the operating conditions, it is possible that W_{air} becomes equal to W_{sol} at some point along a LAMEE, in which case dm_e^* will be discontinuous.

2.6.2.1.Simplified Extended $\epsilon_m - NTU_m$ Model

Due to the coupling between heat and moisture transfer, and also because W_{sol} depends on both X_{sol} and T_{sol}, it is difficult to make any assumption with regards to the profile or value of dm_e^* along a LAMEE. However, assuming a linear profile for W_{air} along the exchanger, $\overline{dm_e^*}$ and m_e^* would be equal, and Eq. (2.38) can be simplified to

$$\epsilon_m = \frac{1 - \exp[-NTU_m \, (1 - m_e^*)]}{1 - m_e^* \exp[-NTU_m \, (1 - m_e^*)]} \tag{2.42}$$

Comparing Eq. (2.42) with the standard $\epsilon_m - NTU_m$ model, Eq. (2.43), it is clear that the simplified-extended model has a form identical to that of the standard model and the only difference is that the simplified-extended model is in terms of m_e^* and NTU_m instead of m^* and NTU_m.

2.6.3. Summary

In this section, the extended effectiveness $\epsilon_s - NTU$ and $\epsilon_m - NTU_m$ models were presented, per Eq. (2.31) and Eq. (2.38), which express ϵ_s and ϵ_m as functions of dimensionless parameters Cr_e, $\overline{dCr_e}$, NTU, m_e^*, $\overline{dm_e^*}$, and NTU_m. Then, the simplified-extended $\epsilon - NTU$ and $\epsilon - NTU_m$ models, collectively denoted the simplified-extended effectiveness models, were developed, per Eq. (2.37) and Eq. (2.42), which express sensible heat transfer effectiveness and moisture transfer effectiveness in terms of dimensionless parameters NTU, Cr_e, NTU_m and m_e^*. However, it was noted that in LAMEEs, depending on the operating conditions, dCr_e and dm_e^* might be undefined at some point along the exchanger and therefor the extended effectiveness models are not always valid. Moreover, in order to obtain the simplified-extended effectiveness models, it was necessary to adopt the assumptions that profiles of T_{air} and W_{air} can be approximated as linear functions of the position along the exchanger.

2.7. Results and Discussions

In this section, some experimental data presented for LAMEEs in the literature are used to verify that, despite the assumptions adopted to develop the simplified-extended $\epsilon - NTU$ and $\epsilon - NTU_m$ models, sensible heat transfer effectiveness and moisture transfer effectiveness of LAMEEs can be modelled in terms of dimensionless parameters NTU, Cr_e, NTU_m and m_e^* for some typical summer operating conditions. Experimental results previously published by Ghadiri Moghaddam

et al. [23], [22] for a small-scale LAMEE and also experimental results published by Zhang [18] for a hollow fiber membrane contactor are analyzed and used for verification.

2.7.1. Verification with Small-Scale LAMEE Experimental Data

The first two experimental datasets chosen for analysis are published by Ghadiri Moghaddam et al. [23] [22]. The LAMEE used in these experiments is composed of one air channel between two solution channels, similar to the design presented in Figure 2.12. To support the flexible membranes, a screen composed of rows of horizontal bars and columns of vertical bars is inserted inside the air channel. Dimensions of the small-scale LAMEE are presented in Table 2.2. In dataset M1 [23] $MgCl_2$ and $LiCl$ were used as the working fluid, while in dataset M2 [22] ordinary water was used as the working fluid. Each data point in datasets M1 and M2 represents the average between 5 experiments [23], and thus the uncertainties in the data points of datasets M1 and M2 due to the random errors in measurements are negligible.

Table 2.2 Dimensions of the small-scale LAMEE used in datasets M1 and M2

Dimension	**Value**
Exchanger length, $L\ (m)$	0.49
Exchanger aspect ratio, L/H	5.2
Air channel width, $d_{air}\ (mm)$	5
Solution channels width (each) , $d_{sol}\ (mm)$	0.8
Membrane thickness $d_m\ (mm)$	0.265

2.7.1.1.Dataset M1: Desiccant Solutions

Dataset M1 covers different operation modes of LAMEEs: cooling and dehumidification (C&D), cooling and humidification (C&H), heating and dehumidification (H&D) and heating and humidification (H&H), which refer to the air stream being cooled and dehumidified, and so on.

Inlet operating conditions for each mode are presented in Figure 2.3. Each operating mode is investigated at four different heat capacity rate ratios Cr of $1,\ 1/3,\ 1/5$ and $1/7$. In order to change the Cr, the mass flow rate of the solution stream was changed, while the mass flow rate of the air stream was kept constant, hence NTU and NTU_m are assumed to be the same for all of the experiments.

Initially, Ghadiri Moghaddam et al. assumed that $Nu = 8.24$ for the air channel [23], which is the value corresponding to fully developed laminar flow between two infinite parallel plates with constant heat flux on both walls [24]. However, due to the existence of the inserts, the flow inside the air channel of the small-scale LAMEE is best characterized as low-Reynolds-number turbulent flow [32, p. 432]. A later study by Oghabi et al. [39] experimentally investigated heat transfer in a flat-plate exchanger augmented with these inserts at different Reynolds number. Based on the studies by Oghabi et al., Ghadiri Moghaddam et al. published a subsequent paper [31] and reported 11.2 as the updated average Nusselt number for dataset M1. In the same paper [31], Ghadiri Moghaddam et al. also reported updated the values for water vapor diffusion resistance of the porous membrane used in the small-scale LAMEE. They concluded that the VDR of the membrane is closer to $24\ s/m$, rather than the originally reported value of $56\ s/m$. NTU and NTU_m calculated for dataset M1 using the originally reported values and also using the updated values of Nu_{air} and VDR are presented in Table 2.3.

Table 2.3 Variation of NTU and NTU_m for dataset M1 [23] [31]

$Nusselt$	8.24 (original **[23]**)		11.2 (updated **[31]**)	
NTU	3		3.8	
$VDR\ (s/m)$	56 (original [23])	24 (updated [31])	56 (original [23])	24 (updated [31])
NTU_m	1.7	2.5	1.9	2.9

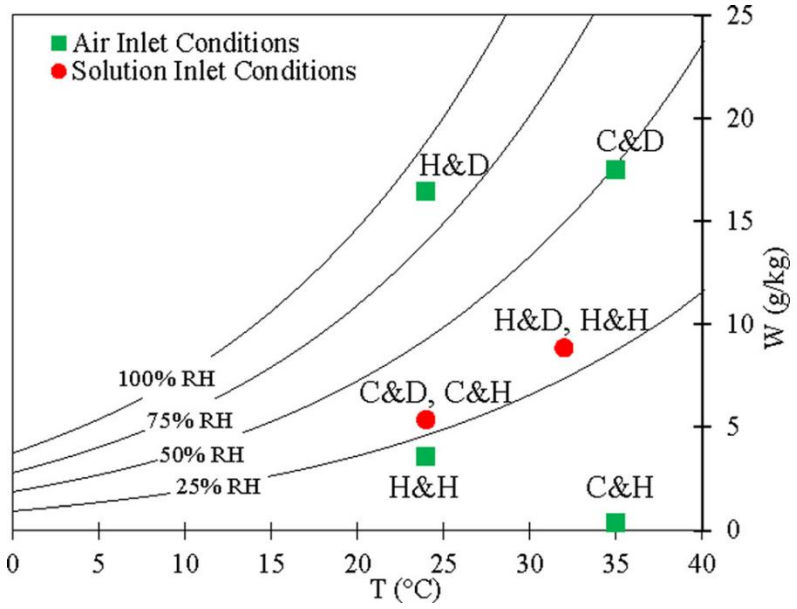

Figure 2.3 Inlet operating conditions of air and solution streams for dataset M1 [23]

2.7.1.1.1. Sensible Effectiveness

Figure 2.4(a) shows experimentally measured values of sensible effectiveness for dataset M1 plotted against Cr_e. In the same plot, effectiveness curves obtained using the simplified-extended $\epsilon - NTU$ model are presented for comparison. For the cooling modes, the maximum discrepancy between the values measured and the values estimated using the simplified-extended $\epsilon - NTU$ model is 12% at either $NTU = 3$ or $NTU = 3.8$. However, for the heating modes, the experimental data is consistently overestimated by the simplified-extended $\epsilon - NTU$ model and the maximum discrepancy is 15% at $NTU = 3.0$ and 19% at $NTU = 3.8$. Ghadiri Moghaddam

et al. cite the uncertainty in the sensible energy balance due to heat exchange with the environment as a reason for the lower heat transfer effectiveness in the heating modes [31], which is probable, since temperature of the solution in the heating modes is different than the room temperature ($T_{sol,in} = 32\ °C$ for the heating modes).

2.7.1.1.2. Moisture Transfer Effectiveness

Figure 2.4-(b) shows the experimental ϵ_m plotted against m_e^*. In the same plot, ϵ_m is estimated using the simplified-extended $\epsilon_m - NTU_m$ model, Eq. (2.42). Assuming that $NTU_m = 1.7$, the maximum discrepancy between the estimated values for ϵ_m and the experimental ϵ_m is 11% and the experimental data is underestimated by 4% on average. Assuming that $NTU_m = 2.9$, the maximum discrepancy increases to 17% and the experimental data is overestimated by 9% on average. It can be concluded that the actual NTU_m is possibly between 1.7 and 2.9. This conclusion is expected, because due to the maldistribution in LAMEEs, which in particular might be introduced by the bulging of the flexible membranes, the actual NTU and NTU_m values are expected to be different that those reported based on the assumption that there is no maldistribution.

(a) (b)

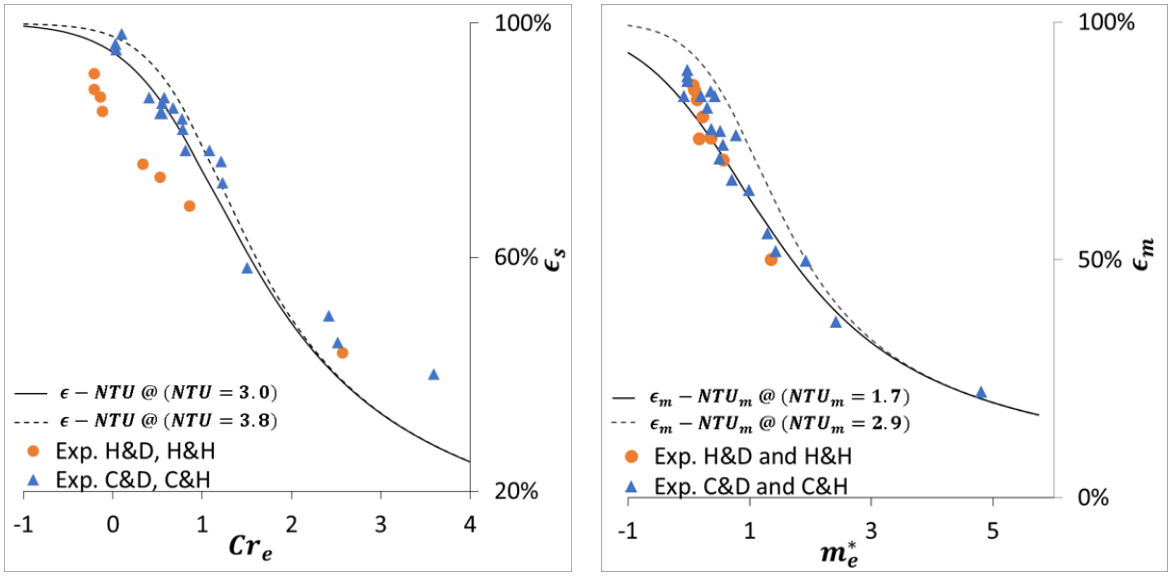

Figure 2.4 (a) heat exchange effectiveness ϵ_s and (b) moisture exchange effectiveness ϵ_m plotted against the dimensionless parameters Cr_e and m_e^* for the experiments of dataset M1, compared with the effectiveness curves obtained using the simplified-extended $\epsilon - NTU$ and $\epsilon_m - NTU_m$ models, Eq. (2.37) and Eq. (2.42), with NTU and NTU_m equal to the originally reported values of 3.0 and 1.7 [23], and also the updated values of 3.8 and 2.9 [31].

2.7.1.1.3. Standard $\epsilon - NTU$ and $\epsilon_m - NTU_m$ Models

To reemphasize the distinction between the standard effectiveness models and the simplified-extended models, assume that for LAMEEs, ϵ_s was a function of NTU and Cr instead of NTU and Cr_e, and ϵ_m was a function of NTU_m and m^* instead of NTU_m and m_e^*. That is, assume the standard $\epsilon - \text{NTU}$ and $\epsilon_\text{m} - \text{NTU}_\text{m}$ models, Eqs. (2.3) and (2.43), could model LAMEEs.

$$\epsilon_m = \frac{1 - \exp[-NTU_m\,(1 - m^*)]}{1 - m^*\,\exp[-NTU_m\,(1 - m^*)]} \tag{2.43}$$

To verify these propositions, consider Figure 2.5(a) and Figure 2.5(b), where the experimental ϵ_s and ϵ_m for dataset M1 are plotted against Cr and m^*, respectively. The reader should be reminded that NTU and NTU_m are the same for all the experiments in dataset M1. As

evident, the standard $\epsilon - \text{NTU}$ and $\epsilon_m - \text{NTU}_m$ models cannot account for the variations in the experimental ϵ_s and ϵ_m among different operating modes. In fact, since at each Cr the effectiveness values vary significantly depending on the operating conditions, it can be concluded that the pair Cr and NTU are not the preferred governing dimensionless parameters for heat transfer in LAMEEs. Similarly, it can be concluded that the pair m^* and NTU_m are not the preferred governing dimensionless parameters for moisture transfer in LAMEES. This is an important distinction between LAMEEs and air-to-air energy exchangers, since in the latter the dimensionless parameters NTU and Cr govern the heat transfer, and the dimensionless parameters NTU_m and m^* govern the moisture transfer [27].

(a) (b)

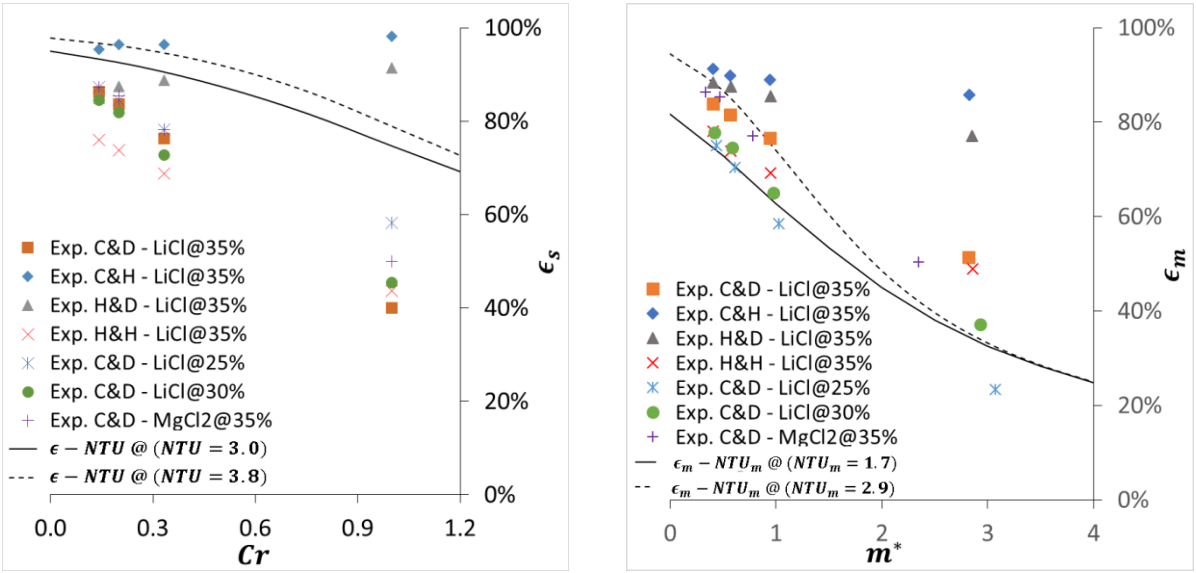

Figure 2.5 (a) heat exchange effectiveness ϵ_s and (b) moisture exchange effectiveness ϵ_m plotted against the dimensionless parameters Cr and m^* for the experiments of dataset M1, compared with the effectiveness curves obtained using the standard $\epsilon - NTU$ and $\epsilon_m - NTU_m$ models, Eq. (2.3) and Eq. (2.43), with NTU and NTU_m equal to the originally reported values of 3.0 and 1.7 [23], and also the updated values of 3.8 and 2.9 [31].

2.7.1.2.Dataset M2: Ordinary Water

The working fluid in dataset M2 is ordinary water [22]. The operating modes that have been investigated include cooling and dehumidification, cooling and humidification and heating and humidification. The operating parameters for these modes are presented in Table 2.4. Each experiment is performed at three different NTU values, but for all of the experiments $Cr = 1/7$. Ghadiri Moghaddam et al. originally assumed that $Nu = 8.24$ and $VDR = 56\,m/s$ [11]. However, as discussed earlier, it is possible to obtain an updated set of values by accounting for the increase in Nu caused by the inserts inside the air channel of the small-scale LAMEE, and also using an updated value of $24\,m/s$ for VDR. NTU and NTU_m calculated for this dataset using the originally reported and also using the updated values of Nu and VDR are presented in Table 2.5.

Table 2.4 Operating conditions for different operating modes of dataset M2

$\boldsymbol{Exp}$	$\boldsymbol{Cr}$	$\boldsymbol{T_{sol,in}}$ $(°\boldsymbol{C})$	$\boldsymbol{X_{sol,in}}$ (%)	$\boldsymbol{W_{sol,in}}$ $(\boldsymbol{g/kg})$	$\boldsymbol{T_{air,in}}$ $(°\boldsymbol{C})$	$\boldsymbol{W_{air,in}}$ $(\boldsymbol{g/kg})$
$\boldsymbol{C\&D}$	1/7	16	~0	11.5	35	19.5
$\boldsymbol{C\&H}$	1/7	22	~0	16	35	7
$\boldsymbol{C\&D}$	1/7	30	~0	25.5	22	8.5

Table 2.5 $\boldsymbol{NTU}$ and $\boldsymbol{NTU_m}$ values for dataset M2

	$\{NTU, NTU_m\}$
Effect of inserts excluded and $VDR = 56\,m/s$ (original [23])	{2.5, 1.4},{3.5,2.0},{4.5, 2.6}
Effect of inserts included and $VDR = 24\,m/s$ (updated [31])	{3.5, 2.6},{4.2, 3.3},{4.9,3.9}

2.7.1.2.1. Sensible Effectiveness

As evident in Figure 2.6(a), the trend in the variation of ϵ_s among the different experiments is well captured using the simplified-extended $\epsilon - NTU$ model and the maximum discrepancy between the measured and the estimated values is no more than 8%.

2.7.1.2.2. Moisture Transfer Effectiveness

The maximum discrepancy between the measured and the estimated values is 15% and the trend in the variation of ϵ_m among the different experiments is well captured using the simplified-extended $\epsilon_m - NTU_m$ model as shown in Figure 2.6(b).

2.7.1.2.3. Standard $\epsilon - NTU$ and $\epsilon_m - NTU_m$ Models

Figure 2.7(a) and Figure 2.7(b) present the experimental ϵ_s and ϵ_m for dataset M2 plotted against Cr and m^*, respectively. It should be reminded that Cr and m^* are constant for all the experiments of dataset M1. Figure 2.7 demonstrates that the standard $\epsilon - NTU$ and $\epsilon_m - NTU_m$ models, Eq. (2.3) and Eq. (2.43), cannot account for the variations in the experimental ϵ_s and ϵ_m among different operating modes.

2.7.1.3.Summary

The estimations for ϵ_s and ϵ_m of experiments of datasets M1 and M2 obtained by substituting the updated values of NTU and NTU_m in the simplified-extended $\epsilon - NTU$ and $\epsilon_m - NTU_m$ models, do not deviate by more than 16% from the experimental values for ϵ_s and ϵ_m, as can be seen in Figure 2.42 and Figure 2.6. Furthermore, assuming a one to one relationship between the estimations by the simplified-extended $\epsilon - NTU$ and $\epsilon_m - NTU_m$ models and the experimental data, one can account for 92% and 68% of the variance in the measured ϵ_s and ϵ_m values among the experiments (coefficient of determination $R^2 = 0.92$ and 0.68). In contrast,

the estimations for ϵ_s and ϵ_m of experiments of datasets M1 and M2 obtained by substituting the updated values of NTU and NTU_m in the standard $\epsilon - NTU$ and $\epsilon_m - NTU_m$ models, deviate by up to 50% from the experimental values for ϵ_s and ϵ_m, as can be seen in Figure 2.52 and Figure 2.7. Furthermore, assuming a one to one relationship between the estimations by the standard $\epsilon - NTU$ and $\epsilon_m - NTU_m$ models and the experimental data, one account for none and only 22% of the variance in the measured ϵ_s and ϵ_m values among the experiments ($R^2 = -0.35$ and 0.22).

(a) (b)

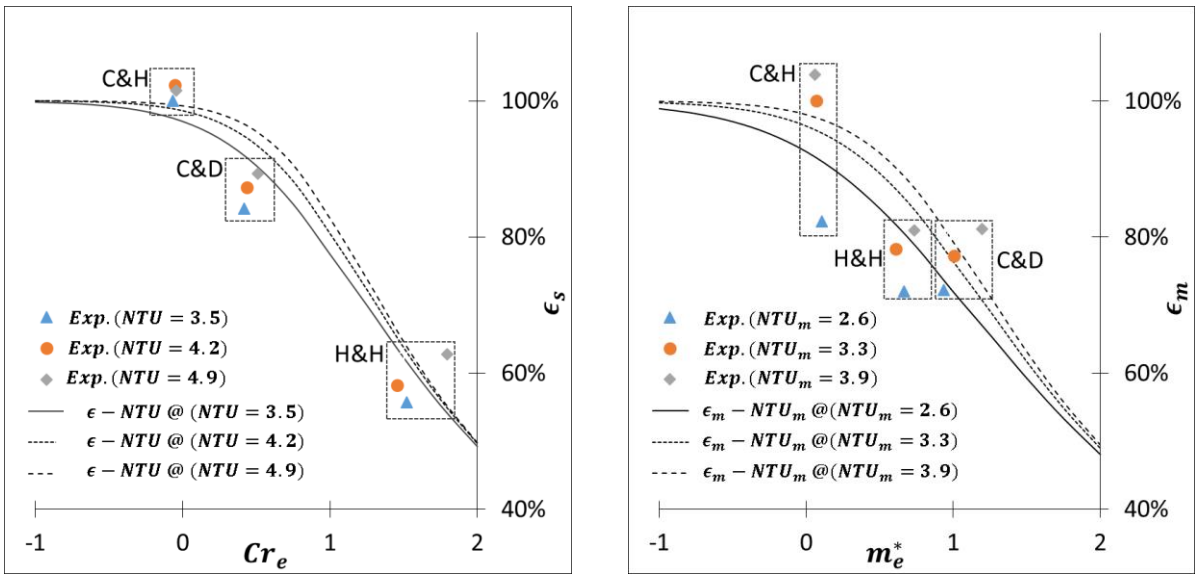

Figure 2.6 (a) heat exchange effectiveness ϵ_s and (b) moisture exchange effectiveness e_m plotted against the dimensionless parameters Cr and m^* for the experiments of dataset M2, compared with the effectiveness curves obtained using the simplified-extended $\epsilon - NTU$ and $\epsilon_m - NTU_m$ models.

(a) (b)

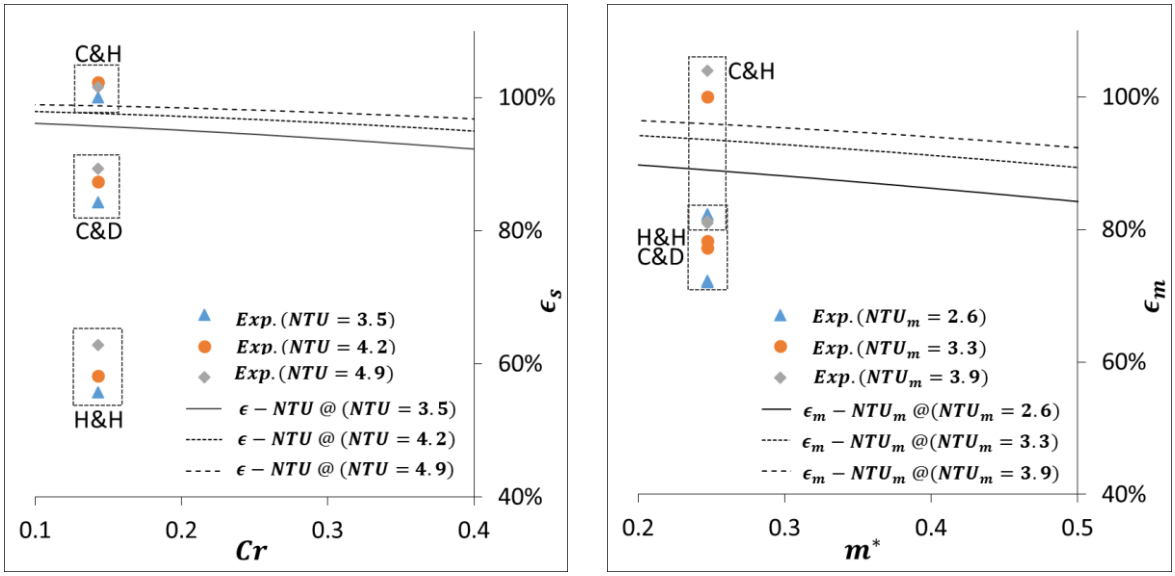

Figure 2.7 (a) heat exchange effectiveness ϵ_s and (b) moisture exchange effectiveness e_m plotted against the dimensionless parameters Cr and m^* for the experiments of dataset M2, compared with the effectiveness curves obtained using the standard $\epsilon - NTU$ and $\epsilon_m - NTU_m$ models

2.7.2. Verification with the Hollow Fiber Membrane Contactor Experimental Data

The design of the hollow fiber membrane contactor (HFMC) investigated by Zhang [18] is similar to a shell and tube exchanger with a counter-flow arrangement, as shown in Figure 2.8. Zhang investigated the performance of the HFMC under cooling and dehumidification mode at different operating condition. The specifications of the experiments are provided in Table 2.6. These experiments are denoted dataset Z. The desiccant is an aqueous solution of $LiCl$ for all the experiments. Zhang provides an $NTU = 4.42$ for the base experiment, conducted at $\dot{m}_{air} = 0.0021\ kg/s$, which results in $UA = 0.00923\ W/K$. To calculate NTU for the other experiments, it is assumed that UA is constant for all the experiments. Zhang also provides an NTU/NTU_m ratio of 2.8 for the same base experiment, which is assumed to be constant for all the experiments, and is used to calculate NTU_m of the other experiments. The uncertainty associated with the measurements of the temperature and the relative humidity of the air are $\pm 0.25\ °C$ and 2.5%, respectively.

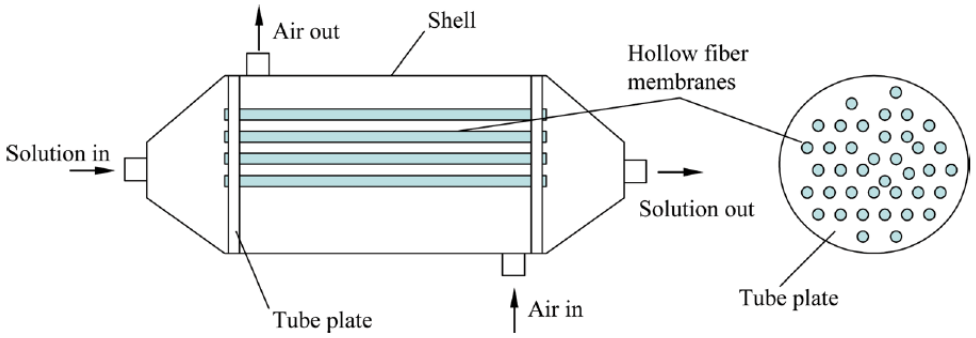

Figure 2.8 Schematics of the hollow fiber membrane contactor by Zhang [18]

Table 2.6 Specifications of the experiments in dataset Z [18]

Exp	$\dot{m}_{air}$ (kg/h)	$\dot{m}_{sol}$ (kg/h)	NTU	NTU_m	Cr	$T_{sol,in}$ $(°C)$	$X_{sol,in}$ (%)	$W_{sol,in}$ (g/kg)	$T_{air,in}$ $(°C)$	$W_{air,in}$ (g/kg)
A	1.6	1.6	4.4	1.6	0.27	25.1	35.0	5.7	34.8	21.0
B	1.9	1.9	5.2	1.9	0.23	24.9	34.0	6.2	33.9	18.0
C	1.4	1.4	3.8	1.4	0.32	25.3	35.0	5.8	35.2	22.0
D	1.0	1.0	2.7	1.0	0.45	25.2	35.0	5.8	34.9	21.0
E	0.8	0.8	2.1	0.8	0.64	25.2	33.0	6.8	33.7	19.0
F	1.0	1.0	2.7	1.0	0.84	25.5	34.0	6.4	33.8	21.0
G	1.6	1.6	4.4	1.6	0.26	24.5	35.0	5.5	35.3	22.0
H	1.6	1.6	4.5	1.6	0.28	24.6	35.0	5.6	32.8	19.0
I	1.6	1.6	4.5	1.6	0.27	24.6	35.0	5.6	29.8	18.0
J	1.6	1.6	4.5	1.6	0.28	25.6	30.0	8.6	27.2	16.0
K	1.6	1.6	4.4	1.6	0.29	25.4	31.0	8.0	25.7	15.0
Min	0.8	0.8	2.1	0.8	0.23	24.5	30	5.0	25.7	15
Max	1.9	1.9	5.2	1.9	0.84	25.6	35	8.6	35.3	22

2.7.2.1.Sensible Effectiveness

Zhang used the absolute temperature values to compare the experimental results for dataset Z with the analytical model that he developed for the HFMC in his paper [18]. Here, the same approach is used. Figure 2.9(a) presents the estimated changes in T_{air}, using both the standard $\epsilon - NTU$ and the simplified-extended $\epsilon - NTU$ models, plotted against the measured changes in T_{air} for dataset Z. As evident, the standard model consistently overestimates the measured changes in T_{air}, with a maximum discrepancy of 5.0 $°C$ between the estimated and the measured values. In contrast, the simplified-extended $\epsilon - NTU$ model underestimates the measured changes in T_{air}, however, the discrepancy between the estimated and the measured values does not exceed 1.6 $°C$ and the average discrepancy is only 0.9 $°C$.

2.7.2.2.Latent Effectiveness

Zhang also used the absolute humidity ratio values to compare the experimental results for dataset Z with the analytical model that he developed for the HFMC in his paper [18]. Figure 2.9-(b) presents the estimated changes in W_{air}, using both the standard $\epsilon_m - NTU_m$ and the simplified-extended $\epsilon_m - NTU_m$ models, plotted against the measured changes in W_{air} for dataset Z. As evident, the standard model consistently underestimates the measured changes in W_{air}, with an average discrepancy of 1.5 g/kg between the estimated and the measured values. However, although the simplified-extended $\epsilon - NTU$ model also underestimates the measured changes in W_{air} for most of the experiments, the average discrepancy between the estimated and the measured values is only 0.5 g/kg, with a maximum discrepancy of 1.3 g/kg.

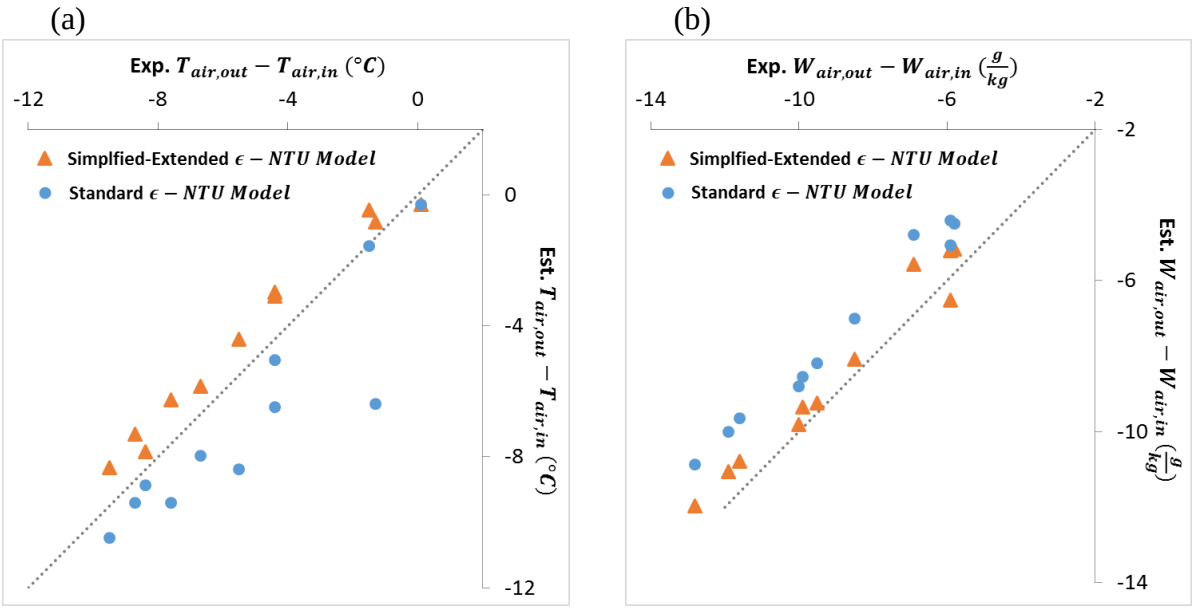

Figure 2.9 (a) Change in T_{air} estimated using the standard and the simplified-extended $\epsilon - NTU$ models compared with the experimental data (b) change in W_{air} estimated using the standard and the simplified-extended $\epsilon_m - NTU_m$ models compared with the experimental data for dataset Z [18]

2.8. Conclusions

In this paper, new dimensionless parameters $\overline{dCr_e}$ and Cr_e were introduced and a new extended $\epsilon - NTU$ model was developed to demonstrate that unless $\overline{dCr_e} = Cr_e = Cr$, the standard $\epsilon - NTU$ model is not exactly valid. In order to calculate $\overline{dCr_e}$, detailed profiles of the temperatures of the air and solution streams along the LAMEEs should be known. In order to estimate ϵ_s for the typical cases for which the temperatures of the streams are available only at the inlet and outlet of the LAMEEs, the simplified-extended $\epsilon - NTU$ model was developed which expresses ϵ_s as a function of NTU and Cr_e.. Analogous developments were provided to model moisture exchange in LAMEEs. The extended $\epsilon_m - NTU_m$ and the simplified-extended $\epsilon_m - NTU_m$ models were developed, which are identical in form to the extended and the simplified-extended $\epsilon - NTU$ models, with $\overline{dCr_e}$, Cr_e and NTU replaced with $\overline{dm_e^*}$, m_e^* and NTU_m.

It was analytically proved that if the temperature profile of the air stream inside LAMEE is linear, the simplified-extended $\epsilon - NTU$ model provides an exact solution for ϵ_s; and, analogously, it was proved that if the humidity ratio profile of the air stream inside LAMEE is linear, the simplified-extended $\epsilon_m - NTU_m$ model provides an exact solution for ϵ_m.

Experimental data for some typical summer operating conditions of LAMEEs were used to demonstrate that the simplified-extended $\epsilon - NTU$ and $\epsilon_m - NTU_m$ models can be used to model ϵ_s and ϵ_m of LAMEEs for practical application (for which the temperature and humidity ratio profiles of the air stream deviate from the linear profiles assumption) in terms of dimensionless parameters NTU, NTU_m, Cr_e and m_e^*. The average discrepancy between the measured values and the values estimated by the correlations was less than 10%. In particular, these models could account for the strong dependency of ϵ_s and ϵ_m of LAMEEs on the inlet

operating conditions. Since NTU_m and NTU do not change with the inlet temperatures and humidity ratios of the air and solution streams, it can be concluded that the dependency of ϵ_s and ϵ_m of LAMEEs on the inlet operating conditions is a result of dependency of Cr_e and m_e^* on the inlet operating conditions. Therefore, LAMEEs are analogous to a heat exchanger for which Cr is variable and strongly dependent on the temperatures of the streams.

2.9. Appendix: Proofs of the Equations

Proofs of the extended $\epsilon - NTU$ model Eq. (2.31) and the extended $\epsilon_m - NTU_m$ model Eq. (2.38) are presented in this section. As a result of the analogy between heat and mass transfer, the proofs are essentially identical. However, since the effectiveness models for mass transfer are less common, first, a detailed proof is provided for the $\epsilon_m - NTU_m$ model, Eq. (2.38), and then the less detailed proof for Eq. (2.31) should be easy to follow.

2.9.1. Proof of Eq. (2.38)

Taking derivatives of both sides of the equation for total moisture exchange Eq. (2.21) with respect to l, one can obtain

$$\frac{d\dot{m}_W}{dl} = A\, U_m (W_{sol} - W_{air})_l \tag{2.44}$$

Then, using mass balance in terms of W_{air} Eq. (2.23) and definition of NTU_m, Eq. (2.41), it is possible to rewrite Eq. (2.44) as

$$\frac{dW_{air}}{dl} = NTU_m (W_{sol} - W_{air})_l \tag{2.45}$$

Then, assuming that $(W_{sol} - W_{air})_l \neq 0$, it is possible to use the definition of dm_e^*, Eq. (2.39), and obtain

$$\frac{1}{(W_{sol}-W_{air})_l}\frac{d(W_{sol}-W_{air})_l}{dl} = NTU_m\,(1-dm_e^*) \tag{2.46}$$

Taking integral of both sides of Eq. (2.46) from $l = 0$ to $l = 1$ results in

$$\frac{(W_{sol}-W_{air})_1}{(W_{sol}-W_{air})_0} = \frac{1}{\exp\left[\int_0^1 -NTU_m\,(1-dm_e^*)\,dl\right]} \tag{2.47}$$

Finally, after some algebraic manipulations, one can obtain

$$\epsilon_m = \frac{1-\exp\left[\int_0^1 -NTU_m\,(1-dm_e^*)\,dl\right]}{1+m_e^*\,\exp\left[\int_0^1 -NTU_m\,(1-dm_e^*)\,dl\right]} \tag{2.48}$$

Eq. (2.48) is valid as long as dm_e^* and NTU_m are continuous. Since NTU_m is calculated for the air side in this paper per Eq. (2.41), it can be assumed to be constant and Eq. (2.48) will result in Eq. (2.38).

2.9.2. Proof of Eq. (2.31)

As a result of the analogy between heat and mass transfer, proof of Eq. (2.31) is analogous to the proof of Eq. (2.38) and hence the details of the steps are omitted and only the main intermediate equation is provided. Using the equations for total heat exchange Eq. (2.20), differential sensible heat transfer to the air stream Eq. (2.24), the definition for dCr_e Eq. (2.32), and the definition for NTU Eq. (2.34), and assuming that $(T_{sol}-T_{air})_l \neq 0$, it is possible to obtain

$$\frac{1}{(T_{sol}-T_{air})_l}\frac{d(T_{sol}-T_{air})_l}{dl} = (T_{sol}-T_{air})_l\,NTU\,(1-dCr_e) \tag{2.49}$$

Then, taking integral of both sides of Eq. (2.49) from $l = 0$ to $l = 1$ and performing some algebraic manipulations, and assuming that NTU is constant, Eq. (2.49) results in Eq. (2.31).

Chapter 3

Estimating Cr_e and m_e^*

3.1. Overview of Chapter 3

In chapter 2, the dimensionless parameters effective heat capacity rate ratio Cr_e and effective mass flow rate ratio m_e^* were developed, and defined per Eq. (2.5) and Eq. (2.9), and the simplified-extended $\epsilon - NTU$ and $\epsilon_m - NTU_m$ models were developed, and presented by Eq. (2.37) and Eq. (2.42). Furthermore, in section 2.7, it was verified that the simplified-extended $\epsilon - NTU$ and $\epsilon_m - NTU_m$ models can be used to correlate the effectiveness of LAMEEs for heat exchange ϵ_s to the dimensionless parameters NTU and Cr_e and correlate the effectiveness of LAMEEs for moisture exchange ϵ_m to the dimensionless parameters NTU_m and m_e^*, respectively. However, in chapter 2, both the inlet and outlet temperatures and humidity ratios of the air stream, in addition to the inlet temperature and equilibrium humidity ratio of the solution stream were used to calculate Cr_e and m_e^* corresponding to each experiment.

In this chapter a set of methods are introduced to calculate Cr_e and m_e^* as a function of the LAMEEs' design parameters (geometric ratios and material properties) and only the inlet operating conditions of the streams. Then, it is verified that these methods result in estimations for Cr_e and m_e^* that are accurate enough such that, if these estimations are substituted into the simplified-extended $\epsilon - NTU$ and $\epsilon_m - NTU_m$ models to estimate ϵ_s and ϵ_m, the change in the temperature and humidity ratio of the air stream can be accurately predicted for a number of experimental data points and a large number of numerical data points for different designs of LAMEEs over a wide range of operating conditions typical to summer air-conditioning applications. The theories were developed and the manuscript #2 was written by the author of this

thesis (Houman Kamali), and the co-authors (Gaoming Ge, Robert W. Besant and Carey J. Simonson) provided feedback on the research and on the manuscript #1.

Manuscript #2: H. Kamali, R. W. Besant, C. J. Simonson, "Estimating Changes in the Temperature and Humidity Ratio of the Air Stream inside Liquid-to-Air Membrane Energy Exchangers using Analogs of the Effectiveness-NTU Model," to be submitted to ASME Journal of Heat Transfer

3.2. Summary

Background: As a result of the coupling between heat and moisture exchange in liquid-to-air membrane energy exchangers (LAMEEs), the standard effectiveness-NTU model is not directly applicable to LAMEEs. The main objective of this paper is to use extensions of the standard effectiveness-NTU model to predict the outlet air temperature and humidity ratio for isolated LAMEEs (i.e. isolated to avoid heat and mass exchange with the surroundings).

Method of approach: The authors, previously, developed the simplified-extended effectiveness models as extensions of the standard effectiveness-NTU model for LAMEEs, which correlated the effectiveness of LAMEEs for sensible energy exchange to the dimensionless parameters number of transfer units and effective heat capacity rate ratio (effective Cr), and correlated the effectiveness of LAMEEs for moisture exchange to the dimensionless parameters number of moisture transfer units and effective mass flow rate ratio (effective m*). In this paper, a set of methods are developed to estimate the effective Cr and effective m* for isolated LAMEEs working in the summer air-condition operating mode as a function of the design parameters (i.e. exchanger geometric ratios and material properties) and the inlet operating conditions (i.e. temperatures and [equilibrium] humidity ratios) of the air and desiccant solution streams.

Results: A number of previously published experimental data points and numerical data points for different designs of LAMEEs were used to validate the propositions made in this paper. The predictions for the outlet air temperatures and humidity ratios that were obtained by substituting the estimations for effective Cr and effective m* into the simplified-extended effectiveness models differed from the experimental measurements and numerical calculations by less than 2.1 °C and 2.8 g/kg. For comparison, the estimations provided by the standard effectiveness-NTU model for the outlet air temperature differed from the numerical calculations by up to 7.2 °C and from the experimental measurements by up to 5.1 °C.

Conclusions: The methods developed in this paper for estimating the effective Cr and effective m* result in estimations that are reasonably accurate for the purpose of using the simplified-extended effectiveness models, which are analogous to the standard effectiveness-NTU model, to predict the outlet air operating conditions for different designs of LAMEEs for summer air-conditioning applications.

Keywords: LAMEE, heat capacity rate ratio, mass flow rate ratio, liquid desiccants, salt solutions, effectiveness – NTU method

3.3. Abstract

Due to the coupling between heat and moisture exchange in liquid-to-air membrane energy exchangers (LAMEEs), the standard effectiveness-NTU model is not directly applicable to LAMEEs. In this paper, new methods are developed which allow the designers to apply models analogous the standard effectiveness-NTU model for analysis and design of LAMEEs. The predictions provided by these methods for the change in the temperature and humidity ratio of the air stream inside LAMEEs for a number of experimental and a large number of numerical data

differed from the experimental measurements and numerical calculations by less than 2.1 °C and 2.8 g/kg.

3.4. Introduction

Liquid-to-air membrane energy exchangers (LAMEEs) are composed of parallel rectangular channels of air and aqueous desiccant solution streams that are separated by porous membranes. These porous membranes are permeable to water vapor but not to liquid water (under the normal operating pressures of LAMEEs, which are $\sim 1\ atm$), and thus enable simultaneous heat and moisture exchange between the air and the desiccant solution streams. LAMEEs can be used to design liquid desiccant air conditioning (LDAC) systems that can achieve small sensible cooling to total cooling ratios in the range of $0.3 - 0.5$ [40], which makes them a desirable choice for reducing energy consumption in summer air-conditioning applications when the latent cooling demand is significant compared to the sensible cooling demand [41], [42].

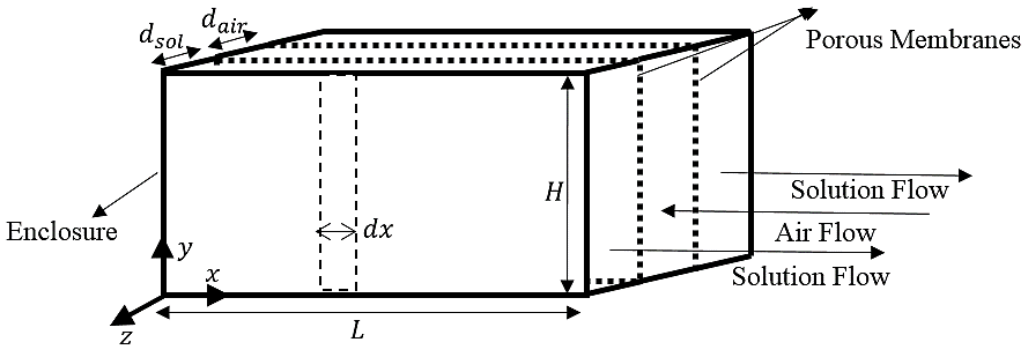

Figure 3.1 Schematics of a counter-flow single-panel LAMEE with an air channel and two adjacent solution channels. Hdx represents a differential area of a membrane, through which heat and moisture are exchanged between two adjacent air and solution streams [43].

The performance of LAMEEs can be uniquely quantified in terms of the sensible heat exchange effectiveness ϵ_S and the moisture exchange effectiveness ϵ_m. In this paper, the air stream has been assumed to have the minimum heat capacity rate ratio ($C_{air} = C_{min}$), and, following the

conventions of ASHRAE standard 84-2013 [8] for the case of $C_{air} = C_{min}$, ϵ_S and ϵ_m for LAMEEs are defined as

$$\epsilon_s = \frac{actual\ sensible\ energy\ transfer}{inlet\ potential\ for\ heat\ transfer} = \frac{T_{air,out} - T_{air,in}}{T_{sol,in} - T_{air,in}} \tag{3.1}$$

$$\epsilon_m = \frac{actual\ moisture\ transfer}{inlet\ potential\ for\ moisture\ transfer} = \frac{W_{air,out} - W_{air,in}}{W_{sol,in} - W_{air,in}} \tag{3.2}$$

Subscripts air and sol refer to the air and solution streams, and the subscripts in and out refer to the respective inlets and outlets of each stream. T $(°C)$ refers to the bulk temperature of a fluid W_{air} (kg/kg) refers to the bulk humidity ratio of the air stream and W_{sol} (kg/kg) refers to the equilibrium humidity ratio of the solution stream, which indicates equilibrium humidity ratio of air at the air-solution interface.

Similar to air-to-air energy exchangers [27], the performance of LAMEEs is dependent on the dimensionless design parameters number of transfer units NTU, number of moisture transfer units NTU_m, and heat capacity rate ratio Cr. However, as a result of the coupling between heat and moisture exchange in LAMEEs, the performance of LAMEEs, unlike heat exchangers and air-to-air energy exchangers, is also strongly dependent on the inlet operating conditions, i.e. $T_{air,in}$, $W_{air,in}$, $T_{sol,in}$ and $W_{sol,in}$, and inlet mass flow rates of the streams. Previously, the performance of different designs of LAMEEs for a wide range of inlet operating conditions had been investigated using experimentation [11], [23], [22], [10], a numerical model [44], and also a simplified analytical model [18] [11]. Although the numerical and the analytical models are accurate for predicting the performance of LAMEEs for typical summer air-conditioning applications, they do not directly provide an explanation for the dependency of the performance of LAMEEs on the inlet operating conditions. In order to fill this gap and develop a model that

could explain the reason for dependency of the performance of LAMEEs on the inlet operating conditions, the authors, in another paper [43], introduced the simplified-extended $\epsilon - NTU$ model, Eq. (3.3), and the simplified-extended $\epsilon_m - NTU_m$ model, Eq. (3.4). These models expressed ϵ_s and ϵ_m in terms of the dimensionless parameters number of transfer units NTU, effective heat capacity rate ratio Cr_e, number of moisture transfer units NTU_m and effective mass flow rate ratio m_e^* as follows

$$\epsilon_s = \frac{1 - \exp[-NTU\ (1 - Cr_e)]}{1 -\ Cr_e\ \exp[-NTU\ (1 - Cr_e)]} \tag{3.3}$$

$$\epsilon_m = \frac{1 - \exp[-NTU_m\ (1 - m_e^*)]}{1 -\ m_e^*\ \exp[-NTU_m\ (1 - m_e^*)]} \tag{3.4}$$

The dimensionless parameters NTU and NTU_m are defined as follows

$$NTU = \frac{UA}{C_{air}} \tag{3.5}$$

$$NTU_m = \frac{U_m A}{\dot{m}_{air}} \tag{3.6}$$

$U\ (W/K.m^2)$ and $U_m(kg/s.m^2)$ are the overall heat and moisture transfer coefficients, respectively. $A\ (m^2)$ is total area of the membranes. C_{air} is the heat capacity rate of the air stream, defined as follows

$$C_{air} = \left(c_p \dot{m}\right)_{air} \tag{3.7}$$

$c_p\ (J/kg \cdot K)$ and $\dot{m}\ (kg/s)$ are specific heat capacity rate and mass flow rate.

The dimensionless parameters Cr_e and m_e^* are defined as follows

$$Cr_e = -\frac{T_{sol,out}\ -\ T_{sol,in}}{T_{air,out}\ -\ T_{air,in}} \tag{3.8}$$

$$m_e^* = -\frac{W_{sol,out} - W_{sol,in}}{W_{air,out} - W_{air,in}} \tag{3.9}$$

The authors, in another paper [42], analytically demonstrated that if the temperature profile (humidity ratio profile) of the air stream can be assumed to be linear along the exchanger and also if U (U_m) is constant throughout the exchanger, then the simplified-extended $\epsilon - NTU$ ($\epsilon_m - NTU_m$) model, Eq. (3.3) (Eq. (3.4)), provides an exact solution for the ϵ_s (ϵ_m), despite the coupling between heat and moisture exchange in LAMEEs.

For the air-to-air energy exchangers, for which the heat and moisture exchange are uncoupled, one can obtain [27]

$$Cr_e = Cr \tag{3.10}$$

$$m_e^* = m^* \tag{3.11}$$

where heat capacity rate ratio Cr and mass flow rate ratio m^* are defined as follows

$$Cr = \frac{C_{air}}{C_{sol}} \tag{3.12}$$

$$m^* = \frac{\dot{m}_{air}}{\dot{m}_{sol}} \tag{3.13}$$

And thus it can be concluded that m^* and Cr are merely the values for m_e^* and Cr_e for the air-to-air exchangers. However, as a result of the coupling between heat and moisture exchange in LAMEEs, m^* and Cr are not the values for m_e^* and Cr_e.

The authors, in another paper [43], used the measured inlet and also the measured outlet operating conditions for some experimental data for a small-scale LAMEE [23], [22] and also a hollow fiber membrane contactor [18] to calculate m_e^* and Cr_e for each experimental data point. In the same paper, the authors demonstrated that the values of Cr_e and m_e^* that were calculated using both the inlet and outlet operating conditions can be substituted in the simplified-extended $\epsilon - NTU$ and $\epsilon_m - NTU_m$ models, Eq. (3.3) and Eq. (3.4), to obtain reasonably accurate

estimations for ϵ_s and ϵ_m (the maximum discrepancy between the estimations for and the experimentally measured values of ϵ_s and ϵ_m did not exceed 16%).

An important assumption that is implied in the use of the simplified-extended effectiveness models, and also the standard $\epsilon - NTU$ model, is that the overall heat and mass transfer coefficients, U and U_m, can be accurately predicted. However, in practice, even the best available heat transfer correlations for heat exchangers can result in uncertainty of $\pm 30\%$ in the overall effectiveness, so the heat exchanger designer always needs to be ready to compensate for such uncertainty when the exchanger is subjected to a wide range of operating conditions. Furthermore, a small uncertainty in the effectiveness of a certain exchanger at a certain operating conditioning does not rule out significant uncertainties in the effectiveness of the same exchanger at all the other operating conditions. This observation implies that the user of heat exchangers and LAMEEs must always be cautious for design and application studies when using only the highest values of effectiveness (with the lowest uncertainties) when the cost of under-sizing the exchangers is large.

It should also be pointed out that the performance of systems including several heat/energy exchangers is sometimes only presented as being only dependent on the effectiveness of each exchanger. Such information cannot indicate whether, under each operational condition of the exchanger system, the system is saving energy and/or cost (i.e. it may be working, but losing operating energy and money). To show that the operation of the system is a benefit and not a loss, we need to determine at each time the energy benefit versus the auxiliary energy inputs for fans, pumps and controls (or the equivalent dollars for each). This ratio is called coefficient of performance (COP), and its transition value is 1.0 for energy saving (but for dollars ratios it will be likely less than 1.0, because typically the thermal energy sources are worth less than the electrical sources at a selected location).

3.5. The Governing Equations of LAMEEs

A thorough discussion on the governing equations of LAMEEs can be found in either [45] or [44]. Here, a short summary of the most important equations is provided, which can be derived following a number of simplifying assumptions, including those presented in Table 3.1 [45], [44], [46]. Differential heat transfer rate dq_s (W) and differential moisture transfer rate $d\dot{m}_W$ (kg/s) in LAMEEs can be calculated as

$$dq_s = C_{air}\, NTU\, (T_{sol} - T_{air})_l\, dl \tag{3.14}$$

$$d\dot{m}_W = \dot{m}_{air}\, NTU_m\, (W_{sol} - W_{air})_l\, dl \tag{3.15}$$

where l is the dimensionless position along the length of the exchanger

$$l = \frac{x}{L} \tag{3.16}$$

U $(W/K.m^2)$ and $U_m(kg/s.m^2)$ are the overall heat and moisture transfer coefficients, respectively. A (m^2) is total area of the membranes.

Assuming no mass exchange with the environment, the principle of conservation of mass can be used to express the ideal mass balance equation for LAMEEs as

$$\frac{d\dot{m}_{air}}{dl} = \frac{d\dot{m}_{sol}}{dl} = \frac{d\dot{m}_W}{dl} \tag{3.17}$$

In terms of the change in the humidity ratio of the air stream, mass balance results in

$$\frac{dW_{air}}{dl} = \frac{1}{\dot{m}_{air}} \frac{d\dot{m}_W}{dl} \tag{3.18}$$

where it has been assumed that the mass flow rate of the dry air is nearly equal to that of the moist air, because, for air conditioning applications, W_{air} is typically less than $0.04\ kg/kg$ and the

percentage changes in $\dot{m}_{air}$ are nearly two orders of magnitude smaller than the percentage changes in W_{air}.

In terms of the change in the concentration of the solution stream, mass balance results in

$$\frac{dX_{sol}}{dl} = \frac{X_{sol}}{\dot{m}_{sol}} \frac{d\dot{m}_W}{dl} \tag{3.19}$$

where concentration of the salt solution is defined as the ratio between mass flow rates of the salt $\dot{m}_{salt}\ (kg/s)$ in the solution stream and the total mass flow rate of the solution stream $\dot{m}_{sol}\ (kg/s)$

$$X_{sol} = \frac{\dot{m}_{salt}}{\dot{m}_{sol}} \tag{3.20}$$

Assuming no energy exchange with the environment, the differential change in the temperature of the air stream can be calculated as

$$\frac{dT_{air}}{dl} = \frac{1}{C_{air}} \frac{dq_s}{dl} \tag{3.21}$$

and the differential change in the temperature of the solution stream can be calculated as

$$\frac{dT_{sol}}{dl} = \frac{1}{C_{sol}} \left(\frac{dq_s}{dl} + \frac{dq_L}{dl} \right) \tag{3.22}$$

q_L is the latent energy exchange and the differential change in it can be calculated as

$$\frac{dq_L}{dl} = h_{fg} \frac{d\dot{m}_W}{dl} \tag{3.23}$$

and $h_{fg}\ (J/kg)$ is the specific heat of evaporation of water. Therefore, the ideal energy balance equation in LAMEEs can be expressed as

$$C_{air}\left[\left(T_{air,out}-T_{air,in}\right)+\frac{h_{fg}}{c_{p,air}}\left(W_{sol,out}-W_{sol,in}\right)\right] \tag{3.24}$$
$$=-C_{sol}\left(T_{sol,out}-T_{sol,in}\right)$$

Table 3.1 Major assumptions used to simplify the governing equations of LAMEEs

1) Exchangers are operating in steady-state conditions.
2) Fluid properties are uniform along the height of the exchanger.
3) Heat and mass exchange occurs only between the two streams through the membranes.
4) Heat and moisture transfer occur only in the direction normal to the membranes.
5) Deflection of the porous membranes and flow mal-distributions of flow have a negligible impact.
6) Overall heat and mass transfer coefficients are approximately constant inside LAMEEs (excluding the entrance regions).
7) Mass flow rates and heat capacity rates of the flows are constant inside LAMEEs.

3.5.1. Properties of Desiccant Solutions

The equilibrium humidity ratio of a solution W_{sol} which indicates the equilibrium humidity ratio of the air adjacent to the solution can be calculated as [46]

$$W_{sol}=\frac{0.622P_v}{P-P_v} \tag{3.25}$$

where $P\ (Pa)$ is the total pressure of the solution and $P_v\ (Pa)$ is the partial water vapor pressure. P_v of a salt solution is a function of the salt type, concentration, X_{sol} , and temperature, T_{sol} , of the salt solution, as follows

$$P_v(\text{salt solution})=f(salt,T_{sol},X_{sol}) \tag{3.26}$$

In this paper, the correlations developed by Conde [32], Cisternas and Lam [37], and Zaytsev and Aseyev [33] have been used to obtain P_v and other properties of $LiCl$ and $MgCl_2$ salt solutions, and the correlations in ASHRAE Fundamentals [47] have been used to obtain the same for ordinary

water. In this paper, it is assumed that $P - P_v = 1\ atm$. It can be verified that W_{sol} increases exponentially with the temperature of the solution T_{sol}, but decreases linearly with the concentration of the solution X_{sol}. Hence, it is proposed that a linear-exponential correlation be used to directly calculate W_{sol} as a function of X_{sol} and T_{sol}, as follows

$$W_{sol}\,@(X_{sol}, T_{sol}) = (\alpha_1 X + \alpha_2)_{sol} \exp(\beta_{sol} T_{sol}) \tag{3.27}$$

where α_1 and α_2 are emperical dimensionless coeficients which express dependency of W_{sol} on the solution type and concentration, and $\beta\ (1/K)$ is another empirical coefficient which expresses dependency of W_{sol} on the temperature of the solution. The values of these empirical coefficients are dependent on the salt solution type and the desired range of applicability of X_{sol} and T_{sol}.

The parameters of the linear-exponential equation can be estimated by fitting Eq. (3.27) to the equilibrium humidity ratio curves obtained using Eq. (2.28). Then, it can be observed that for the solutions and the range of temperatures considered in this paper, β_{sol} can be assumed to be approximately equal to 0.058. The values for α_1 and α_2 of the linear-exponential correlation are presented in Table 3.2. The root-mean-square and maximum discrepancies between W_{sol} obtained using Eq. (2.28) and W_{sol} obtained using Eq. (3.27) are also presented in Table 3.2. These root-mean-square and maximum discrepancies are, respectively, less than 0.8 [g/kg] and 1.1 [g/kg], or, equivalently stated, less than 4% and 6% relative humidity at the room temperature ($T = 24\ °C$), for the range of study in this paper. Figure 2.2 presents a comparison between equilibrium humidity ratio curves of different solutions calculated using Eq. (2.28) and also calculated using Eq. (3.27), with α_1 and α_2 and β used as presented in Table 3.2; as evident, both Eq. (2.28) and Eq. (3.27) result in essentially the same curves.

3.5.1.1.The Dehumidification and the Regeneration Operating Modes

For the summer air-conditioning, LAMEEs have two distinct functions: (1) to condition (dry and cool) the air stream or (2) condition (dry and cool) the solution stream. In order to condition the hot and/or humid air stream, the solution enters the LAMEE at a low temperature, corresponding to a small W_{sol}, and the air stream is cooled and/or dehumidified from its inlet to its outlet. This operating mode is thus denoted the dehumidification operating mode. A heat pump can be employed to arbitrarily control the temperature of the solution stream. However, although the concentration of the desiccant solution decreases little from the solution inlet to the solution outlet inside LAMEEs as the humid air stream is dehumidified, these changes in the concentration can eventually accumulate over time and result in a noticeable decrease in the concentration of the solution stream, which in turn decreases the potential of the salt solution for dehumidification. To reduce the water content of the salt solution stream and thus increase its concentration, the solution at an elevated temperature, corresponding to a large W_{sol}, and dry air ($W_{air} < W_{sol}$), e.g. building exhaust air, enter the LAMEE. As a result of the moisture exchange between the dry air and the solution at an elevated temperature, the solution stream loses its water content and thus its concentration increases. This operating mode thus is denoted the regeneration operating mode.

Table 3.2 Specifications of the linear-exponential correlation Eq. (3.27)

Salt Solution Type		$LiCl$	$MgCl_2$	Pure Water
Reference Correlations for P_v		Conde [33]	C&L [38]	ASHRAE [47]
Parameters of Eq. (3.27)	α_1	-12.2	-10.3	-
	α_2	5.63	5.70	4.8
	β	0.058	0.058	0.058
Range of Usage	T_{sol}	15 °C . . 45 °C	$15\ °C\ ..\ 45\ °C$	$15\ °C\ ..\ 45\ °C$
	X_{sol}	25% . . 35%	25% . . 35%	-
Discrepancy	Average	0.4 g/kg	0.3 g/kg	0.8 g/kg
	Max	0.4 g/kg	0.5 g/kg	1.1 g/kg

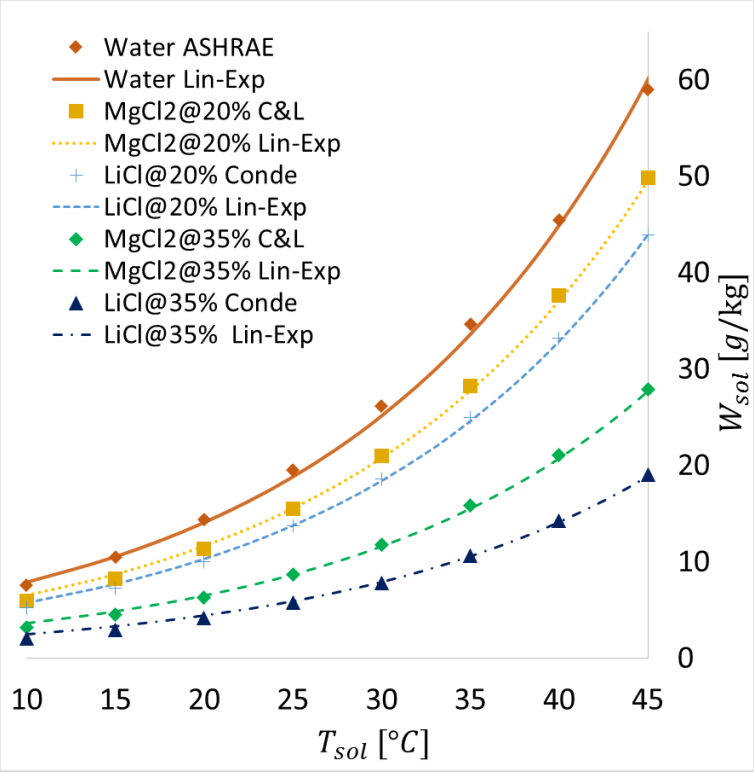

Figure 3.2 Comparison between the W_{sol} curves obtained by using the linear-exponential equation Eq. (3.27) with the values of the parameters as presented in Table 3.2 and the W_{sol} curves obtained by using the correlations for p_v in Eq. (2.28)

3.6. Estimating Cr_e and m_e^* for LAMEEs

In this section, methods for estimating Cr_e and m_e^* for LAMEEs as a function of design parameters NTU, NTU_m and Cr, and inlet operating conditions $T_{air,in}$, $W_{air,in}$, $T_{sol,in}$ and $W_{sol,in}$, are developed. To estimate Cr_e, first a hypothetical case when the LAMEE works exclusively as a heat exchanger (the moisture exchange between the air and the solution streams is negligible) is analyzed. Similarly, to estimate m_e^*, first a hypothetical case when the LAMEE works exclusively as a moisture exchanger (the sensible energy exchange between the streams is negligible) is analyzed. Then, the relationships between these hypothetical cases and the actual case of coupled sensible energy exchange and moisture exchange in LAMEEs are developed.

3.6.1. Dominant Sensible Energy Exchange and Negligible Moisture Exchang

Consider the hypothetical case for which the energy exchange between the streams in LAMEEs is primarily by sensible energy exchange between the streams. In particular, assume that

$$\frac{NTU_m}{NTU} \cong 0 \tag{3.28}$$

Substituting Eq. (3.28) into the energy balance equation, Eq. (3.24), and using the definitions for ϵ_s and ϵ_m, Eq. (2.1) and Eq. (3.2), one can obtain

$$\frac{h_{fg}}{c_{p,air}} \frac{W_{air,out} - W_{air,in}}{T_{air,out} - T_{air,in}} = H^* \frac{\epsilon_m}{\epsilon_s} \cong 0 \tag{3.29}$$

where H^* is the operating factor, a dimensionless parameter defined as

$$H^* = \frac{h_{fg}}{c_{p,air}} \frac{W_{sol,in} - W_{air,in}}{T_{sol,in} - T_{air,in}} \tag{3.30}$$

If Eq. (3.29) is applicable to a LAMEE, then that LAMEE is functioning as a heat exchanger (HX). Indeed, substituting Eq. (3.29) into the energy balance equation, Eq. (3.24), and using the definitions for Cr_e and Cr, Eq. (2.5) and Eq. (3.12), it can be verified that

$$Cr_{e,HX} = Cr \tag{3.31}$$

3.6.2. Dominant Latent Energy Exchange and Negligible Sensible Energy Exchange

First, note that, as discussed before, W_{air} is less than $0.04\ kg/kg$ for typical air-conditioning applications. Thus, it can be concluded that the relative change in X_{sol} inside LAMEEs is negligible [23] and the concentration of the solution is practically constant inside LAMEEs. That is, in LAMEEs

$$\frac{dX_{sol}/dl}{X_{sol}} \ll 1 \rightarrow X_{sol,out} \cong X_{sol,in} \tag{3.32}$$

The observation that $X_{sol,out} \cong X_{sol,in}$ for typical operating conditions of LAMEEs means that to estimate the change in W_{sol} inside LAMEEs, it suffices to consider the change only in T_{sol}. Then, consider the hypothetical case for which the energy exchange between the streams in LAMEEs is primarily by latent energy exchange between the streams. In particular, assume that

$$\frac{NTU}{NTU_m} \cong 0 \tag{3.33}$$

Substituting Eq. (3.33) into the energy balance equation, Eq. (3.24), and using the definitions for ϵ_s and ϵ_m, Eq. (2.1) and Eq. (3.2), results in

$$\frac{c_{p,air}}{h_{fg}} \frac{T_{air,out} - T_{air,in}}{W_{air,out} - W_{air,in}} = \frac{1}{H^*} \frac{\epsilon_s}{\epsilon_m} \cong 0 \tag{3.34}$$

If Eq. (3.34) is applicable, the LAMEE operates as a moisture exchanger (MX). Substituting Eq. (3.34) into the energy balance equation, Eq. (3.24), it can be verified that

$$\left(-\frac{T_{sol,out}-T_{sol,in}}{W_{air,out}-W_{air,in}}\right)_{MX}=\left(-\frac{dT_{sol}}{dW_{air}}\right)_{MX}=Cr\frac{h_{fg}}{c_{p,air}} \tag{3.35}$$

Furthermore, using the linear-exponential correlation for ϵ_m Eq. (3.9), one can obtain

$$m_e^*=-W_{sol,in}\frac{\exp\left[\beta\left(T_{sol,out}-T_{sol,in}\right)\right]-1}{W_{air,out}-W_{air,in}} \tag{3.36}$$

Then, it can observed that if Eq. (3.34) is valid, Eq. (3.36) can be simplified for LAMEEs operating exclusively as moisture exchangers as follows

$$m_{e,MX}^*=m_{e,in,MX}^*\frac{\exp\left(m_{e,IWD,MX}^*\,\epsilon_m\right)-1}{m_{e,IWD,MX}^*\epsilon_m} \tag{3.37}$$

where the inlet effective mass flow rate ratio $m_{e,in}^*$ and the inlet humidity ratio difference (IWD) effective mass flow rate ratio $m_{e,IWD}^*$ are a set of dimensionless parameters defined as follows for LAMEEs operating as moisture exchangers

$$m_{e,in,MX}^*=Cr\,\frac{h_{fg}}{c_{p,air}}\,\beta\,W_{sol,in} \tag{3.38}$$

$$m_{e,IWD,MX}^*=Cr\,\frac{h_{fg}}{c_{p,air}}\,\beta\,\left(W_{air,in}-W_{sol,in}\right) \tag{3.39}$$

ϵ_m in Eq. (3.37) can be calculated as a function of NTU_m and m_e^* using the simplified-extended ϵ_m-NTU_m model, Eq. (3.4), and thus provided with NTU_m, $m_{e,in,MX}^*$ and $m_{e,IWD,MX}^*$, Eq. (3.36) can be iteratively solved for m_e^*. Then, m_e^* and NTU_m can be used in the simplified-extended ϵ_m-NTU_m model, Eq. (3.4), to obtain ϵ_m. Hence, the moisture transfer effectiveness curves in LAMEEs operating as a moisture exchanger can be calculated as a function of the dimensionless parameters NTU_m, $m_{e,in,MX}^*$ and $m_{e,IWD,MX}^*$, as presented in Figure 3.3.

Further insight into the Eq. (3.37) can be gained by noting that

$$Cr\ \frac{h_{fg}}{c_{p,air}} = \left(-\frac{dT_{sol}}{dW_{air}}\right)_{MX} \tag{3.40}$$

$$\beta\ W_{sol,in} = \frac{dW_{sol}}{dT_{sol}} \tag{3.41}$$

Then, it can be observed that for LAMEEs working exclusively as moisture exchangers, the dimensionless parameter $m^*_{e,in,MX}$ indicates the value of m^*_e calculated at the solution inlet

$$m^*_{e,in,MX} = -\left(\frac{dW_{sol}}{dW_{air}}\right)_{MX,@W_{sol}=W_{sol,in}} \tag{3.42}$$

The analogy between $m^*_{e,in,MX}$ and Cr becomes clear once reminded that for heat exchangers

$$Cr = -\frac{dT_{sol}}{dT_{air}} \tag{3.43}$$

The phase change energy associated with moisture exchange between the air and solution streams causes T_{sol} to change, which in turn changes W_{sol}, inside LAMEEs. The dimensionless parameter $m^*_{e,IWD,MX}$ reflects the effect of change in W_{sol} inside LAMEEs on m^*_e and indicates the difference between m^*_e calculated at $W_{air,in}$ and m^*_e calculated at $W_{sol,in}$ for LAMEE operating as moisture exchangers

$$m^*_{e,IWD,MX} = -\left[\left(\frac{dW_{sol}}{dW_{air}}\right)_{MX,@W_{sol}=W_{air,in}} - \left(\frac{dW_{sol}}{dW_{air}}\right)_{MX,@W_{sol}=W_{sol,in}}\right] \tag{3.44}$$

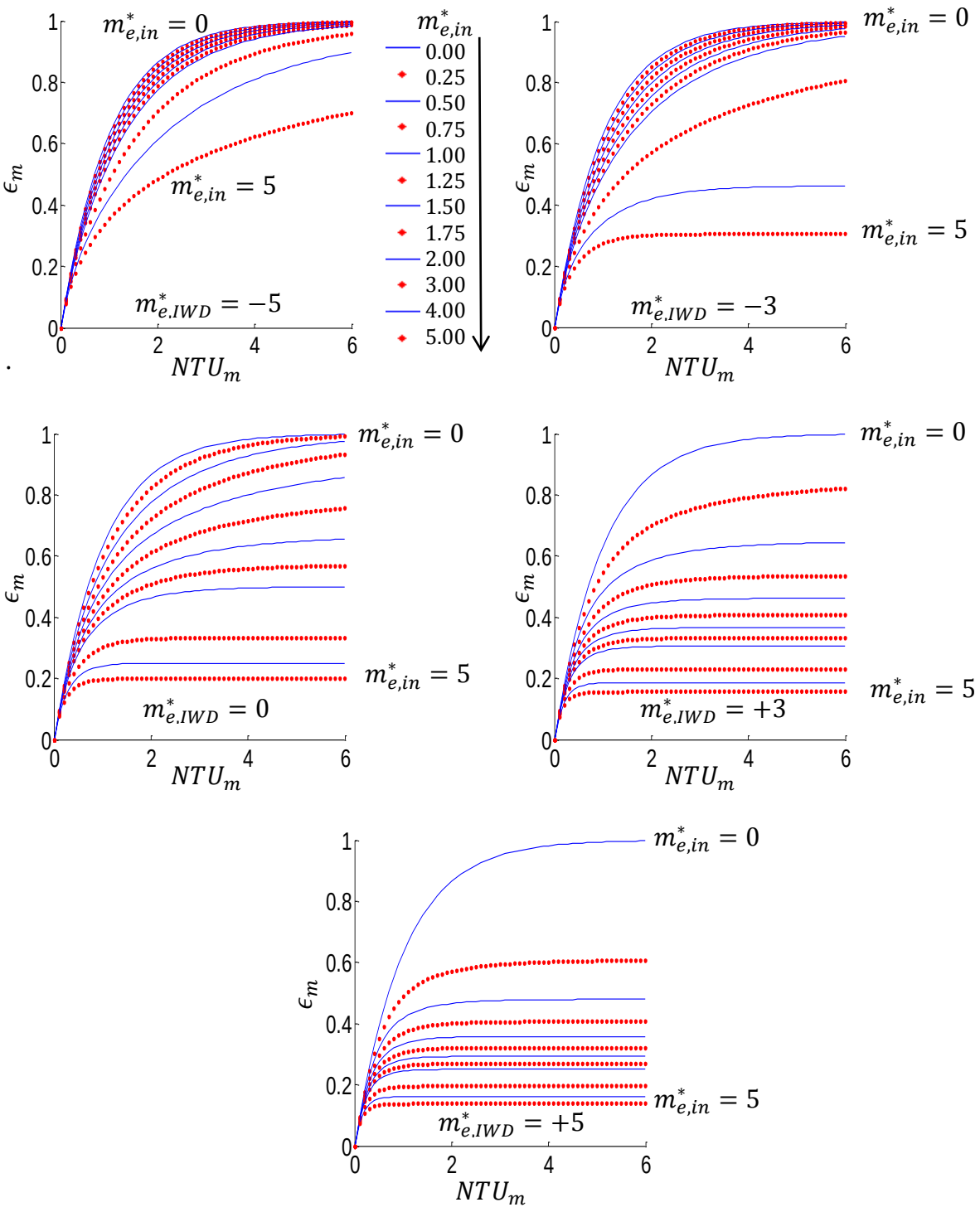

Figure 3.3 Moisture exchange effectiveness curves for LAMEEs operating as moisture exchangers, with negligible sensible energy exchange between the streams

3.6.3. Coupled Sensible Energy Exchange and Latent Energy Exchange

The first objective of this paper is achieved in this section and the methods for estimating Cr_e and m_e^* for LAMEEs as a function of design parameters and the inlet operating conditions are developed. Using the definition of the operating factor H^* Eq. (3.30) to rewrite the energy balance equation Eq. (3.24), one can find that if the sensible energy exchange and the moisture exchange in LAMEEs are coupled, then

$$-\frac{T_{sol,out}-T_{sol,in}}{T_{air,out}-T_{air,in}} = Cr\left(1+H^*\frac{\epsilon_m}{\epsilon_s}\right) \tag{3.45}$$

$$-\frac{T_{sol,out}-T_{sol,in}}{W_{air,out}-W_{air,in}} = Cr\frac{h_{fg}}{c_{p,air}}\left(\frac{1}{H^*}\frac{\epsilon_s}{\epsilon_m}+1\right) \tag{3.46}$$

Comparing the definition for Cr_e, Eq. (2.5), with Eq. (3.45), and noting from Eq. (3.31) that $Cr_{e,HX} = Cr$, one can conclude that for LAMEEs

$$Cr_e = -\frac{T_{sol,out}-T_{sol,in}}{T_{air,out}-T_{air,in}} = Cr\left(1+H^*\frac{\epsilon_m}{\epsilon_s}\right) = Cr_{HX}\left(1+H^*\frac{\epsilon_m}{\epsilon_s}\right) \tag{3.47}$$

H^* can be readily calculated as a function of inlet operating temperatures and humidity ratios. To estimate ϵ_m/ϵ_s, as a first guess, it is possible to consider only the difference between the values of NTU and NTU_m, and calculate ϵ_s and ϵ_m at $Cr_e = m_e^* = 0$. Hence, in this paper, to estimate ϵ_m and ϵ_s for Eq. (3.45) and Eq. (3.46), it is assumed that

$$\frac{\epsilon_m}{\epsilon_s} \cong \left(\frac{\epsilon_m}{\epsilon_s}\right)_{@\ Cr_e=m_e^*=0} = \frac{1-\exp(-NTU_m)}{1-\exp(-NTU)} \tag{3.48}$$

Then, using the approximation of Eq. (3.48), Cr_e for LAMEEs, Eq. (3.49), can be estimated as follows

$$Cr_e \cong Cr\left(1 + H^* \frac{1 - \exp(-NTU_m)}{1 - \exp(-NTU)}\right) \tag{3.49}$$

To calculate m_e^* for LAMEEs, Eq. (3.46) can be substituted into Eq. (3.36) to obtain

$$m_e^* = m_{e,in}^* \frac{\exp\left(m_{e,IWD}^* \, \epsilon_m\right) - 1}{m_{e,IWD}^* \epsilon_m} \tag{3.50}$$

where the dimensionless parameters $m_{e,in}^*$ and $m_{e,IWD}^*$ are calculated as follows

$$m_{e,in}^* = m_{e,in,MX}^* \left(\frac{1}{H^*}\frac{\epsilon_s}{\epsilon_m} + 1\right) = \left[Cr \, \frac{h_{fg}}{c_{p,air}}\left(\frac{1}{H^*}\frac{\epsilon_s}{\epsilon_m} + 1\right)\right] \beta \, W_{sol,in} \tag{3.51}$$

$$m_{e,IWD}^* = m_{e,IWD,MX}^* \left(\frac{1}{H^*}\frac{\epsilon_s}{\epsilon_m} + 1\right) = \left[Cr \, \frac{h_{fg}}{c_{p,air}} \left(\frac{1}{H^*}\frac{\epsilon_s}{\epsilon_m} + 1\right)\right] \beta \left(W_{air,in} - W_{sol,in}\right) \tag{3.52}$$

Then, using the approximation of Eq. (3.48), $m_{e,in}^*$ and $m_{e,IWD}^*$ for LAMEEs, Eq. (3.51) and Eq. (3.52), can be estimated as follows

$$m_{e,in}^* = \left[Cr \, \frac{h_{fg}}{c_{p,air}}\left(\frac{1}{H^*}\frac{1 - \exp(-NTU)}{1 - \exp(-NTU_m)} + 1\right)\right] \beta \, W_{sol,in} \tag{3.53}$$

$$m_{e,IWD}^* = \left[Cr \, \frac{h_{fg}}{c_{p,air}} \left(\frac{1}{H^*}\frac{1 - \exp(-NTU)}{1 - \exp(-NTU_m)} + 1\right)\right] \beta \left(W_{air,in} - W_{sol,in}\right) \tag{3.54}$$

Finally, after assuming a value for the ratio ϵ_s/ϵ_m, the procedure discussed earlier for solving Eq. (3.36) for m_e^* can be applied to iteratively solve Eq. (3.50) for m_e^*. It perhaps might be useful to note that, using the 3rd order Maclaurin expansion of the exponential function, Eq. (3.50) can be simplified as follows

$$m_e^* \cong m_{e,in}^* \left[1 + \frac{1}{2}\left(m_{e,IWD}^* \, \epsilon_m\right) + \frac{1}{6}\left(m_{e,IWD}^* \, \epsilon_m\right)^2\right] \tag{3.55}$$

Solving Eq. (3.55) for m_e^* is easier than solving Eq. (3.50) for m_e^*, as there is no need to be cautious about division by zero as a result of the denominator in Eq. (3.50) becoming zero.

3.6.4. Summary and Discussion

The first objective of this paper was to develop methods for estimating Cr_e and m_e^* as a function of the design parameters and the inlet operating conditions of LAMEEs. In this section, it was demonstrated that once provided with the ratio ϵ_s/ϵ_m, this objective could be achieved: Cr_e was expressed in Eq. (3.47) as a function of the ratio ϵ_s/ϵ_m, the design parameters and the inlet operating conditions; similarly, m_e^* was correlated to the dimensionless parameters NTU_m, $m_{e,in}^*$ and $m_{e,IWD}^*$ in Eq. (3.50), where the parameters $m_{e,in}^*$ and $m_{e,IWD}^*$ were expressed in Eq. (3.51) and Eq. (3.52) as a function of the ratio ϵ_s/ϵ_m, the design parameters and the inlet operating conditions.

However, in lieu of the exact value for the ratio ϵ_s/ϵ_m (which is known only if the air outlet operating conditions are available), it was proposed that the ratio ϵ_s/ϵ_m could be assumed to be equal to the approximation of Eq. (3.48), which expresses the ratio ϵ_s/ϵ_m at $Cr_e = m_e^* = 0$. Then, Cr_e, $m_{e,in}^*$ and $m_{e,IWD}^*$, can be estimated per Eq.(3.49), Eq. (3.53) and Eq. (3.54), as a function of only the design parameters and the inlet operating conditions. Finally, provided with the estimations for $m_{e,in}^*$ and $m_{e,IWD}^*$, m_e^* can be calculated by solving Eq. (3.50) for m_e^*.

3.7. Results

In this section, the second objective of this paper is achieved, which is to validate whether using the methods developed in the previous section for estimating Cr_e and m_e^* result in values that can be used to accurately evaluate the performance of LAMEEs as a function of the design parameters and the inlet operating conditions. To achieve this objective, a number of experimental and numerical data points pertaining to summer air-conditioning applications are selected. Then, firstly, Cr_e of these data points are estimated per Eq. (3.49) and m_e^* of these data points are

estimated by solving Eq. (3.50) for m_e^*, with $m_{e,in}^*$ and $m_{e,IWD}^*$ in Eq. (3.50) estimated per Eq. (3.53) and Eq. (3.54). Secondly, the estimated Cr_e and m_e^* are substituted into the simplified-extended $\epsilon - NTU$ and $\epsilon_m - NTU_m$ models, Eq. (3.3) and Eq. (3.4), in order to estimate ϵ_s and ϵ_m of these data points. Thirdly, the estimated ϵ_s and ϵ_m are used to calculate the change in the temperature of the air stream and the change in the humidity ratio of the air stream, i.e. ΔT_{air} and ΔW_{air}, for these data points. Here, the parameters ΔT_{air} and ΔW_{air} are defined as follows

$$\Delta T_{air} = T_{air,out} - T_{air,in} \tag{3.56}$$

$$\Delta W_{air} = W_{air,out} - W_{air,in} \tag{3.57}$$

Finally, in order to demonstrate that the estimations closely match the numerical and the experimental data, the estimated ΔT_{air} and ΔW_{air} are compared with the experimentally measured and the numerically calculated values of ΔT_{air} and ΔW_{air} for the same data points.

3.7.1. Verification against the Experimental Data

Experimental data points used in this paper are those published by (a) Ghadiri Moghaddam et al. for a small-scale LAMEE, as presented in [23] and in [22], which are denoted dataset M1 and dataset M2, (b) Ge et al. [11] for another small-scale LAMEE, which is denoted dataset G, and (c) Zhang [18] for a hollow fiber membrane contactor, which is denoted dataset Z. Relevant details of these experiments are presented in the following subsections. In Figure 3.4, the measured changes in T_{air} and W_{air} for these data points are plotted against the estimated changes in T_{air} and W_{air} of these data points. The estimated ΔT_{air} and ΔW_{air} are calculating by using the simplified-extended $\epsilon - NTU$ and $\epsilon_m - NTU_m$ models, with Cr_e and m_e^* corresponding to each experiment calculated using Eq. (3.47) and Eq. (3.50), with $m_{e,in}^*$ and $m_{e,IWD}^*$ estimated per Eq.

(3.51) and Eq. (3.52). The estimations for ΔT_{air} and ΔW_{air} account for most of the variations in the experimentally measured ΔT_{air} and ΔW_{air} ($R^2 \geq 0.97$). The maximum discrepancy between the experimentally measured values and the estimations by the simplified-extended $\epsilon - NTU$ model for ΔT_{air} is 2.1 $°C$ and the root-mean-square discrepancy between the two is 1.0 $°C$. The maximum discrepancy between the experimentally measured values and the estimations by the simplified-extended $\epsilon_m - NTU_m$ model for ΔW_{air} is 1.9 $\frac{g}{kg}$and the root-mean-square discrepancy between the two is 0.8 $\frac{g}{kg}$. For comparison, if instead of Cr_e, Cr was substituted into the simplified-extended $\epsilon - NTU$ model to predict ΔT_{air}, which then would be identical to using the standard $\epsilon - NTU$ model [49] to predict ΔT_{air}, the maximum discrepancy between the experimentally measured values and the predictions would increase to 5.0° C.

(a)

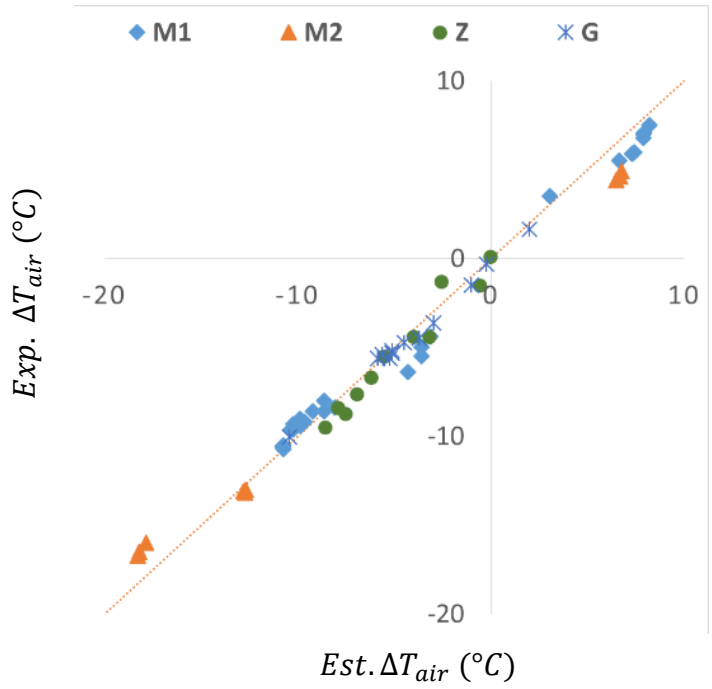

(b)

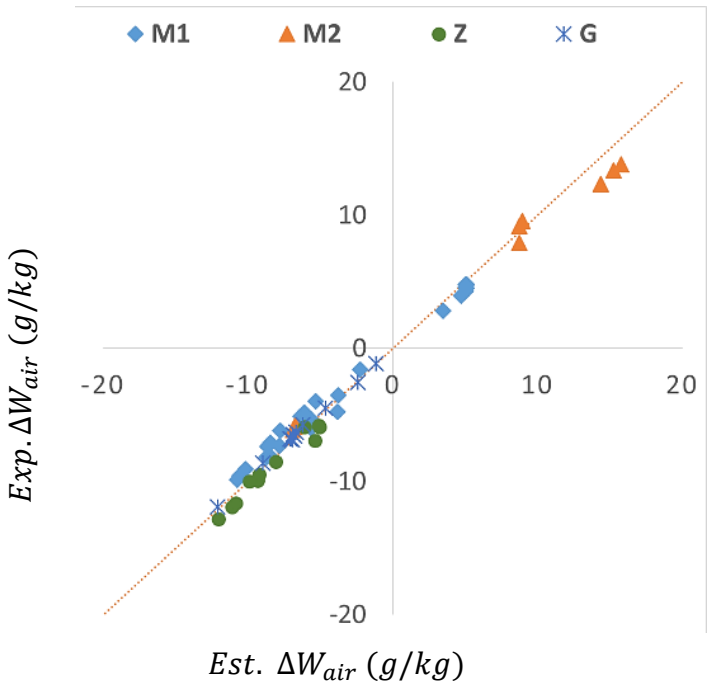

Figure 3.4 Comparison between the experimentally measured values and the estimations for (a) ΔW_{air} and (b) ΔT_{air} for data sets M1, M2, Z and G

3.7.1.1.Dataset M1 and M2

The small-scale LAMEE used in datasets M1 and M2 is composed of one rectangular air channel between two rectangular solution channels, of lengths of $520mm$ and heights of $94\ mm$, and with a counter-flow arrangement for the streams. In dataset M1 [23], $MgCl_2$ and $LiCl$ salt solutions were used as the working fluid and Ghadiri Moghaddam et al. investigated performance of the LAMEE under cooling and dehumidification (C&D), cooling and humidification (C&H), heating and dehumidification (H&D) and heating and humidification (H&H) modes at four different Cr values of $1, 1/3, 1/5$ and $1/7$, but at the same pair of NTU and NTU_m values of 3.8 and 2.9 for all the experiments. In dataset M2 [22], ordinary water was used as the working fluid and Ghadiri Moghaddam et al. investigated performance of the LAMEE under C&D, C&H and H&H modes at the same Cr value of $1/7$ for all the experiments, but at three different pair of NTU and NTU_m values. NTU and NTU_m values for datasets M1 and M2 were calculated as instructed by Ghadiri Moghaddam et al. per reference [45].

3.7.1.2.Dataset G

The small-scale LAMEE used in datasets G [11] is composed of one rectangular air channel between two rectangular solution channels, of lengths of $990mm$ and heights of $94\ mm$, and with a counter-flow arrangement for the streams. Ge et al. investigated cooling and dehumidification mode at different operating conditions, with $LiCl$ salt solution used as the working fluid. The specifications of experiments of dataset G are provided in Table 3.5.

3.7.1.3.The Hollow Fiber Membrane Contactor

The hollow fiber membrane contactor (HFMC) analyzed by Zhang [18] is similar to a shell and tube exchanger with a counter-flow arrangement. Zhang investigated the performance of the HFMC under cooling and dehumidification mode at different operating conditions, with $LiCl$ salt

solution used as the working fluid. Zhang provided an NTU value of 4.4 and NTU/NTU_m ratio of 2.8 for the experiment A of dataset Z, as presented in Table 3.3. To calculate NTU and NTU_m values for the rest of the experiments of dataset Z, in this paper, it was assumed that UA and NTU/NTU_m ratio for all the experiments are the same as those of the experiment A.

Table 3.3 Specifications of the experiments of dataset M1 [23] [45]

$\boldsymbol{Exp.}$	$\{\boldsymbol{NTU}, \boldsymbol{NTU_m}\}$	$\boldsymbol{Cr}$	$\boldsymbol{T_{sol,in}}$ $(°\boldsymbol{C})$	**Salt**	$\boldsymbol{X_{sol,in}}$ (%)	$\boldsymbol{W_{sol,in}}$ $(\boldsymbol{g/kg})$	$\boldsymbol{T_{air,in}}$ $(°\boldsymbol{C})$	$\boldsymbol{W_{air,in}}$ $(\boldsymbol{g/kg})$
C&D	$\{3.8, 2.9\}$	$1, \frac{1}{3}, \frac{1}{5}, \frac{1}{7}$	24	$LiCl$	25	10.3	35	17.3
					30	7.7		
					35	5.3		
				$MgCl_2$	35	8.0		
C&H	$\{3.8, 2.9\}$	$1, \frac{1}{3}, \frac{1}{5}, \frac{1}{7}$	24	$LiCl$	34	5.7	35	0.3
H&D	$\{3.8, 2.9\}$	$1, \frac{1}{3}, \frac{1}{5}, \frac{1}{7}$	32	$LiCl$	34	9.1	24	16.5
H&H	$\{3.8, 2.9\}$	$1, \frac{1}{3}, \frac{1}{5}, \frac{1}{7}$	32	$LiCl$	34	9.1	24	3.5

Table 3.4 Specifications of the experiments of dataset M2 [22] [45]

$Exp.$	$\{NTU, NTU_m\}$	Cr	$T_{sol,in}$ ($°C$)	$X_{sol,in}$ (%)	$W_{sol,in}$ (g/kg)	$T_{air,in}$ ($°C$)	$W_{air,in}$ (g/kg)
C&D	{3.5, 2.6}, {4.2,3.3}, {4.9,3.9}	1/7	16	~0	11	35	19
C&H	{3.5, 2.6}, {4.2,3.3}, {4.9,3.9}	1/7	22	~0	16	35	7
H&H	{3.5, 2.6}, {4.2,3.3}, {4.9,3.9}	1/7	30	~0	26	22	8

Table 3.5 Specifications of the experiments of dataset G [11]

Exp	NTU	NTU_m	Cr		$T_{sol,in}$ ($°C$)	$X_{sol,in}$ (%)	$W_{sol,in}$ (g/kg)	$T_{air,in}$ ($°C$)	$W_{air,in}$ (g/kg)
D1	5	3.1	0.25		24	32	6.7	30	14
D2	6	3.7	0.25		24	32	6.8	30	14
D3	7	4.3	0.25		24	32	6.8	30	14
D4	5	3.1	0.25		24	32	6.8	25	14
D5	5	3.1	0.25		24	32	6.8	35	14
D6	5	3.1	0.25		24	32	6.8	30	20
D7	5	3.1	0.25		24	32	6.8	30	8
D8	5	3.1	0.50		24	32	6.7	30	14
D9	5	3.1	0.17		24	32	6.7	30	14
D10	5	3.1	0.25		28	32	8.7	30	14
D11	5	3.1	0.25		32	32	11.1	30	14
D12	5	3.1	0.25		24	37	4.5	30	14
D13	5	3.1	0.25		24	27	9.1	30	14
Min	5	3.1	0.17		24	27	4.5	25	8
Max	7	4.3	0.5		32	37	11.1	35	20

Table 3.6 Specifications of the experiments of dataset Z [18]

Exp	$\dot{m}_{air}$ (kg/h)	$\dot{m}_{sol}$ (kg/h)	NTU	NTU_m	Cr		$T_{sol,in}$ $(°C)$	$X_{sol,in}$ (%)	$W_{sol,in}$ (g/kg)	$T_{air,in}$ $(°C)$	$W_{air,in}$ (g/kg)
A	1.6	1.6	4.4	1.6	0.27		25.1	35.0	5.7	34.8	21.0
B	1.9	1.9	5.2	1.9	0.23		24.9	34.0	6.2	33.9	18.0
C	1.4	1.4	3.8	1.4	0.32		25.3	35.0	5.8	35.2	22.0
D	1.0	1.0	2.7	1.0	0.45		25.2	35.0	5.8	34.9	21.0
E	0.8	0.8	2.1	0.8	0.64		25.2	33.0	6.8	33.7	19.0
F	1.0	1.0	2.7	1.0	0.84		25.5	34.0	6.4	33.8	21.0
G	1.6	1.6	4.4	1.6	0.26		24.5	35.0	5.5	35.3	22.0
H	1.6	1.6	4.5	1.6	0.28		24.6	35.0	5.6	32.8	19.0
I	1.6	1.6	4.5	1.6	0.27		24.6	35.0	5.6	29.8	18.0
J	1.6	1.6	4.5	1.6	0.28		25.6	30.0	8.6	27.2	16.0
K	1.6	1.6	4.4	1.6	0.29		25.4	31.0	8.0	25.7	15.0
Min	0.8	0.8	2.1	0.8	0.23		24.5	30	5.0	25.7	15
Max	1.9	1.9	5.2	1.9	0.84		25.6	35	8.6	35.3	22

3.7.2. Verification against the Numerical Model

The system of ordinary differential equations (ODEs) that describes counter-flow LAMEEs in steady-state operating condition is a boundary-value problem, which is presented in Table 3.9. The numerical solution used in this paper, which is elaborated in the appendix, solves this boundary-value problem to obtain $T_{air,out}$ and $W_{air,out}$ as a function of the inlet operating conditions and the design parameters. In total, 10,000 data points were selected for the verification of the simplified-extended models against the numerical model. NTU, NTU_m, Cr and the salt type of each of these data points were randomly selected from the ranges of the values presented in Table 3.7.

The inlet operating conditions for each of the data points were randomly selected from the range of the values presented in Table 3.8, and the resulting inlet operating conditions are plotted

in Figure 3.5. Half of the data points belong to the dehumidification operating mode and the other half to the regeneration operating mode.

(a)

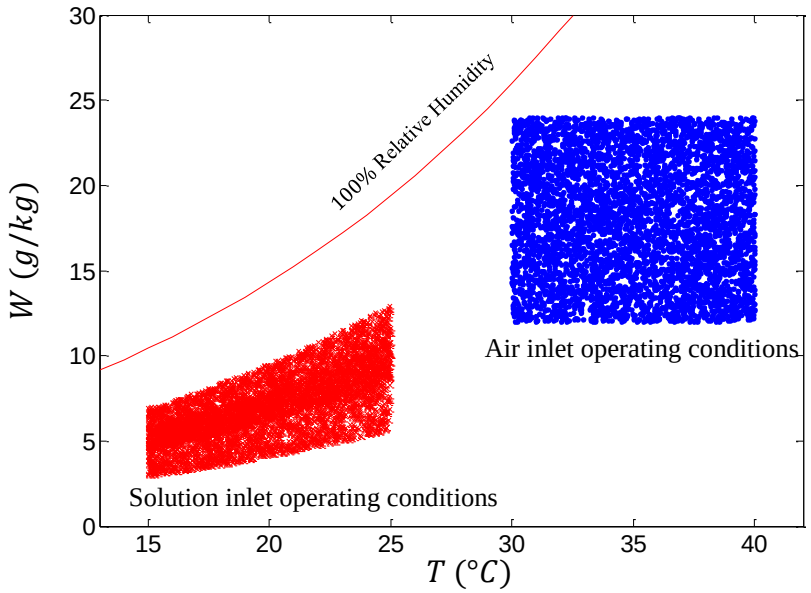

(b)

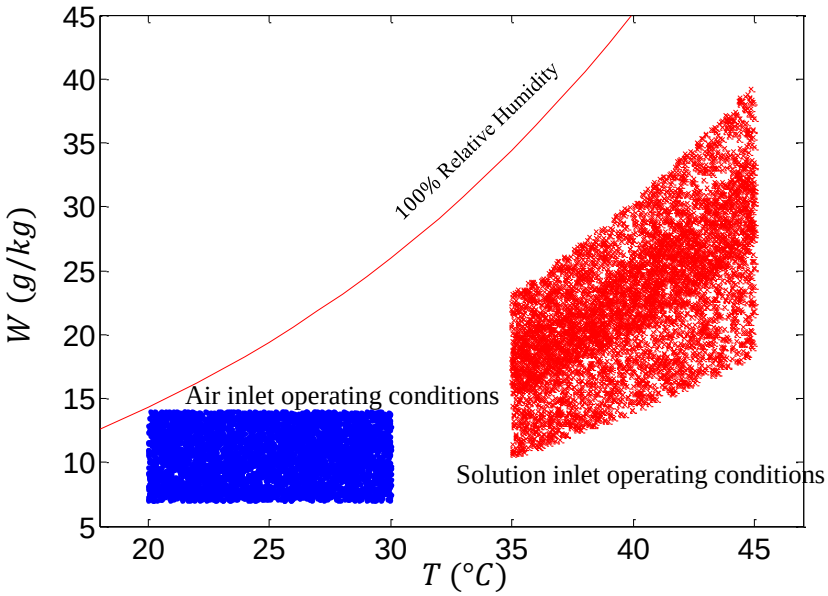

Figure 3.5 The inlet operating conditions of the numerical data points plotted on the psychometric chart for (a) the dehumidification mode and (b) the renegenration mode

The numerical solution directly calculates $T_{air,out}$ and $W_{air,out}$ for each data point. The simplified-extended models can estimate ϵ_s and ϵ_m, which in turn can be used to calculate the estimations for ΔT_{air} and ΔW_{air}, for each data point. The values of ΔT_{air} and ΔW_{air} for each data point as calculated by the numerical solution are plotted against ΔT_{air} and ΔW_{air} as estimated by the simplified-extended models in Figure 3.7 and Figure 3.6. For the 10,000 data points used for the verification, the root-mean-square discrepancies between the numerically calculated values and the estimated values for ΔT_{air} and ΔW_{air} are, respectively, $0.3\,°C$ and $0.2\,g/kg$. The maximum discrepancies between the estimated and numerical values are $2.2\,°C$ and $0.5\,g/kg$ for the dehumidification mode and $1.1\,°C$ and $2.8\,g/kg$ for the regeneration mode.

For comparison, if instead of the estimations for Cr_e and m_e^*, the values for Cr and m_e^* are substituted into the simplified-extended effectiveness models in order to estimate ϵ_s and ϵ_m, and then in turn to estimate ΔT_{air} and ΔW_{air} for each of the 10,000 data points used for the verification, then the root-mean-square discrepancies between these new estimations and the numerically calculated values for ΔT_{air} and ΔW_{air} increase to $1.7\,°C$ and $1.9\,g/kg$. Moreover, the maximum discrepancies between the estimated and numerical values increase to $6.2\,°C$ and $4.0\,g/kg$ for the dehumidification mode and $7.2\,°C$ and $11.2\,g/kg$ for the regeneration mode (i.e. the discrepancies increase by a factor of $5-10$).

It is important to note that, if instead of the estimations for Cr_e and m_e^*, the exact values for Cr_e and m_e^* (calculated by using both the inlet and the numerically calculated outlet operating conditions of each data point) were substituted into the simplified-extended effectiveness models, there would have been little reduction in the maximum discrepancy between the numerical results and the estimations for ΔT_{air} and ΔW_{air}. However, if the profiles of T_{air} and W_{air} were approximately linear along the exchanger, then the estimations of the simplified-extended

effectiveness models, obtained by using the exact values of Cr_e and m_e^*, should have closely matched the numerical results. Thus, it can be concluded that the main reason for the higher discrepancies between the numerical results and the estimations of the simplified-effectiveness models for some data points is that the assumption of linear profiles of T_{air} and W_{air} for those data points is not entirely accurate. A method to improve the accuracy of the estimations for ΔT_{air} and ΔW_{air} for such data points could be dissecting the exchanger along its length to more than one section, and applying the simplified-extended models for each section, because in doing so the profiles of T_{air} and W_{air} can be better approximated as linear profiles.

Table 3.7 The range of the design parameters for the numerical data points

NTU	NTU_m/NTU	Cr	$Salt\ Solution$
$1-6$	$0.2-0.8$	$0.1-0.5$	$LiCl\ , MgCl_2$

Table 3.8 The range of the inlet operating conditions of the numerical data points

Operating Mode	$T_{air,in}$	$W_{air,in}$	$T_{sol,in}$	$X_{sol,in}$
Dehumidification	$30-40$	$12-24$	$15-25$	$25-35$
Regeneration	$20-30$	$7-14$	$35-45$	$25-35$

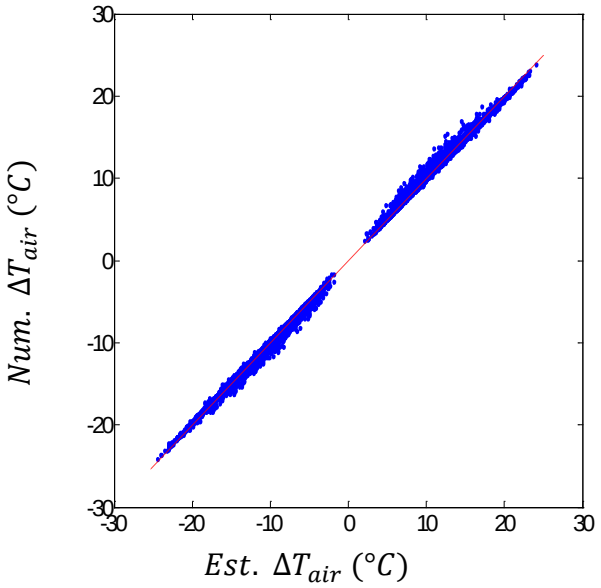

Figure 3.6 Comparison between the numerically calculated values and the estimations for ΔT_{air} for the numerical data points with design parameters Table 3.7 of and inlet operating conditions of Table 3.8

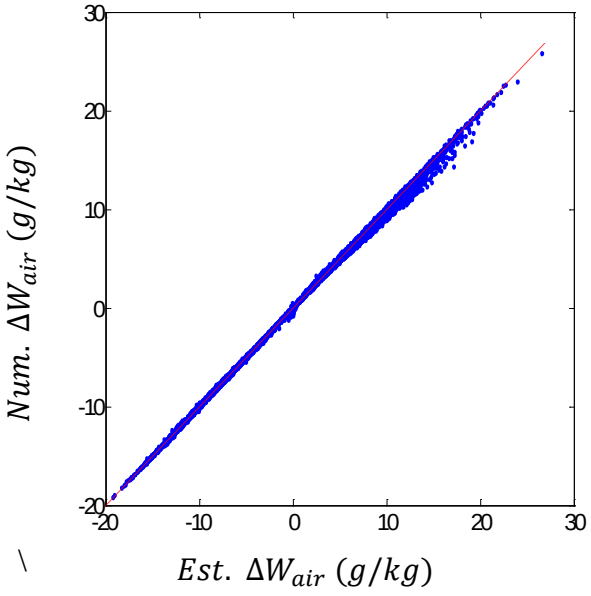

Figure 3.7 Comparison between the numerically calculated values and the estimations for ΔW_{air} for the numerical data points with design parameters Table 3.7 of and inlet operating conditions of Table 3.8

3.8. Conclusions

In section 3.3., it was demonstrated that if the ratio ϵ_s/ϵ_m is provided, then the exact values for Cr_e and m_e^* can be calculated as a function of the inlet operating conditions and the design parameters of LAMEEs using Eq. (3.47) and Eq. (3.50). However, in lieu of the exact value for the ratio ϵ_s/ϵ_m (which is known only if the air outlet operating conditions are available), it was proposed that the ratio ϵ_s/ϵ_m could be assumed to be equal to the approximation of Eq. (3.48), which expresses the ratio ϵ_s/ϵ_m at $Cr_e = m_e^* = 0$. Then, Cr_e, $m_{e,in}^*$ and $m_{e,IWD}^*$, could be estimated per Eq.(3.49), Eq. (3.53) and Eq. (3.54), as a function of only the design parameters and the inlet operating conditions. Finally, provided with the estimations for $m_{e,in}^*$ and $m_{e,IWD}^*$, m_e^* can be calculated per Eq. (3.50). Then, these equations were used to estimate Cr_e and m_e^* for the data points of the experimental data sets M1, M2, G and Z (as discussed in section 4.1.), and also for the 10,000 randomly generated numerical data points belonging to different designs of LAMEEs working either in the dehumidification or in the regeneration mode (as discussed in section 4.2). Finally, these estimations for Cr_e and m_e^* were substituted into the simplified-extended $\epsilon - NTU$ and $\epsilon_m - NTU_m$ models, Eq. (3.3) and Eq. (3.4), to obtain ϵ_s and ϵ_m, and, in turn, to obtain ΔT_{air} and ΔW_{air} of these experimental and numerical data points. The comparison between the estimations and the experimental and numerical data points showed that the estimated ΔT_{air} and ΔW_{air}, which were obtained using the simplified-extended models as a function of the inlet operating conditions and the design parameters of each data point, could account for more than 97% the variation in the experimentally measured or the numerically calculated changes in the temperature and humidity ratio of the air stream, i.e. ΔT_{air} and ΔW_{air}.

3.9. Future Research

In this paper, the validation of the simplified-extended models was limited to the operating conditions typical for summer air-conditioning applications, because the experimental data available for other applications were limited. Provided with an extended range of experimental data, the application of the simplified-extended models for evaluating the performance of LAMEEs can be validated for an extended range of air-conditioning applications. Moreover, it is worthwhile to investigate whether, in addition to LAMEEs, the simplified-extended models can be used to evaluate the performance of other equipment with coupled heat and moisture exchange, such as cooling towers. A common approach for decreasing the discrepancy between the approximate solutions of the differential equations and the numerical solutions of the same is to divide the problem into more than one interval along the independent variable, i.e. length of the exchanger in this paper, and apply the approximate solution to each section [28]. It should be worthwhile to investigate if the accuracy of the simplified-extended models can be increased by adopting this approach.

3.10. Appendix: The Numerical Model

To solve the boundary value problem for counter-flow LAMEEs, a shooting method was used. First, it was assumed that for each sample data point, in addition to the solution inlet operating conditions, $T_{sol,in}$ and $X_{sol,in}$, the air outlet operating conditions $T_{air,out}$ and $W_{air,out}$ were also available. Then, the problem was changed into solving a system of ODEs with prescribed initial-values for the air and the solution streams. To solve this system of ODEs, 'ode45' function in MATLAB™ [50] was used, which is an implementation of the Runge-Kutta formula [51]. For each assumed pair of $T_{air,out}$ and $W_{air,out}$, the solution of this system of ODEs results in a corresponding set of calculated $T_{sol,out}$ and $X_{sol,out}$, $T_{air,in}$ and $W_{air,in}$. Then, the function

'lsqnonlin' in MATLAB was used to find the pair of $T_{air,out}$ and $W_{air,out}$ that result in a corresponding pair of calculated $T_{air,in}$ and $W_{air,in}$ that are the same as the actual inlet temperature and humidity ratio of the air stream; this pair of $T_{air,out}$ and $W_{air,out}$ is the solution to the boundary-value problem. To increase the speed of shooting process, the initial starting point for the 'lsqnonlin' function was set to the pair of $T_{air,in}$ and $W_{air,in}$ that are obtained using the simplified-extended effectiveness models for each sample data point. As an alternative approach to the shooting method for finding the outlet conditions for a counter-flow exchange, one can solve the transient heat and mass transfer problem and then find the steady-state response of the transient system of ODEs by marching through time. To calculate W_{sol} for the numerical solution, Eq. (2.28) was used, with the correlations by Conde [33] and Cisternas and Lam [38] used to calculate p_v of $LiCl$ and $MgCl_2$ desiccant solutions, respectively. The calculations of this numerical model for the outlet operating conditions of the air and solution streams closely matches the experimental data for LAMEEs working in the dehumidification mode and also the results provided by the numerical model previously developed for LAMEEs by Seyed-Ahmadi et. al [44].

Table 3.9 System of ODEs and the boundary conditions for counter-flow LAMEEs

Differential Equations	Boundary Conditions
$dq_s = C_{air}\, NTU\, (T_{sol} - T_{air})_l\, dl$ $d\dot{m}_W = \dot{m}_{air}\, NTU_m\, (W_{sol} - W_{air})_l\, dl$ $\frac{dW_{air}}{dl} = \frac{1}{\dot{m}_{air}} \frac{d\dot{m}_W}{dl}$ $\frac{dX_{sol}}{dl} = \frac{X_{sol}}{\dot{m}_{sol}} \frac{d\dot{m}_W}{dl}$ $\frac{dT_{air}}{dl} = \frac{1}{C_{air}} \frac{dq_s}{dl}$ $\frac{dT_{sol}}{dl} = \frac{1}{C_{sol}} \left(\frac{dq_s}{dl} + h_{fg} \frac{d\dot{m}_W}{dl} \right)$	$T_{sol} = T_{sol,in}$ @ $l = 1$ $X_{sol} = X_{sol,in}$ @ $l = 1$ $T_{air} = T_{air,in}$ @ $l = 0$ $W_{air} = W_{air,in}$ @ $l = 0$

Chapter 4

Summary, conclusions and future research

This thesis had two main objectives: (a) to identify and introduce a new set of dimensionless parameters to which the effectiveness of LAMEEs for heat and moisture exchange can be correlated, and (b) to develop methods to predict the effectiveness of LAMEEs based on these new dimensionless parameters. The new dimensionless parameters effective heat capacity rate ratio Cr_e and effective mass flow rate ratio m_e^* were introduced in chapter 2 (as analogs of the dimensionless parameter heat capacity rate ratio Cr). Cr_e and m_e^* were defined per Eq. (2.5) and Eq. (2.9), as follows

$$Cr_e = -\frac{T_{sol,out} - T_{sol,in}}{T_{air,out} - T_{air,in}} \tag{4.1}$$

$$m_e^* = -\frac{W_{sol,out} - W_{sol,in}}{W_{air,out} - W_{air,in}} \tag{4.2}$$

The analogs of the standard $\epsilon - NTU$ model were also developed in chapter 2 as models that can correlate the effectiveness of LAMEEs for heat and moisture exchange to the dimensionless parameters Cr_e and m_e^*. These analogs were termed the simplified-extended $\epsilon - NTU$ and $\epsilon_m - NTU$ models, and were presented by Eq. (2.37) and Eq. (2.42). Using the definitions for ϵ_s and ϵ_m, Eq. (2.1) and Eq. (2.2), the simplified-extended effectiveness models result in the followings

$$\epsilon_s = \frac{T_{air,out} - T_{air,in}}{T_{sol,in} - T_{air,in}} = \frac{1 - \exp[-NTU\ (1 - Cr_e)]}{1 - Cr_e\ \exp[-NTU\ (1 - Cr_e)]} \tag{4.3}$$

$$\epsilon_m = \frac{W_{air,out} - W_{air,in}}{W_{sol,in} - W_{air,in}} = \frac{1 - \exp[-NTU_m\ (1 - m_e^*)]}{1 - m_e^*\ \exp[-NTU_m\ (1 - m_e^*)]} \tag{4.4}$$

where NTU and NTU_m are the dimensionless parameters number of heat transfer units and number of moisture transfer units, defined per Eq. (2.34) and Eq. (2.41), respectively, as follows

$$NTU = \frac{UA}{C_{air}} \tag{4.5}$$

$$NTU_m = \frac{U_m A}{\dot{m}_{air}} \tag{4.6}$$

Then, in section 2.7, it was demonstrated that the simplified-extended $\epsilon - NTU$ model can correlate the effectiveness of LAMEEs for heat exchange ϵ_s to NTU and Cr_e, and the simplified-extended $\epsilon_m - NTU_m$ model can correlate the effectiveness of LAMEEs for moisture exchange ϵ_m to NTU_m and m_e^*. However, to calculate Cr_e and m_e^* per Eq. (4.1) and Eq. (4.2), in addition to the inlet operating conditions of both of the streams, the outlet operating conditions of the air stream is also needed, which is an inconvenience for design purposes.

In section 3.6, a set of methods were developed to estimate Cr_e and m_e^* as a function of inlet operating conditions of the air and solution streams and design parameters (LAMEEs' geometric ratios and material properties), with a summary of these methods provided in section 3.6.4. Cr_e was expressed in Eq. (3.47) as a function of the ratio ϵ_s/ϵ_m, the design parameters and the inlet operating conditions; similarly, m_e^* was correlated to the dimensionless parameters NTU_m, $m_{e,in}^*$ and $m_{e,IWD}^*$ in Eq. (3.50), as follows

$$Cr_e = Cr\left(1 + H^* \frac{\epsilon_m}{\epsilon_s}\right) \tag{4.7}$$

$$m_e^* = m_{e,in}^* \frac{exp\left(m_{e,IWD}^* \epsilon_m\right) - 1}{m_{e,IWD}^* \epsilon_m} \tag{4.8}$$

where the parameters $m_{e,in}^*$ and $m_{e,IWD}^*$ were expressed in Eq. (3.51) and Eq. (3.52) as a function of the ratio ϵ_s/ϵ_m, the design parameters and the inlet operating conditions, as follows

$$m^*_{e,in} = \left[Cr \, \frac{h_{fg}}{c_{p,air}} \left(\frac{1}{H^*} \frac{\epsilon_s}{\epsilon_m} + 1 \right) \right] \beta \, W_{sol,in} \tag{4.9}$$

$$m^*_{e,IWD} = \left[Cr \, \frac{h_{fg}}{c_{p,air}} \left(\frac{1}{H^*} \frac{\epsilon_s}{\epsilon_m} + 1 \right) \right] \beta \left(W_{air,in} - W_{sol,in} \right) \tag{4.10}$$

and H^* is the operating factor, defined per Eq. (3.30), as follows

$$H^* = \frac{h_{fg}}{c_{p,air}} \frac{W_{sol,in} - W_{air,in}}{T_{sol,in} - T_{air,in}} \tag{4.11}$$

However, in lieu of the exact value for the ratio ϵ_s/ϵ_m (which is known only if the air outlet operating conditions are available), it was proposed that the ratio ϵ_s/ϵ_m could be assumed to be equal to the approximation of Eq. (3.48), which expresses the ratio ϵ_s/ϵ_m at $Cr_e = m^*_e = 0$. That is, it was proposed to assume that

$$\frac{\epsilon_m}{\epsilon_s} \cong \left(\frac{\epsilon_m}{\epsilon_s} \right)_{@\, Cr_e = m^*_e = 0} = \frac{1 - \exp(-NTU_m)}{1 - \exp(-NTU)} \tag{4.12}$$

Then, Cr_e, $m^*_{e,in}$ and $m^*_{e,IWD}$, can be estimated per Eq. (4.7), Eq. (4.9) and Eq. (4.10), as a function of only the design parameters and the inlet operating conditions. Finally, provided with the estimations for $m^*_{e,in}$ and $m^*_{e,IWD}$, a first estimation for m^*_e can be calculated by solving Eq. (4.8) for m^*_e. (Noting that ϵ_m in Eq. (4.8) is a function of m^*_e and NTU_m. As seen in Eq. (4.4), it becomes evident that an iterative method is required to solve for m^*_e.) A sample calculation based on these steps is presented in Appendix B.

Finally, these methods were used to estimate Cr_e and m^*_e for a number of experimental and a large number of numerical data points[2]. These estimated Cr_e and m^*_e values were substituted into

[2] The MATLAB™ scripts and functions used to implement the numerical solution are provided in Appendix A.

the simplified-extended $\epsilon - NTU$ and $\epsilon_m - NTU$ models in order to predict ϵ_s and ϵ_m for each data point. The predicted ϵ_s and ϵ_m were, in turn, used to estimate the change in the temperature and humidity ratio of the air stream inside the LAMEEs, i.e. ΔT_{air} and ΔW_{air}, for each data point. The discrepancies between these predictions for ΔT_{air} and ΔW_{air} and the measured or the numerically calculated values were less than less than $2.1\ °C$ and $2.8\ g/kg$.

4.1. Conclusions

In this thesis, it was concluded that LAMEEs operate analogously to heat exchangers for which Cr is dependent on the inlet operating conditions. Furthermore, it was demonstrated that if the concept of heat capacity rate ratio is properly extended to the coupled heat and moisture exchanger in LAMEEs, then it becomes possible to use models analogous to the standard $\epsilon - NTU$ model to predict the change in the temperature and humidity ratio of the air stream inside different designs of LAMEEs over a wide range of operating conditions pertaining to summer air-conditioning applications as a function of the inlet operating conditions and design parameters.

4.2. Future Research

In this paper, the application of the simplified-extended effectiveness models for predicting the performance of counter-flow LAMEEs was presented. As a next step, development of methodical design procedures for LAMEEs based on these models can be pursued. Furthermore, application of these models to LAMEEs with other flow arrangements (e.g. parallel flow and cross flow), and also other equipment with coupled heat and moisture exchange (e.g. cooling towers) can be investigated.

Another objective for future research can be improvement of the accuracy of the simplified-extended effectiveness models. In chapter 2, it was proved that if the profiles of temperature and

humidity ratio of the air stream inside LAMEEs are linear, the simplified-extended effectiveness models provide an exact solution for the heat and moisture exchange effectiveness of LAMEEs. However, it is known that these profiles not only can deviate from the assumed linear form, but there might be even an inflection in the profiles of the temperature and humidity ratio of the air stream inside LAMEEs. To account for the possible deviations of these profiles from the assumed linear form, one solution is to divide the exchanger into smaller intervals along its length and apply the simplified-extended effectiveness models to each interval, which is similar to the approach taken by Jaber and Webb for analysis of the coupled heat and moisture exchange in cooling towers [28].

References

[1] B. Erb, 2009, *Run-Around Membrane Energy Exchanger Performance and Operational Control Strategies,* Saskatoon: University of Saskatchewan.

[2] G. Ge, M. R. H. Abdel-Salam, R. W. Besant and C. J. Simonson, 2013, "Research and applications of liquid-to-air membrane energy exchangers in building HVAC systems at University of Saskatchewan: A review," *Renewable and Sustainable Energy Reviews,* vol. 26, p. 464–479.

[3] M. Rasouli, S. Akbari and C. J. B. R. W. Simonson, 2014, "Energetic, economic and environmental analysis of a health-care facility HVAC system equipped with a run-around membrane energy exchanger," *Energy and Buildings,* vol. 69, p. 112–121.

[4] Office of Energy Efficiency, Natural Resources Canada, 2012, "Energy Efficiency Trends in Canada 1990 to 2009," Natural Resources Canada, Ottawa.

[5] K. Daou, R. Wang and Z. Xia, 2006, "Desiccant cooling air conditioning: a review," *Renewable and Sustainable Energy Reviews,* vol. 10, no. 2, p. 55–77.

[6] R. K. Shah and D. P. Sekulic, 2003, Fundamentals of Heat Exchanger Design, John Wiley & Sons, Inc.

[7] F. P. Incropera and D. P. DeWitt, 1985, Fundamental of Heat and Mass Transfer, second ed., New York: Wiley.

[8] ASHRAE, ANSI/ASHRAE Standard 84-2013, 2013, Method of Testing Air-to-Air Heat/Energy Exchangers (ANSI Approved), Atlanta: American Society of Heating, Refrigerating and Air-Conditioning Engineers, Inc.

[9] B. Erb, C. J. Simonson, M. Seyed-Ahmadi and R. W. Besant, 2009, "Experimental Measurements of a Run-Around Membrane Energy Exchanger (RAMEE) with Comparison to a Numerical Model," *ASHRAE Transactions,* vol. 115, pp. 689-705.

[10] R. Namvar, D. Pyra, G. Ge, C. J. Simonson and R. W. Besant, 2012, "Transient characteristics of a liquid-to-air membrane energy exchanger (LAMEE) experimental data with correlations," *International Journal of Heat and Mass Transfer,* p. 6682–6694.

[11] G. Ge, D. G. Moghaddam, A. H. Abdel-Salam, R. W. Besant and C. J. Simonson, 2014, "Comparison of experimental data and a model for heat and mass transfer performance of a liquid-to-air membrane energy exchanger (LAMEE) when used for air dehumidification and salt solution regeneration," *International Journal of Heat and Mass Transfer,* p. 119–131.

[12] K. Mahmud, G. Mahmood, C. Simonson and R. Besant, 2010, "Performance testing of a counter-cross-flow run-around membrane energy exchanger (RAMEE) system for HVAC applications," *Energy and Buildings,* vol. 42, pp. 1139-1147.

[13] A. Vali, C. J. Simonson, R. W. Besant and G. Mahmood, 2009, "Numerical model and effectiveness correlations for a run-around heat recovery system with combined counter and cross flow exchangers," *International Journal of Heat and Mass Transfer,* vol. 52, no. 25-26, p. 5827–5840.

[14] M. Seyed-Ahmadi, B. Erb, S. J. Carey and R. W. Besant, 2009, "Transient behavior of run-around heat and moisture exchanger system. Part I: Model formulation and verification," *International Journal of Heat and Mass Transfer,* vol. 52, no. 25-26, p. 6000–6011.

[15] H. Hemingson, C. Simonson and R. Besant, 2011, "Steady-state performance of a run-around membrane energy exchanger (RAMEE) for a range of outdoor air conditions," *International Journal of Heat and Mass Transfer,* vol. 54, pp. 1814-1824.

[16] S. Akbari, C. Simonson and R. Besant, 2012, "Application of neural networks to predict the transient performance of a Run-Around Membrane Energy Exchanger for yearly non-stop operation," *International Journal of Heat and Mass Transfer,* vol. 55, p. 5403–5416.

[17] S. Akbari, H. B. Hemingson, D. Beriault, C. J. Simonson and R. W. Besant, 2012, "Application of neural networks to predict the steady state performance of a Run-Around Membrane Energy Exchanger," *International Journal of Heat and Mass Transfer,* vol. 55, no. 5-6, p. 1628–1641.

[18] L. Z. Zhang, 2011, "An Analytical Solution to Heat and Mass Transfer in Hollow Fiber Membrane Contactors for Liquid Desiccant Air Dehumidification," *ASME, Journal of Heat Transfer,* vol. 133, pp. 092001-1–092001-8.

[19] C. B. Field, V. R. Barros, D. Dokken, K. J. Mach, M. D. Mastrandrea, T. E. Bilir, M. Chatterjee, K. L. Ebi, Y. O. Estrada, R. C. Genova, B. Girma, E. S. Kissel, A. N. Levy, S. MacCracken, P. R. Mastrandrea and L. L. White, IPCC, 2014: Climate Change 2014: Impacts, Adaptation, and Vulnerability. Working Group II Contribution to the Fifth

Assessment Report of the Intergovernmental Panel on Climate Change, Cambridge University Press (in press).

[20] ASHRAE, 2007, Air Conditioning System Design Manual, 2nd ed., Burlington: Butterworth-Heinemann.

[21] A. H. Abdel-Salam, G. Ge and C. J. Simonson, 2013, "Performance analysis of a membrane liquid desiccant air-conditioning system," *Energy and Buildings,* vol. 62, p. 559–569.

[22] D. G. Moghadam, P. LePoudre, G. Ge, R. W. Besant and C. Simonson, 2013, "Small-scale single-panel liquid-to-air membrane energy exchanger (LAMEE) test facility development, commissioning and evaluating the steady-state performance," *Energy and Buildings,* no. 66, pp. 424-436.

[23] D. G. Moghadam, P. LePoudre, R. W. Besant and C. Simonson, 2013, "Steady-State Performance of a Small-Scale Liquid-to-Air Membrane Energy Exchanger for Different Heat and Mass Transfer Directions, and Liquid Desiccant Types and Concentrations: Experimental and Numerical Data," *Journal of Heat Transfer*, vol. 135.

[24] F. Incropera and D. DeWitt, 1985, Fundamental of Heat and Mass Transfer, second ed., New York: Wiley.

[25] C. J. Simonson and R. W. Besant, 1999, "Energy wheel effectiveness: part I—development of dimensionless groups," *International Journal of Heat and Mass Transfer,* vol. 42, no. 12, p. 2161–2170.

[26] C. J. Simonson and R. W. Besant, 1999, "Energy wheel effectiveness: part II—correlations," *International Journal of Heat and Mass Transfer,* vol. 12, no. 42, p. 2171–2185.

[27] L. Z. Zhang and J. L. Niu, 2002, " Effectiveness Correlations for Heat and Moisture Transfer Processes in an Enthalpy Exchanger With Membrane Cores," *Journal of Heat Transfer,* vol. 124, no. 5, pp. 922-929.

[28] H. Jaber and R. L. Webb, 1989, "Design of Cooling Towers by the Effectiveness-NTU Method," *Journal of Heat Transfer,* vol. 111, no. 4, pp. 837-843.

[29] ASHRAE, 2013, ASHRAE Handbook-Fundamentals, Atlanta: American Society of Heating, Refrigerating and Air-Conditioning Engineers, Inc.

[30] G. P. Narayan, K. H. Mistry, M. H. Sharqawy, S. M. Zubair and J. H. Lienhard V, 2010, "Energy Effectiveness of Simultaneous Heat and Mass Exchange Devices," *Frontiers in Heat and Mass Transfer*.

[31] D. Ghadiri Moghaddam, A. Oghabi, G. Ge, R. W. Besant and C. J. Simonson, 2013, "Numerical model of a small-scale liquid-to-air membrane energy exchanger: Parametric study of membrane resistance and air side convective heat transfer coefficient," *Applied Thermal Engineering,* vol. 61, no. 2, p. 245–258.

[32] R. K. Shah and D. P. Sekulic, 2003, Fundamentals of Heat Exchanger Design, John Wiley & Sons, Inc.

[33] M. Conde, 2004, "Properties of aqueous solutions of lithium and calcium chlorides: formulations for use in air conditioning equipment design," *International Journal of Thermal Sciences,* vol. 43, p. 367–382.

[34] I. D. Zaytsev and G. Aseyev, 1992, Properties of Aqueous Solutions of Electrolytes, Boca Raton, FL: CRC Press.

[35] ASHRAE, 2013, ASHRAE Handbook-Fundamentals, Atlanta: American Society of Heating, Refrigerating and Air-Conditioning Engineers, Inc.

[36] L. Z. Zhang, S. M. Huang, J. H. Chi and L. X. Peia, 2012, "Conjugate heat and mass transfer in a hollow fiber membrane module for liquid desiccant air dehumidification: A free surface model approach," *International Journal of Heat and Mass Transfer,* vol. 55, no. 13-14, p. 3789–3799.

[37] S. M. Huang, L. Z. Zhang, K. Tang and L. X. Peia, 2012, "Fluid flow and heat mass transfer in membrane parallel-plates channels used for liquid desiccant air dehumidification," *International Journal of Heat and Mass Transfer,* vol. 55, no. 9-10, p. 2571–2580.

[38] L. A. Cisternas and E. J. Lam, 1991, "Analytic Correlation for the Vapour Pressure of Aqueous and Non-Aqueous Solutions of Single and Mixed Electrolytes. Part II. Application and Extension," *Fluid Phase Equilibria,* vol. 62, pp. 11-27.

[39] A. Oghabi, D. Ghadiri Moghaddam, C. J. Simonson and R. W. Besant, 2013, "Measurement of Heat Transfer Enhancement and Pressure Drop Across Eddy Promoter Air Screens in a

Liquid-to-Air-Membrane Energy Exchanger (LAMEE)," in *ASME 2013 Heat Transfer Summer Conference*, Minneapolis, MN.

[40] A. H. Abdel-Salam, G. Ge and C. J. Simonson, 2013, "Performance analysis of a membrane liquid desiccant air-conditioning system," *Energy and Buildings,* vol. 62, p. 559–569.

[41] ASHRAE, 2007, Air Conditioning System Design Manual, 2nd ed., Burlington: Butterworth-Heinemann.

[42] K. Daou, R. Wang and Z. Xia, 2006, "Desiccant cooling air conditioning: a review," *Renewable and Sustainable Energy Reviews,* vol. 10, no. 2, p. 55–77.

[43] H. Kamali, G. Ge, R. W. Besant, C. J. Simonson, "Extension of the Concepts of Heat Capacity Rate Ratio and Effectiveness-NTU Model to the Coupled Heat and Moisture Exchange in Liquid-to-Air Membrane Energy Exchangers," to be submitted to *ASME Journal of Heat Transfer*

[44] M. Seyed-Ahmadi, B. Erb, S. J. Carey and R. W. Besant, 2009, "Transient behavior of run-around heat and moisture exchanger system. Part I: Model formulation and verification," *International Journal of Heat and Mass Transfer,* vol. 52, no. 25-26, p. 6000–6011.

[45] D. Ghadiri Moghaddam, A. Oghabi, G. Ge, R. W. Besant and C. J. Simonson, 2013, "Numerical model of a small-scale liquid-to-air membrane energy exchanger: Parametric study of membrane resistance and air side convective heat transfer coefficient," *Applied Thermal Engineering,* vol. 61, no. 2, p. 245–258.

[46] R. K. Shah and D. P. Sekulic, 2003, Fundamentals of Heat Exchanger Design, John Wiley & Sons, Inc.

[47] ASHRAE, 2005, ASHRAE Handbook - Fundamentals, Atlanta: American Society of Heating, Refrigerating and Air Conditioning, Engineers Inc.

[48] I. D. Zaytsev and G. Aseyev, 1992, Properties of Aqueous Solutions of Electrolytes, Boca Raton, FL: CRC Press.

[49] F. Incropera and D. DeWitt, 1985, Fundamental of Heat and Mass Transfer, second ed., New York: Wiley.

[50] MathWorks, Inc., *MATLAB Release 2013a*, Natick, MA.

[51] J. R. Dormand and P. J. Prince, 1980, "A family of embedded Runge-Kutta formulae," *J. Comp. Appl. Math.*, vol. 6, p. 19–26.

[52] D. Kadylak, P. Cave and W. Mérida, 2009, "Effectiveness correlations for heat and mass transfer in membrane humidifiers," *International Journal of Heat and Mass Transfer,* vol. 52, no. 5-6, p. 1504–1509.

Appendix A: MATLAB Codes

This appendix includes the MATLAB [50] functions and scripts that were developed by the author to implement the numerical solution for LAMEEs.

- **The script that creates the random data points and the respective numerical solutions and the predictions provided by the simplified-extended effectiveness models**

```
% Creates random data points and invokes the numerical solution to calculate the numerical outlet data and the simplified-extended effectiveness models to calculate the estimated outlet data, for each data point for the stead state operating conditions

clc
% clears the MATLAB command screen
clear
% clears all the variables

global gTau gTair gWair gTsol gXsol;
% defines the global variables that will be accessible to all the functions
% gTau is the variable that holds the dimensionless points along the exchanger at which discretization is applied
% gTair, gWair, gTsol and gXsol are, respectively, the temperature and humidity ratio profiles of the air stream and temeprature and concetration profiles of the solution stream, along the exchange

m = 1
n = 5000
% total number of data points equals to n-m+1

for p = m:n
% the loop to generate the random inlet operating conditions and design paramerters for the data points
  Cr_(p)= random('unif',0.1,0.5);
  % assigns the heat capacity rate ratio
  NTU_(p) = random('unif',1,6);
  % assigns the NTU
  NTU_ratio_(p) = random('unif',0.2,0.8);
  % assigns the ratio NTU_m/NTU
  NTU_m(p) = NTU_(p) * NTU_ratio_(p);
  % calculates and assigns NTU_m

  if random('unif',0,2) >= 1
     salt_{p} = 'LiCl';
  else
     salt_{p} = 'MgCl2';
  end
  % assigns the salt type

  Tsol_in_(p) = random('unif',15,25);
  % assigns the inlet solution temperature
  Xsol_in_(p) = random('unif',25,35);
  % assigns the inlet solution concentration
```

```
  Wsol_in_(p) = W(VP(salt_{p}, Tsol_in_(p), Xsol_in_(p)));
  % calculates and assigns the inlet solution equilibirum humidity ratio

  Tair_in_(p) = random('unif', 30,40);
  % assigns the inlet air temperature
  Wair_in_(p) = random('unif',12,24);
  % assigns the inlet air humidity ratio

  h_fg(p) = 2.501 - 0.0024 * Tsol_in_(p);
  % calculates and assigns the specific heat of evaporation
  cp_sol(p) = HeatCapacity(salt_{p}, (Tsol_in_(p)), Xsol_in_(p));
  % calculates and assigns the specific heat of solution
  h_star(p) = h_fg(p) * ( Wsol_in_(p) - Wair_in_(p))/(Tsol_in_(p) - Tair_in_(p));
  % calculates and assigns h_star

end

for p=m:n
% the loop for numerical calculations and also estimations of the simplified-extended
% method for outlet air operating conditions

  % start of the calculations for the estimations provided by the simplified-extended effectiveness models
  mse_in_MX(p) = 0.058 * Wsol_in_(p) * Cr_(p) * h_fg(p);
  % calculates and assigns mse_in_MX
  mse_IWD_MX(p) = 0.058 * (Wair_in_(p)-Wsol_in_(p)) * Cr_(p) * h_fg(p);
  % calculates and assigns mse_IWD_MX
  f = @(x) (x - m_star_e_de(mse_in_MX(p), mse_IWD_MX(p), NTU_m(p),x));
  % assigns the function f which will be solved to find x, where x is the m_star_e_MX
  fval = 0.01;
  % sets the initial residue of the solver
  trial = 1;
  % initializes the number of trials to 1
  options = optimset('Display','off');
  % sets the display option to off
  while fval>=0.01 && trial <= 150
  % the loop that will continue for at most 150 trials until fval is less than 0.01
    if trial == 1
    % for the first trial, the starting point of the solver is set to x=20
    % m_star_e_decoupled is the variable that represents the solution for x, which in turn is m_star_e_MX
      [m_star_e_decoupled(p),fval] = lsqnonlin(f, 20,-100,100,options);
    else
    % for the other trials, the starting point of the solver is randomly selected between -100 and 100
      [m_star_e_decoupled(p),fval] = lsqnonlin(f, random('unif',-100,100),-1e3,1e3,options);
    end
    trial = trial+1;
    % increases the trial number after each attempt to solve for x
  end

  eff_r(p) = eff(NTU_m(p),0)/eff(NTU_(p),0);
  % calculates and assigns the approximation for the ratio e_m/e_s


  Cr_e_emp(p) = Cr_(p) * (1 + h_star(p) * eff_r(p));
  % calculates and assigns the estimated Cr_e
```

```
eff_s_emp(p) = eff(NTU_(p), Cr_e_emp(p));
% calculates and assigns eff_s estimated based on the estimated Cr_e
dTair_emp(p) = eff_s_emp(p)*(Tsol_in_(p) - Tair_in_(p));
% calculates and assigns dTair (change in the temperature of the air stream) estimated based on the estimated eff_s


mse_in(p) = 0.058 * Wsol_in_(p) * Cr_(p) * h_fg(p) * (1+1/(h_star(p) * eff_r(p)));
% calculates and assigns mse_in
mse_IWD(p) = 0.058 * (Wair_in_(p)-Wsol_in_(p)) * Cr_(p) * h_fg(p) * (1 + 1 /(h_star(p) * eff_r(p)));
% calculate and assigns mse_IWD
f = @(x) (x - m_star_e_de(mse_in(p), mse_IWD(p), NTU_m(p),x));
% assigns the function f which will be solved to find x, where x is the m_star_e

fval = 0.1;
trial = 1;
options = optimset('Display','off');
while fval>=0.01 && trial <= 150
   if trial == 1
   % m_star_e_coupled is the variable that represents the solution for x, which in turn is m_star_e
      [m_star_e_coupled(p),fval] = lsqnonlin(f, 20,-100,100,options);
   else
      [m_star_e_coupled(p),fval] = lsqnonlin(f, random('unif',-100,100),-1e3,1e3,options);
   end
   trial = trial+1;
end
if fval>0.1
% if the residua of the solver is greater than 0.1, sets fail flag to 1
   failed_emp(p)=1;
else
   failed_emp(p)=0;
end

eff_m_emp(p) = eff(NTU_m(p), m_star_e_coupled(p));
% calculates and assigns eff_m based on the estimated values for m_star_e
dWair_emp(p) = eff_m_emp(p)*(Wsol_in_(p) - Wair_in_(p));
% calculates and assigns dWair (change in the humidity ratio of the air stream) based on the estimated eff_m
dHair_emp(p) = dTair_emp(p) + h_fg(p) * dWair_emp(p);
% calculates and assigns dHair based on the estimated  dTair and dWair

Tair_out_emp (p) = Tair_in_(p) + dTair_emp(p);
% calcualtes and assigns Tair_out based on the estimated dTair
Wair_out_emp (p) = Wair_in_(p) + dWair_emp(p);
% calculates and assigns Wair_out based on the estimated dWair
% the calculations for the estimations provided by the simplified-extended effectiveness models end here


% Calculations for the numerical model start here
fval = 0.1;
trial = 1;
while fval>=0.1 && trial <= 50
   if trial == 1
      % 1st guess solution = empirical output
      x01 = Tair_out_emp (p);
      x02 = Wair_out_emp (p);
```

```
        trial_emp = [p, x01, x02]
    else
        % other guess solutions = randomly selected
        x01 = max(0.5,random('norm',Tair_out_emp (p),15));
        Wsat_x01 = W(VP(salt_{p}, x01, 0.1));
        x02 = max(0.5,random('norm',Wair_out_emp (p),15));
        trial_ran = [p,trial, x01, x02]
    end
    [x,fval] = lsqnonlin(@(x) LAMEE_ode(salt_{p}, NTU_(p) , NTU_ratio_(p), ...
        Cr_(p),...
        x(1),x(2), Tsol_in_(p), Xsol_in_(p))...
        -[ Tair_in_(p), Wair_in_(p)],[x01 ,  x02],[0.5 0.5], [80 W(VP(salt_{p}, 80, 0.1))],options);
    % solves for x(1) and x(2), which are Tair_out_(p) and Wair_out_(p). The solution for  x(1) and x(2)
    % results in Tair_in and Wair_in that are the same as (or closest to) Tair_in_(p) and Wair_in_(p)
    trial = trial+1;
  end
  if fval>1
    failed_num(p)=1
  else
    failed_num(p)=0;
  end

  Tair_out(p) = real(gTair(1));
  % the variable gTair holds the temperature profile of the air along the exchanger
  Wair_out(p) = real(gWair(1));
  % the variable gWair holds the humidity ratio profile of the air along the exchanger

  dTair_num(p) = Tair_out(p) - Tair_in_(p);
  dWair_num(p) = Wair_out(p) - Wair_in_(p);

  Table{p,1} = gTau;
  Table{p,2} = gTair;
  Table{p,3} = gWair;
  Table{p,4} = gTsol;
  Table{p,5} = gXsol;
  % store profiles of Tair, Wair, Tsol and Xsol, and gTau (the points along the exchangers which data is available)

end
```

- **The function that calculates differential changes in Tair, Wair, Tsol and Xsol along the exchanger**

```
function dy = dLAMEE(x,y)
% calculates differential changes in Tair, Wair, Tsol and Xsol along the exchanger

global salt_ NTU_ NTUm_ Cr_
% instructs the function dLAMEE of the global variables that it should use

test = 'dLAMEE';

dy = zeros(4,1);
```

```
h_fg = min(2.501, abs(2.501 - 0.0024 * y(3)));
% calcultes and assigns the specific heat of evaporation at Tair=Tsol
cp_sol = min(4.2, abs(HeatCapacity(salt_, y(3), y(4))));
% calculates and assigns the specific heat capacity of the solution
Wsol = min(200, abs(W(VP(salt_, y(3), y(4)))));
% calculates and assigns the equilibirum humidity ratio of the solution

dy(1) = -NTU_ * (y(3) - y(1));
dy(2) = -NTUm_ * (Wsol - y(2));
dy(3) = Cr_ * ( dy(1) + h_fg * dy(2));
dy(4) = -y(4) * Cr_ * cp_sol * dy(2) * 1/1000;
% calculate and assign the differential changes to the variable d

end
```

- **The function that calculates effectiveness for the counter-flow heat exchangers**

```
function [ eff_ ] = eff( NTU, Cr )
% calculates effectiveness for the counter-flow heat exchangers at NTU==NTU and Cr==Cr

   if Cr == 1
      eff_ = NTU/(1+NTU);
      % formula for calculating effective of counter-flow heat exchangers at Cr==1
   else
      eff_ = (1-exp(-NTU*(1-Cr)))/(1-Cr*exp(-NTU*(1-Cr)));
      % formula for calculating effective of counter-flow heat exchangers at Cr!=1
   end
   eff_ = max(0.001,eff_);
   % assigns the effectiveness values. The minimum of 0.001 is chosen to prevent division by zero
end
```

- **The function that solves the differential equations for 1D flow inside LAMEEs**

```
function out = LAMEE_ode (salt, NTU, NTUr, Cr, Tair, Wair, Tsol, Xsol)
% solves the differential equations for 1D flow inside LAMEEs

global salt_ NTU_ NTUm_ Cr_ gTau gTair gWair gTsol gXsol
% instructs the function 'LAMEE_ode' of the global variables that it should use

salt_ = salt;
NTU_ = NTU;
NTUm_ = NTU * NTUr;
% calculates and assigns NTUm
Cr_ = Cr;

Tair = max(0.5,min(80,Tair));
Tsol = max(0.5,min(80,Tsol));
Wair = max(0.5,min(200,Wair));
% verifying the values for Tair, Tsol and Wair are reasonable as the solution progresses

options = odeset('AbsTol',1e-12,'MaxStep',0.01);
% sets the option for the ODE solver ode45
[T,Y] = ode45(@dLAMEE,[0,1],[Tair Wair Tsol Xsol]);
% invokes ode45 solver, with the differential changes in Tair, Wair, Tsol and Xsol calculated and returned by the
function 'dLAMEE'

out(1) = Y(length(Y),1);
% returns Tair_out as out(1)
out(2) = Y(length(Y),2);
% returns Wair_out as out(1)

gTau = T;
% global function gTau stores the dimensionless intervals at which the differential equation is discretized
gTair = Y(:,1);
gWair = Y(:,2);
gTsol = Y(:,3);
gXsol = Y(:,4);
```

```
% global functions that store Tair, Wair, Tsol and Xsol along the exchanger
```

- **The function that calculates the right side of the Eq. (4.6)**

```
function [ m_star_e ] = m_star_e_de( mse_in, mse_IWD, NTUm, guess)
%calculates the right side of the Eq 4.6 for m_star_in=mse_in, m_star_IWD=mse_IWD, NTUm=NTUm, and
m_star_e=guess

if mse_IWD==0
   m_star_e = mse_in;
else
   m_star_e = mse_in*(exp(mse_IWD*eff(NTUm,guess))-1)/(mse_IWD*eff(NTUm,guess));
end
end
```

- **The function that calculates the equilibrium humidity ratio of the air adjacent to the solution**

```
function W_ = W (VP)
% calculates   the equilibrium humidity ratio of the air adjacent to the solution at (partial vapour pressure=VP) per
Eq. (3.25)

global P_total
% instructs the function 'W' that P_total is a global variable provided to the function

W_ = 0.62198 * (VP / (101325 / 1000- VP)) * 1000;
% calculats Wsol per Eq. 3.25

end
```

Appendix B: Sample Calculations

This appendix includes the calculations for estimating the change in the temperature and humidity ratio of a sample data point. Data point F, from dataset Z [18] is chosen as the sample data point for this purpose.

From Table 2.6:

- $X_{sol,in} = 34.0\%,\ T_{sol,in} = 25.5\ °C$

Then, noting that the salt for dataset Z is $LiCl$, the corresponding coefficients for the linear-exponential correlation for W_{sol}, Eq. (3.27), can be obtained from Table 3.2 to conclude that

- $W_{sol,in}\ @\left(X_{sol,in}, T_{sol,in}\right) = (-12.2 \text{ x } 0.34 + 5.63)\exp(0.058 \text{ x } 25.5) = 6.50\ g/kg$

From Table 2.6:

- $W_{air,in} = 21\frac{g}{kg}, T_{air,in} = 33.8\ °C$

Substituting $W_{air,in}, T_{air,in}, T_{sol,in}$ and $W_{sol,in}$ into the formula for H^*, Eq. (4.11), one obtains

- $H^* = \frac{h_{fg}}{c_{p,air}}\frac{W_{sol,in}-W_{air,in}}{T_{sol,in}-T_{air,in}} = 2.4\frac{6.5-21}{25.5-33.8} = 4.2$

From Table 2.6:

- $NTU = 2.7, NTU_m = 1.0$

Substituting the values for NTU and NTU_m into Eq. (4.12) to estimate the ratio ϵ_m/ϵ_s, results in

- $\frac{\epsilon_m}{\epsilon_s} \cong \left(\frac{\epsilon_m}{\epsilon_s}\right)_{@\ Cr_e = m_e^* = 0} = \frac{1-\exp -NTU_m}{1-\exp -NTU} = 0.678$

From Table 2.6:

- $Cr = 0.84$

Substituting the values for Cr, H^* and the estimation for the ratio ϵ_m/ϵ_s into Eq. (4.7), Cr_e can be calculated as follows

- $Cr_e = Cr\left(1 + H^*\frac{\epsilon_m}{\epsilon_s}\right) \cong 0.84\ (1 + 4.2\ \text{x}\ 0.678) \cong 3.2$

Substituting the values for Cr_e and NTU into Eq. (4.3), results in

- $\epsilon_s = \frac{T_{air,out}-33.8}{25.5-33.8} = \frac{1-\exp[-2.7\ (1-3.2)]}{1-\ 3.2\ \exp[-2.7\ (1-3.2)]} = 0.31$

  $\rightarrow (\boldsymbol{Estimated})\ \boldsymbol{T_{air,out} = 31.2\ °C}$

From [18] for data point F

- $(\boldsymbol{Experimental})\ \boldsymbol{T_{air,out} = 32.5\ °C}$

Note that if instead of the simplified-extended $\epsilon - NTU$ model, the standard $\epsilon - NTU$ model was used, i.e. if Cr was substituted into the effectiveness formula instead of Cr_e, then

- $\epsilon_s = \frac{T_{air,out}-33.8}{25.5-33.8} = \frac{1-\exp[-2.7\ (1-0.84)]}{1-\ 0.84\ \exp[-2.7\ (1-0.84)]} = 0.77$
- $\rightarrow\ Est.T_{air,out} = 27.4\ °C$

$m^*_{e,in}$ and $m^*_{e,IWD}$ can be calculated, per Eq. (4.9) and Eq. (4.10), as follows

- $m^*_{e,in} = \left[Cr\ \frac{h_{fg}}{c_{p,air}}\left(\frac{1}{H^*}\frac{\epsilon_s}{\epsilon_m}+1\right)\right]\ \beta\ W_{sol,in}$
  $= \left[0.84\ 2.4\left(\frac{1}{4.2}\frac{1}{0.678}+1\right)\right]\ 0.058\ 6.5$
  $= 1.0$
- $m^*_{e,IWD} = \left[Cr\ \frac{h_{fg}}{c_{p,air}}\left(\frac{1}{H^*}\frac{\epsilon_s}{\epsilon_m}+1\right)\right]\beta\ \left(W_{air,in} - W_{sol,in}\right)$

  $= \left[0.84\ 2.4\left(\frac{1}{4.2}\frac{1}{0.678}+1\right)\right]\ 0.058\ (21-6.5)$

  $= 2.3$

To solve for m^*_e, as a 1st guess, it is assumed that

- $(1st\ guess)\ m^*_e = \left(1.0 + \frac{2.3}{2}\right) = 2.2$

Then, from Eq. (4.4), the 1st guess for ϵ_m can be obtained

- $(1st\ guess)\ \epsilon_m = \frac{1-\exp[-NTU_m\ (1-m^*_e)]}{1-\ m^*_e\ \exp[-NTU_m\ (1-m^*_e)]} = \frac{1-\exp[-1\ (1-2.2)]}{1-\ 2.2\ \exp[-1\ (1-2.2)]} = 37\%$

Then, the 2nd guess for m^*_e can be obtained from Eq. (4.8)

- $(2nd\ guess)\ m^*_e = m^*_{e,in}\frac{exp(m^*_{e,IWD}\ \epsilon_m)-1}{m^*_{e,IWD}\epsilon_m} = 1.0\frac{exp(2.3\ 0.37)-1}{2.3\ 0.37} = 1.58$

Then, from Eq. (4.4), the 2nd guess for ϵ_m can be obtained

- $(2nd\ guess)\ \epsilon_m = \frac{1-\exp[-1\ (1-1.58)]}{1-\ 1.58\ \exp[-1\ (1-1.58)]} = 43\%$

Then, the 3rd guess for m^*_e can be obtained from Eq. (4.8)

- $(3rd\ guess)\ m^*_e = 1.0\frac{exp(2.3\ 0.43)-1}{2.3\ 0.43} = 1.7$

Then, from Eq. (4.4), the 3rd guess for ϵ_m can be obtained

- $(3rd\ guess)\ \epsilon_m = \frac{1-\exp[-1\ (1-1.7)]}{1-\ 1.7\ \exp[-1\ (1-1.7)]} = 42\%$

Since the difference between 2nd and 3rd guess for ϵ_m is 1%, we assume that

- $\epsilon_m = (3rd\ guess)\ \epsilon_m = 42\%$

  Then, from Eq. (4.4)

- $\epsilon_m = \frac{W_{air,out} - 21}{6.5 - 21} = 0.42$

  $\rightarrow (\boldsymbol{Estimated})\boldsymbol{W_{air,out} = 14.9\ g/kg}$

  From [18] for data point F

- $(\boldsymbol{Experimental})\boldsymbol{W_{air,out} = 15.1\ g/kg}$